PROCEEDINGS

OF THE

AMERICAN SOCIETY OF CIVIL ENGINEERS

VOL. 71 DECEMBER, 1945 NO. 10

TECHNICAL PAPERS

AND

DISCUSSIONS

Published monthly, except July and August, at Prince and Lemon Streets, Lancaster, Pa., by the American Society of Civil Engineers. Editorial and General Offices at 33 West Thirty-ninth Street, New York 18, N. Y. Reprints from this publication may be made on condition that the full title of Paper, name of Author, page reference, and date of publication by the Society are given.

Entered as Second-Class Matter, September 23, 1937, at the Post Office at Lancaster, Pa., under the Act of March 3, 1879. Acceptance for mailing at special rate of postage provided for in Section 1103, Act of October 3, 1917, authorized on July 5, 1918.

Subscription (if entered before January 1) $8.00 per annum. Price $1.00 per copy

Copyright, 1945, *by the* AMERICAN SOCIETY OF CIVIL ENGINEERS

Printed in the United States of America

	Published	Discussion closes
Bull, Anders. Stresses in the Linings of Shield-Driven Tunnels	Nov., 1944	
Discussion in Jan., Feb., May, June, Sept., Nov., Dec., 1945		Closed*
Kalinske, A. A. Conversion of Kinetic to Potential Energy in Flow Expansions	Dec., 1944	
Discussion in Feb., May, June, Sept., 1945		Closed*
Osgood, William R. Column Formulas	Dec., 1944	
Discussion in Feb., Mar., May, June, Nov., 1945		Closed*
Powell, Ralph W. Flow in a Channel of Definite Roughness	Dec., 1944	
Discussion in June, Oct., Nov., 1945		Closed*
Conkling, Harold. Utilization of Ground-Water Storage in Stream System Development	Jan., 1945	
Discussion in Mar., Apr., May, June, Sept., 1945		Closed*
DeYoung, Isaac. A Plan for a Movable Dam	Feb., 1945	
Discussion in May, June, Oct., 1945		Closed*
Bennett, Preston T. The Effect of Blankets on Seepage Through Pervious Foundations	Jan., 1945	
Discussions in Mar., Apr., June, Oct., 1945		Closed*
Weiss, Camillo. Interrelation of Certain Structural Concepts	Jan., 1945	
Discussion in May, June, Sept., Oct., Nov., 1945		Closed*
Blanks, R. F., and Meissner, H. S. Deterioration of Concrete Dams Due to Alkali-Aggregate Reaction	Jan., 1945	
Discussion in Sept., Dec., 1945		Jan. 1, 1946
Bakhmeteff, Boris A., and Allan, William. The Mechanism of Energy Loss in Fluid Friction	Feb., 1945	
Discussion in Sept., Nov., 1945		Jan. 1, 1946
Hayes, Harry. Elimination of Cross Connections in Los Angeles, Calif.	Mar., 1945	
Discussion in May, Oct., 1945		Jan. 1, 1946
Eliel, Leon T. Economics of Photogrammetry	Mar., 1945	
Discussion in June, Oct., Dec., 1945		Jan. 1, 1946
Genter, A. L. Computing Coagulant Requirements in Sludge Conditioning	Mar., 1945	
Discussion in June, Oct., Dec., 1945		Jan. 1, 1946
Harrold, Lloyd L. Flow from Drainage Basins Determined by Short-Term Records	Apr., 1945	
Discussion in Oct., 1945		Jan. 1, 1946
Camp, Thomas R. Sedimentation and the Design of Settling Tanks	Apr., 1945	
Discussion in Sept., Nov., 1945		Jan. 1, 1946
Eichler, John Oran, and Eves, Howard W. Mathematical Examination of the Highway Transition Spiral	May, 1945	
Discussion in Nov., Dec., 1945		Jan. 1, 1946
Report: Water Supply Engineering: Report of the Committee of the Sanitary Engineering Division for the Two Years Ending December 31, 1944	May, 1945	Jan. 1, 1946
Nelidov, I. M. Determination of Pressures within a Siphon Spillway	Mar., 1945	
Discussion in Dec., 1945		Feb. 1, 1946
Mullis, Ira B. Design of Roadbeds	Apr., 1945	
Discussion in Oct., Nov., Dec., 1945		Feb. 1, 1946
Stevens, J. C. Future of Lake Mead and Elephant Butte Reservoir	May, 1945	
Discussion in Oct., Nov., Dec., 1945		Feb. 1, 1946
Brumfield, R. C. Moving Loads on Restrained Beams and Frames	May, 1945	
Discussion in Oct., Nov., Dec., 1945		Feb. 1, 1946
Johnston, Milan A. Effects of Radiant Heat on Reinforced-Concrete Rigid Frames	June, 1945	
Discussion in Oct., Nov., 1945		Feb. 1, 1946
Ehasz, F. L. Structural Skew Plates	June, 1945	
Discussion in Nov., 1945		Feb. 1, 1946
Laverty, Finley B. Correlating Flood Control and Water Supply, Los Angeles Coastal Plain	June, 1945	
Discussion in Nov., 1945		Feb. 1, 1946
Symposium: Cavitation in Hydraulic Structures	Sept., 1945	
Discussion in Dec., 1945		Feb. 1, 1946
Freudenthal, Alfred M. The Safety of Structures	Oct., 1945	Mar. 1, 1946
Symposium: Design Developments—Structures of the Tennessee Valley Authority	Oct., 1945	
Discussion in Dec., 1945		Mar. 1, 1946
Hopkins, Charles D. Balanced Design in Urban Triangulation	Nov., 1945	Apr. 1, 1946
Fitz Hugh, M. M., Miller, J. S., and Terzaghi, Karl. Shipways with Cellular Walls on a Marl Foundation	Nov., 1945	Apr. 1, 1946

NOTE.—The closing dates herein published are final except when names of prospective discussers are registered for special extension of time.

* Publication of closing discussion pending.

CONTENTS FOR DECEMBER, 1945

PAPERS

PAGE

Uplift Pressure in and Beneath Dams: A Symposium 1473

DISCUSSIONS

Determination of Pressures Within a Siphon Spillway.
By A. Shukry 1537

Mathematical Examination of the Highway Transition Spiral.
By Max C. Koehler 1545

Stresses in the Linings of Shield-Driven Tunnels.
By Louis Balog 1551

Deterioration of Concrete Dams Due to Alkali-Aggregate Reaction.
By J. C. Witt 1556

Computing Coagulant Requirements in Sludge Conditioning.
By Walter H. Brown, Jr. 1559

Design of Roadbeds.
By Delbert L. Lacey 1561

Economics of Photogrammetry.
By W. J. Ryan 1565

Design Developments—Structures of the Tennessee Valley Authority: A Symposium.
By A. T. Larned 1567

Cavitation in Hydraulic Structures: A Symposium.
By C. A. Mockmore 1571

Future of Lake Mead and Elephant Butte Reservoir.
By Berard J. Witzig 1573

CONTENTS FOR DECEMBER, 1945 (*Continued*)

PAGE

Moving Loads and Restrained Beams and Frames.

By J. Kalb, G. Rolsma and F. W. Gieseking, Stanley S. Schure, and Alexander Dodge 1576

INDEXES

Subject and Author Indexes, 1945 *Proceedings* 1601

A list of "Current Papers and Discussions" may be found on the page preceding the table of contents

The Society is not responsible for any statement made or opinion expressed in its publications

HINTS TO AUTHORS

Those who are planning papers for submission to PROCEEDINGS *will expedite Committee action measurably by first studying the standard instructions as to style, content, and format. For reprints, address the Secretary, Committee on Publications, 33 W. 39th St., New York 18, N. Y.*

AMERICAN SOCIETY OF CIVIL ENGINEERS

Founded November 5, 1852

PAPERS

UPLIFT PRESSURE IN AND BENEATH DAMS
A SYMPOSIUM

PAGE

Experiments on Effective Uplift Area in Gravity Dams.
By SERGE LELIAVSKY, ESQ. 1474

Dams on Porous Media.
By MOHAMED AHMED SELIM, ASSOC. M. ASCE..... 1518

NOTE.—Written comments are invited for immediate publication; to insure publication the last discussion should be submitted by May 1, 1946.

EXPERIMENTS ON EFFECTIVE UPLIFT AREA IN GRAVITY DAMS

BY S. LELIAVSKY,[1] ESQ.

SYNOPSIS

In a concrete dam, water filters through the natural pores of the material of the structure and develops an internal pressure or uplift. This paper describes tests made to determine the intensity of the pressure required to cause breakage of the material. Water under pressure was driven into the pores of concrete specimens of various mixtures and the pressure required to burst the concrete was measured on a specially designed testing machine. An empirical relationship between the hydrostatic load and the bursting force is developed.

INTRODUCTION

In the design of masonry or concrete dams the uplift due to the penetration of water into the structure is a factor that has never been completely investigated. There are two essentially different schools of thought in connection with this problem. According to the earlier group of theories—which comprised Maurice Lévy's law (communication to the French Academy of Sciences submitted by Maurice Lévy, on August 5, 1895), the Lieckfeldt method,[2] the Link theory,[3,4] and others[5]—the uplift pressure was assumed to penetrate into the material through cracks (see Fig. 1), and the horizontal or hydrostatic pressure of water was assumed to be exerted externally on the face of the dam. These uplift theories were very popular in Europe in the earlier years of the twentieth century and were incorporated in some of the larger projects of the period; but as experience and knowledge accumulated they were gradually abandoned.

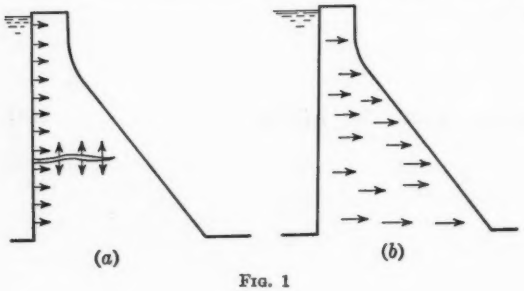

FIG. 1

[1] Chf. of Designing Office, Projects Dept., Ministry of Public Works, Cairo, Egypt.

[2] "Die Standfestigkeit von Staumauern mit offenen Lagerfugen," by G. Lieckfeldt, *Zentralblatt der Bauverwaltung*, Berlin, Vol. 18, February 26, 1898, p. 105.

[3] "Die Bestimmung der Querschnitte von Staumauern und Wehren aus dreieckigen Grundformen," by E. Link, Berlin, 1910.

[4] "Über Sohlenwasserdruck bei Staumauern mit entwässerter Grundungsfläche," by E. Link, *Zeitschrift für Bauweisen*, 1919, p. 525.

"Profils des Barrages en Maçonnerie," by Pelletrau, *Annales des Ponts et Chaussées*, 1897.

The modern principle, accepted by Karl Terzaghi,[6] M. ASCE, P. Fillunger,[7,8] O. Hoffman,[9] and many other research workers in all parts of the world, is that water filters through the natural pores of the material of the dam. For that purpose the structure need not be considered cracked or injured but may be perfectly sound and strong, at the same time being more or less pervious. (Messrs. Terzaghi, Fillunger, and Hoffman are chiefly responsible for the latest developments in the theory of internal uplift in masonry dams. The serious student of this subject is referred to their several published contributions.) That the two effects (strength and porosity) might be superimposed has been suggested from time to time but the idea does not seem to have gained popularity. In one case there is a purely abstract conception of a hypothetical crack whereas the other concerns a physical phenomenon, capable of being investigated by means of the usual methods of experimental science.

As a corollary to the new conception it appears that the horizontal water pressure is not applied to the face of the material, as was formerly believed to be the case, but is totally or partly transferred into the body of the dam (shown by the arrows in Fig. 1(*b*)).

This change in the ideas concerning the point of application of the hydrostatic pressure necessarily must have affected the methods of stress analysis adopted in a given case. It may be shown, however, that the normal stresses on horizontal planes and the shearing stresses are not altered, the normal stresses on vertical planes being the only ones that need to be revised. Although an exhaustive reply to this question might call for model tests, preliminary calculations tend to show that there is no cause for apprehension, at least in so far as the usual type of sections is concerned.

It follows from the foregoing that "uplift" can be defined as a "pressure in the pores" or an "interstitial pressure." The first and obvious problem in this connection is to decide the intensity to which such a pressure should be raised, in order to cause the material to be broken.

Curious as this might seem, the published information on this subject is very scarce and rather inconsistent. In other branches of engineering it is standard practice to test specimens to failure in the laboratory, and thus to ascertain the effect of load upon the resistance for use in practical design; but very little evidence of similar character has been supplied concerning the force of uplift and its effect upon concrete or masonry.

The first set of experiments to be cited in this connection is the well-known investigation, as early as 1900, by Prof. August Föppl.[10] The apparatus he used is shown in Fig. 2.

Water under pressure supplied through the intake was driven into the pores of the material, and so caused the concrete to burst. The following are the

[6] "Die Wirksame Flächenporosität des Betons," by Karl Terzaghi, *Oesterreichischer-ingenieur-und-architekten-verein, Zeitschrift*, Vol. 86, 1934, Heft 1/2, pp. 1–9.

[7] "Der Auftrieb in Talsperren," by P. Fillunger, *Oesterreichische Wochenschrift für den öffentlichen Baudienst*, Vol. 19, 1913.

[8] "Neuere Grundlagen für die statische Berechnung von Talsperren," by Paul Fillunger, *Oesterreichischer-ingenieur-und-architekten-verein, Zeitschrift*, 1914, p. 441.

[9] *Die Wasserwirtschaft*, 1929–1930.

[10] *Mitteilungen aus dem Mechanisch-Technischen Laboratorium der K. Polytechnischenschule in München*, No. 27, 1900, Heft 24, p. 16.

pressures, in atmospheres, which were required in order to produce failure of exactly identical specimens: 11.0, 3.8, 12.0, 6.4, 15.0, 29.0, 7.0, 3.0, and 2.0. Obviously, with such irregular results no conclusions could be reached.

The technical consensus tends to attribute the inconsistency of these experiments to secondary influences and accidental circumstances, the effect of which had not been properly dealt with in designing the apparatus.

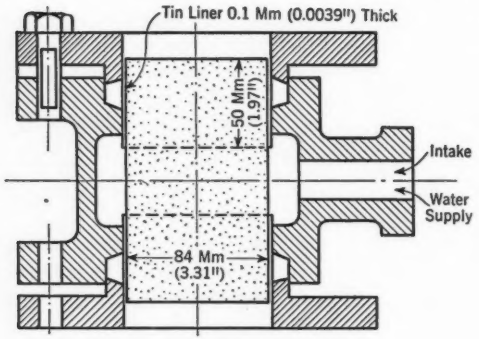

FIG. 2

In addition to Professor Föppl's tests, several others might be cited in which the test pieces were broken (or were intended to be broken) by the direct action of the uplift force: A test at the Bull Run Dam in Oregon; an experimental investigation which formed the subject of an unpublished thesis at the California Institute of Technology at Pasadena; a set of tests made by S. H. Woodard, M. ASCE; and findings reported by the late D. C. Henny,[11,12] M. ASCE.

Although the details of the mechanical devices used in these experiments were not published it appears that they were based upon the same general principle as the Föppl apparatus; but, in addition to this, the tensile breaking stress of the materials experimented upon was determined, in every case, by means of control specimens, on testing machines of the usual type.

The difference in the results derived in these interesting experiments seems to have been very great: The ratio of the interstitial area affected by the uplift pressure to the total sectional area was found to be 3% in one of these tests but appeared to increase to as much as 183% in another experiment.

One might naturally be reluctant to use these results in either design or theory, because the numerical value of the ratio in question must lie logically in between the coefficient of volumetric porosity, as a minimum, and 100%, as a maximum. It is rather difficult to interpret what actually occurred, particularly as the published information about these tests is indeed very scanty; but, according to Mr. Henny (as interpreted by the writer), the fact that the results in this case were far from consistent was most probably due to two causes: (*a*) The control briquettes did not furnish the true value of the tensile breaking stress, and (*b*) the pressure of the water injected into the pores was not uniformly distributed over the entire area of rupture (being undoubtedly less at the center than at the periphery).

These technical causes might have been effective in the two other cases as well, but the main source of the trouble seems to be deeper than that, as explained subsequently herein.

[11] "Problems in Concrete Dam Design," by D. C. Henny, *Engineering News-Record*, Vol. 106, No. 11, March 12, 1931, p. 433.

[12] "Stability of Straight Concrete Gravity Dams," by D. C. Henny, *Transactions*, ASCE, Vol. 99 (1934), p. 1041.

Four other experimental investigations on uplift should be cited—namely, those of Max Rudeloff and Panzerbieter,[13] Fillunger,[14] Terzaghi[15] (1934) and N. Kelen.[16] An example of the testing devices used in these experiments is shown in Fig. 3. These four series of tests differed greatly in value, but they

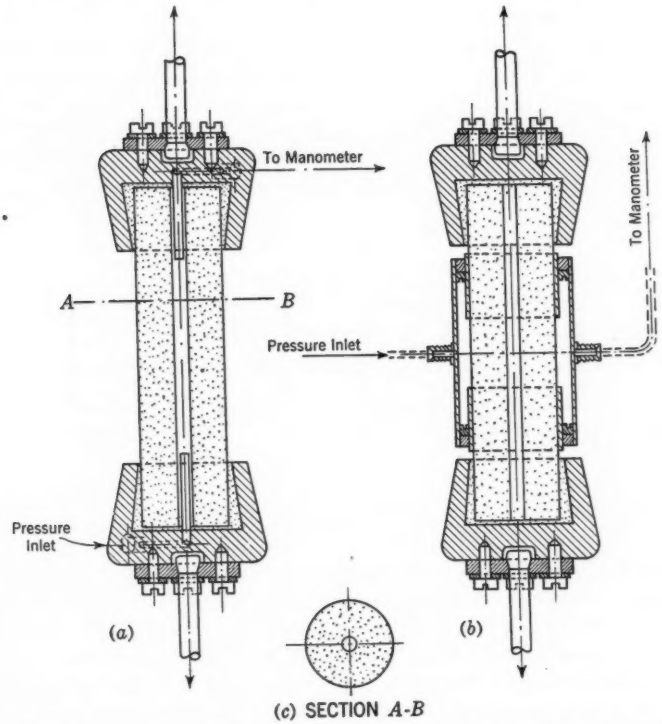

FIG. 3.—TESTING DEVICE USED IN THE EXPERIMENTS BY RUDELOFF AND PANZERBIETER

had one point in common—although the uplift force was present in every case, and the results of the tests were more or less dependent upon it, the failure itself was due to another agency, a mechanically developed load. This led to some ambiguity in interpreting the results obtained, thus rendering their significance difficult to assess, and leading consequently to much controversy as to the true interpretation of the tests.

The existence of uplift (as an interstitial hydraulic force which was capable of causing failure) was still considered in certain circles as not being fully proved; and, even if it existed, opinions were often expressed that the magni-

[13] "Versuche über den Porendruck des Wassers im Mauerwerk," by Max Rudeloff and Panzerbieter, *Mitteilungen aus deutschen Königlichen Materialprüfungsamt zu Gross*, Lichterfelde West, Berlin, 1912.

[14] "Versuche über Zugfestigkeit bei allseitigem Wasserdruck," by Paul Fillunger, *Osterreichische Wochenschrift für den öffentlichen Baudienst*, Vol. 21, Pt. 2, July, 1917, Heft 29, p. 443.

[15] "Simple Tests Determine Hydrostatic Uplift," by Karl Terzaghi, *Engineering News-Record*, Vol. 116, June 18, 1936, p. 872.

[16] "Experimental Determination of the Tangential Foundation Resistance of Gravity Dams," by N. Kelen, *Engineering*, Vol. 144, August 20, 1937, p. 215, and August 27, 1937, p. 242.

tude of that force was a matter of chance and could not be dealt with as a measurable physical quantity.

Therefore, it was believed that, in order to determine a convincing conclusion about the uplift pressure, the first and obvious step in solving the problem was to cause the material to be broken by driving water into the pores of the specimen, as was done by Föppl, but also to design the testing apparatus in such a way as to avoid the irregularity of the results he obtained.

Consequently, a more advanced type of apparatus was called for, but this alone would not have supplied the required solution, because the principle itself, upon which Föppl's device was based, did not contain the elements required for solving the problem. In this connection, attention is called to Fig. 4. The unit pressure of water being p and the sectional area of the

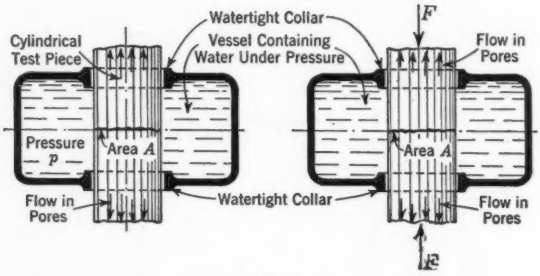

FIG. 4

cylindrical specimen A, the total pressure in the pores will be $p\,A$ multiplied by a certain coefficient of reduction n_a which represents the ratio of the interstitial area subjected to the hydraulic pressure, to the total area of the section, and is the main unknown value to be determined by these tests. (According to the modern school of thought n_a is believed to be a physical constant depending on the arrangement of pores. It is variously described in different works on the subject either as the "uplift factor," or the "reduction coefficient," or as the "effective porosity.") At the moment of failure, when the specimen bursts, the force $n_a\,p\,A$ must be equal to the resistance z of the specimen; that is,

$$n_a\,p\,A = z \qquad (1)$$

Unfortunately, Eq. 1 contains two unknown factors, n_a and z, and it is obvious that it cannot be used for finding either of them. Apart from technical details, therefore, the general layout of Föppl's testing arrangement did not satisfy the conditions of the problem.

In other instances, mentioned previously herein, z was determined by means of control specimens, so that apparently, had the causes of excessive dispersion been removed, these experiments might have supplied at least a partial solution to the problem. It will be shown, however, that, for reasons concerning the range of conditions experimented upon as compared with the probable deviation, consistent results would have been exceedingly difficult to obtain, if this method had been followed.

Proposed Solution of the Problem

The principle of the author's solution of this problem is shown in Fig. 4. The material is arranged the same as in a dam; that is, the specimen is first subjected to the effect of a force F, so that, when the uplift begins to produce its effect, it must not only overcome the resistance of the material, but must also counteract the effect of a certain compressive force, which in a full-sized dam is due to its structural weight. Suppose that, having tested several identical specimens subjected to various forces F_1, F_2, F_3, etc., it is known that the unit pressures at which they broke were p_1, p_2, p_3, etc. The following series of formulas can then be written:

$$\left.\begin{aligned} n_a\, p_1\, A &= z + F_1 \\ n_a\, p_2\, A &= z + F_2 \\ n_a\, p_3\, A &= z + F_3 \\ &\cdots\cdots\cdots \\ n_a\, p_n\, A &= z + F_n \end{aligned}\right\} \qquad (2)$$

from which

$$\left.\begin{aligned} n_a &= \frac{F_2 - F_1}{p_2\, A - p_1\, A} \\ n_a &= \frac{F_4 - F_3}{p_4\, A - p_3\, A} \\ n_a &= \frac{F_n - F_{n-1}}{p_n\, A - p_{n-1}\, A} \end{aligned}\right\} \qquad (3)$$

The result is not only one, but several equations, from which n_a can be determined. The more general form of Eqs. 3 is:

$$n_a = \frac{\Delta F}{A\, \Delta p} \qquad (4a)$$

or

$$n_a = \frac{dF}{A\, dp} \qquad (4b)$$

The physical interpretation of Eqs. 4 is as follows: The additional unit pressure Δp is absorbed in overbalancing the additional force ΔF; therefore, Δp multiplied by the effective area $n_a\, A$ must be equal to ΔF.

This solution is valid only when a relationship is found to exist between $p\, A$ and F. In the absence of definite information on the subject, the problem of proving the existence of this relationship was at least as important as that of estimating it quantitatively; but, once the relationship had been established empirically, the new solution was independent of the precise nature of the physical causes which determined the value of the coefficient n_a. Had the problem been considered from the standpoint of the results of the earlier tests, the existence of this relationship between $p\, A$ and F might have appeared rather doubtful.

This value may be conceived either as being correlated with the inter-structural arrangement of the pores in the normal condition of the material

tested; or, alternatively, this material may be assumed to be already affected before the actual failure takes place, being at that moment in the state of "agony" observed in certain earlier tests. A third interpretation could also be imagined; in fact, one may visualize the effective area as being affected by the crack itself, or, in a strict sense, by the process of its gradual development, so that the failure of the less resistant or more accessible parts facilitates the penetration of water into the material, until, at the moment when the final fracture occurs, a certain (possibly quite a large) part of the area of rupture is already open to the direct action of the pressure.

So long as a measurable relation is found to exist between $p\,A$ and F, it would not really matter which of these three interpretations was taken to be true; or, should another physical explanation be suggested, the results of the tests would still remain valid and applicable to the statical analysis of the dam section. (Nevertheless, when analyzed, the tests themselves supplied a definite indication that the first of the three suggested explanations is the correct one, but this point will be considered subsequently in this paper.)

A certain correction must be introduced into the value of n_a obtained as suggested herein, in order to account for the fact that, apart from producing uplift, the water contained in the pores increases the weight of the material. For a more or less triangular profile the diagram of this additional weight, for any horizontal section considered, is nearly triangular; which means that, at any point, this effect may be assumed to be proportional to the uplift pressure. Therefore, it may be taken into account by a corresponding reduction in the value of n_a. The final value of the uplift factor would then be found from:

$$n = n_a - n_v \qquad (5)$$

in which n_v is the volumetric porosity of the material.

This method of calculation seems to be justified for the reason that n_v is very small. It is evident, however, that an alternative path could also be followed—namely, to take n_v into account by a corresponding adjustment of the structural weight of the dam, and then to multiply the interstitial, pressure intensities by the unreduced value of n_a. The first procedure seems to be more usual because it sets off the difference in the relative values of the two coefficients and therefore gives a better idea of the total effect which the filtering of water may produce upon the mechanical stability of the work.

The problem concerning the calculation of the pressure intensities of filtering water is not specifically discussed in this paper. It is rather more simple and more obvious than that referring to the value of n_a. This subject has been treated extensively in modern technical literature and may now be considered as belonging to the scope of a textbook. For example, Professor Terzaghi has written on the subject in various papers,[17] as have E. W. Lane,[18] M. ASCE, W. Weaver,[19] Hoffman[20] and many others.

[17] "Beanspruchung von Gewichtstaumauern durch das strömende Sickerwasser," by Karl Terzaghi, *Die Bautechnik*, Vol. 12, July 6, 1934, Heft 29, p. 379.

[18] "Security from Under-Seepage Masonry Dams on Earth Foundations," by E. W. Lane, *Transactions*, ASCE, Vol. 100 (1935), p. 1235.

[19] "Uplift Pressure on Dams," by W. Weaver, *Journal of Mathematics and Physics*, M.I.T., Cambridge, Mass., June, 1932, p. 114.

[20] "Permeazioni D'Aqua e loro Effeti nei Muri di Ritenuta," by O. Hoffman, Milan, 1928.

In the study of streamline flow as in many other cases of physical analysis the investigator is fully dependent on boundary conditions, which forces him to adopt graphical and approximate arithmetical solutions, or to use model tests and electrical-analogy methods in connection with the design of weirs and dams built on granular soils. The structural details of the foundations of such works may often create exceedingly complicated boundary conditions in so far as the seepage of water is concerned. As compared with these involved cases, the triangular profile of a gravity dam resting on rock is usually very simple to analyze mathematically. In fact, Hoffman has shown[21] that in this case the field of pressures tends to be delimited by a plane, which means that the pressure diagram is nearly triangular. Many times before Hoffman defined it, this principle was used more or less intuitively, in designs, theoretical analyses, and specifications.

To convert from the conditions applying to an ideal triangular profile to those of a practical dam section, the effect of the roadway at the top and the interruption of continuity at the base must be taken into account. These are chiefly local effects, however, which are of rather secondary importance as compared with the main tendency toward a linear pressure distribution. There is no great difficulty in finding the numerical values of the corresponding corrections.

Occasionally, departures from the accepted theory have been reported in connection with pressure-pipe observations in actual dams. There are reasons to believe that the cause of the trouble is partly in the accidental differences in the value of Darcy's coefficient; but, as in every case reported the number of observation points was far too small for the application of scientific statistical investigation methods, the personal element seems to have played a large part in the interpretation of these results. One must distinguish, however, between the accidental differences in the texture of the material in the dam itself, and the systematic differences in Darcy's coefficient over the line of contact with the foundations. Departures from the theoretical triangle are accidental in the first case, but might be systematic in the second case. They should then be taken into account by means of the same methods of calculation as were adopted for granular foundations. Galleries, drains, and differences in the mixtures and methods used in casting the toe and heel areas of the dam are some other causes that may account for systematic variations.[22,23,24]

After much preliminary work, the engineers working on granular foundations in India have succeeded in showing that theory, model tests, and pipe observations were all in agreement.[25] There is no apparent reason why the same should not apply to rock foundations, except that, in the latter case, the investigator is faced[26] with the much more difficult problem of computing the value of n_a.

---

[21] "Permeazioni D'Aqua e loro Effeti nei Muri di Ritenuta," by O. Hoffman, Milan, 1928, p. 41.

[22] *Ibid.*, pp. 49-73.

[23] "Pressures due to Percolating Water and Their Influence upon Stresses in Hydraulic Structures," by J. H. A. Brahtz, *Transactions*, 2d Cong. on Large Dams, U. S. Government Printing Office, Washington, D. C., Vol. V, 1938, p. 43.

[24] "Beanspruchung von Gewichtstaumauern durch das strömende Sickerwasser," by Karl Terzaghi, *Die Baulechnik*, Vol. 12, July 6, 1934, Heft 29, p. 3.

[25] "Design of Weirs on Permeable Foundations," by A. N. Khosla, Simla, 1936, p. 6.

[26] "Measuring Dam Behavior," by Douglas McHenry and Roy W. Carlson, *Engineering News-Record*, Vol. 122, No 13, March 30, 1939, p. 58.

General Principle Underlying the Design of the Experimental Machine

In detailing the testing apparatus for the proposed study it was essential to insure that, when the test piece broke, the pressure p had already penetrated into the thickness of the material and was the same over the entire area of the surface of rupture. If the specimen failed before the penetration was complete, means had to be provided to ascertain, subsequently, the true intensity that the pressure in the pores had actually attained at the moment of failure. To solve this problem, the part of the test piece in which the failure was intended to take place was made hollow, similar to a ring or a pipe with very thick walls, as shown in Fig. 5. (Rudeloff[13] had previously adopted a somewhat similar arrangement for his experiments, but this was not known to the writer until 1938 when the finished drawings of his own testing machine had been completed.)

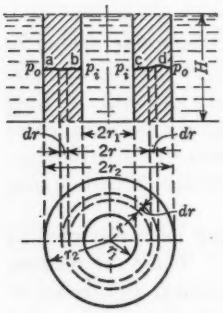

Fig. 5

The sequence of the operations performed in the course of an experiment on the writer's apparatus was as follows: At the beginning of the experiment the test piece was subjected to a certain force F and the water pressure in the container was raised to the intensity p_o, which, hereafter, is denoted as the "outer pressure." At the same time, the empty space inside the test piece was filled with water, connected to a manometer, and closed. The pressure in that space ("inner pressure") was then allowed to rise naturally, until it became constant, or nearly so. In order to prevent this rise from becoming too rapid, or from being abrupted, an air vessel was introduced into the system of pipes connected with the inner space of the specimen.

By that time, if the test piece still remained unbroken, the outer pressure p was increased, and the apparatus was left standing until the inner pressure became constant again. The same procedure was repeated, the pressures being stepped up, until failure finally occurred. Thus, the rise of the inner pressure p_i (which was recorded throughout the duration of the entire test) depended on the quantity of water percolating through the walls of the specimen, and on the velocity of infiltration. It indicated the intensity of the pressure in the pores in immediate contact with the inner periphery of the specimen. A reverse order might have also been adopted—namely, keep the pressure p_o constant and reduce the force F gradually until the specimen broke. This sequence would have been easier but was believed to be inadmissible, because in actual practice the material comprising the dam begins by being compressed by the weight of the superimposed layers; and then only is it subjected to the filtering effect of the water. It was considered essential, therefore, that the sequence of the various causes of stress should be reproduced in the test in the order it occurs in nature.

Had failure occurred when p_i and p_o were equal, the conclusion would be that, at that moment, the pressure in the pores on the outer and inner surfaces of the ring-shaped specimen were the same. In such cases the resultant pressure was calculated by multiplying the sectional area of the specimen by

$p_i = p_o$ (as was originally assumed in explaining the principle of the solution); yet, more often than otherwise, the specimen broke when p_i was less than p_o. (In fact p_i never equals the full value of p_o. A slight difference always remains; but in many cases its effect on the results is almost imperceptible.) Then the resultant depended on the law controlling the distribution of the pressure intensities over the section:

$$p = \frac{Q}{2\pi H K} \log_e r + C \ldots\ldots\ldots\ldots\ldots\ldots (6)$$

in which p is the unit pressure at the radius r; Q is the discharge; K is Darcy's filtering coefficient; and H is as indicated in Fig. 5.

Eq. 6 is the standard formula for radial filters, which is given in various textbooks on the subject,[27] and may be transformed into:

$$p = (p_o - p_i) \frac{\log_e \frac{r}{r_1}}{\log_e \frac{r_2}{r_1}} + p_i \ldots\ldots\ldots\ldots\ldots\ldots (7)$$

The average value of pressure over the cross section is then as follows:

$$p_a = \frac{1}{A} \int_0^A p \, dA = \frac{1}{A} \int_{r_1}^{r_2} 2\pi r p \, dr \ldots\ldots\ldots\ldots\ldots (8)$$

Substituting for p its value obtained from Eq. 7, and integrating:

$$p_a = p_i + (p_o - p_i) \left(\frac{r^2_1}{r^2_2 - r^2_1} - \frac{1}{2 \log_e \frac{r_2}{r_1}} \right) \ldots\ldots\ldots\ldots (9)$$

or

$$p_a = p_i + (p_o - p_i)\Delta \ldots\ldots\ldots\ldots\ldots\ldots (10)$$

in which

$$\Delta = \frac{r^2_1}{r^2_2 - r^2_1} - \frac{1}{2 \log_e \frac{r_2}{r_1}} \ldots\ldots\ldots\ldots\ldots\ldots (11)$$

In conducting the tests the average pressure p_a calculated from Eq. 10 was substituted for p in all the cases in which, at the moment of failure, the inner and outer pressures were not the same.

The physical meaning of Eq. 10 is perfectly clear—the average pressure intensity is equal to the sum of two terms p_i and $(p_o - p_i)\,\Delta$. The first represents the limit reached if the outer pressure falls and becomes equal to p_i; or, conversely, if the inner pressure rises and attains the value p_o. The second term shows the effect of the difference $r_2 - r_1$ and depends on the value of Δ which, in turn, is a function of the ratio $\frac{r_2}{r_1}$ of the outer and inner radii. This

[27] "Hydraulik," by Philipp Forcheimer, B. G. Teubner, Leipzig und Berlin, 1914, p. 433.

function is shown graphically in Fig. 6. Eq. 10 applies also to the case in which $p_i > p_o$ except that the flow is reversed, and, therefore, instead of being convex the curve of pressures must be concave.

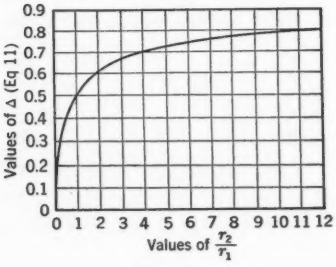

FIG. 6

Referring again to the arrangement actually adopted in the tests (that is, $p_o > p_i$), attention is called to the fact that, thus far, no proof has been offered that n_a is constant. Since this was one of the questions that the experiments were intended to answer, the investigation was conducted in such a manner that the results would have remained significant regardless of whether n_a was found constant or variable. With this object in view the results of each series of tests were represented graphically on a chart, the values of F being plotted as ordinates against $p_a A$ as abscissas.

A series of points was thus obtained, which one could expect to define either as a straight line, or a curve. When the points define a straight line, n_a is shown to be constant (and equal to the tangent of the angle between this straight line and the horizontal). When they define a curve, the variable slope of the curve represents the value of n_a corresponding to various values of $p_a A$ and F. Should the observed points be irregularly dispersed over the entire diagram, defining neither curve nor straight line, this would indicate either that the apparatus was improperly designed or that the uplift was not controlled by any regular law.

In such computations, the greater the range of variation of the variables, the more convincing is the result. In perfecting the details of the testing apparatus, therefore, it was believed convenient to use a device which allowed for reversing the direction of the force F. Thus it was possible to obtain positive as well as negative values of that force, which did not affect the substance of the conclusions, but permitted an increase in the range with the same testing equipment.

THE TEST SPECIMEN

One of the reasons for adopting a ring-shaped type of test specimen has been given. The ring shape also solves the problem of air drainage, as the air contained in the pores in the critical part of the specimen can escape freely into the inner space.

The diameters of the specimens adopted in earlier experiments on uplift were:

	Diameter (cm)
Föppl	8.4
Rudeloff and Panzerbieter	9.0
Terzaghi	8.0
Woodard	5.0

Although sometimes referred to as "concrete," the materials used in these experiments were actually "mortar," being made of cement and sand without

the addition of the coarser aggregate. Since the new experiments were intended to explore a wider range of conditions, however, it was considered essential to introduce broken stone or gravel into the mixtures tested.

To derive consistent results from samples of such a nonhomogeneous substance, the dimensions of the specimens must be more accurate than the irregularities that cause the nonhomogeneity of the material. For that reason, the section of the test piece in the new experiments was made slightly greater than 150 sq cm, the outer diameter being 15 cm when cast, and somewhat less than that when tested, owing to the removal of the "skin"—an operation which was always performed before placing the specimen in the apparatus.

As no marked difference was discovered, later, between the dispersion of the individual tests in the groups prepared, respectively, with and without coarse aggregate, there is sufficient reason for believing that the adopted dimensions of the specimen were adequate.

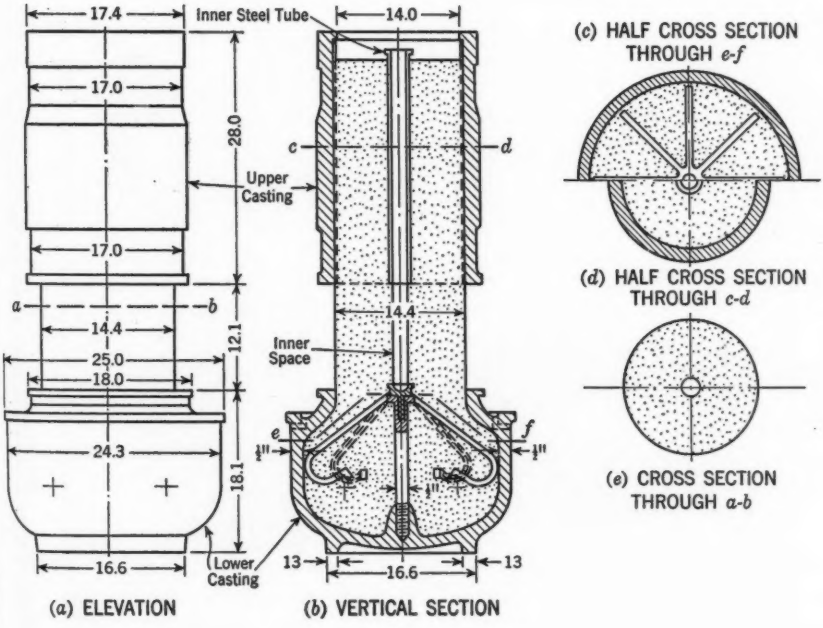

FIG. 7

The general arrangement of the apparatus is shown in Fig. 7, and Fig. 8 is a view of the appearance of the specimen before and after failure. The cast-iron collars by means of which the two castings are held together, when the test piece is cast, are shown in Fig. 9. It will be observed that the apparatus consists of: The inner core, made of the material tested; the upper lining; the lower casting; the pipe in the upper part of the inner space; and the reinforcing bars in the lower part of the core.

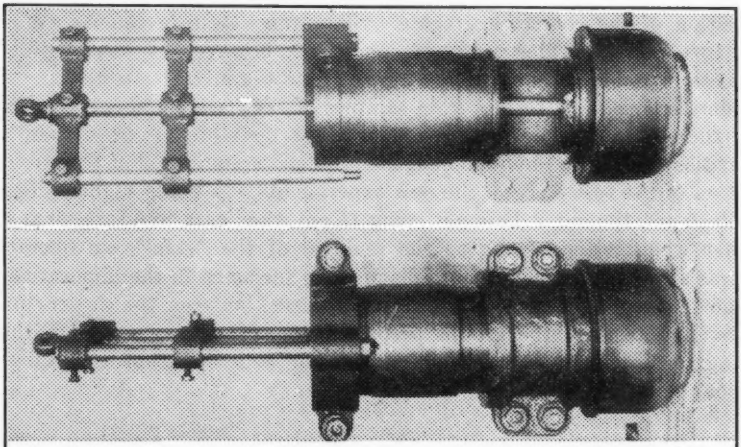

FIG. 9

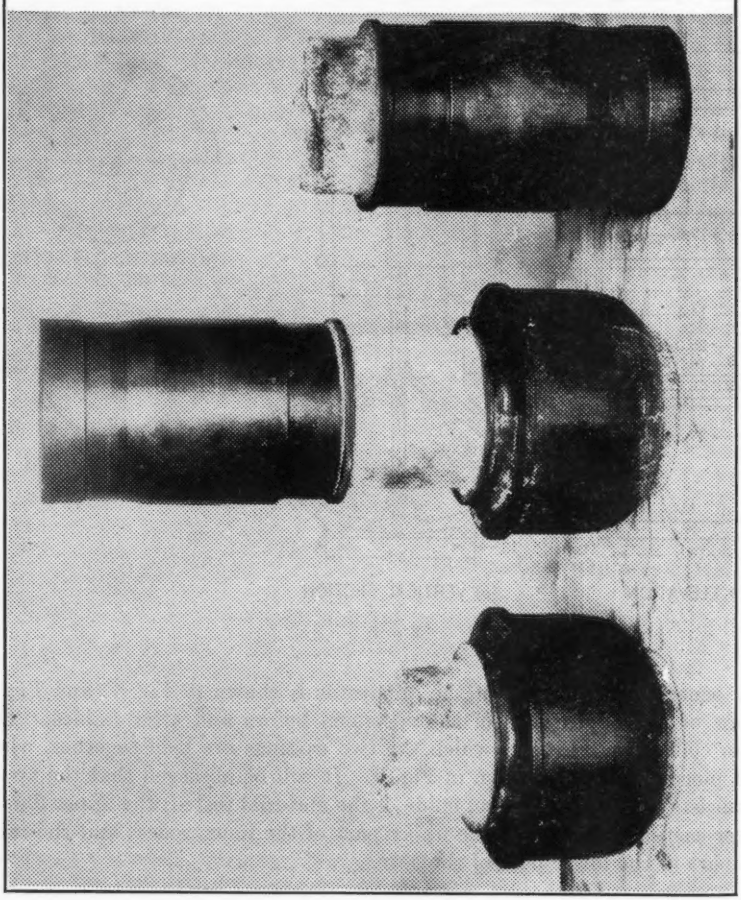

FIG. 8

The first point that calls for comment is the unsymmetrical layout of the specimen. Instead of having both its ends projecting beyond the specimen container, as was done in Föppl's experiments and Rudeloff's experiments, the test piece is entirely enclosed on its lower side, so that only one watertight collar is required instead of two. This arrangement is preferable for technical reasons, both in regard to simplicity of design and facility in conducting tests.

The function of the upper casting is twofold: (1) To provide a watertight and smooth surface for the leather collar to slide over; and (2) to transmit to the material tested the force F—compression or tension as the case may be.

It is essential that this force should not be applied directly to the concrete by means of any object placed on its top surface, because such an objcet would obstruct the exit from the pores through which the water is filtering during the experiment. Should this occur, the conditions would not be the same as in an actual dam. Therefore, the design adopted was as follows: The force F is transmitted by a cup and a brass collar to the upper rim of the top casting, and retransmitted to the specimen through the shearing effect from the inner deformed surface of the lining to the concrete adhering to it. The lower casting (which resembles in shape a common kitchen kettle) has no other function than to maintain the specimen in position.

Both castings were made heavy and strong, and all surfaces that control the position of the specimen relative to the container were machined carefully, thereby avoiding the secondary effects that caused the failure of Föppl's experiments. The remaining parts of the test specimen are of less importance. The pipe in the upper part of the inner space (diameter, 2 cm) is required for fixing the connections to the flexible pipe leading to the air vessel and to the manometer that measures p_i. The reinforcing bars in the lower part of the tested material are introduced in order to prevent the failure from occurring along a curved surface, subject to critical inclined stresses.

A pair of pincers, made of $\frac{3}{4}$-in. round iron, was used to lift and transport the specimens. They were arranged in such a way as to engage with the upper rim of the lower casting, so that no tension stresses, even of the smallest intensity, were set up in the tested material at any moment before the test proper was actually started.

The Testing Machine

The testing machine consists of the four parts: (*a*) Test vessel, or container, in which the specimen is placed for testing; (*b*) lever system, required to develop the compressive or tensile force F; (*c*) accumulator with inverted plunger, frame for carrying the loads, counterweight, manometer for measuring p_o, etc.; and (*d*) air vessel, with manometer for measuring p_i, and a system of flexible pipes designed to connect with the inner space of the specimen.

The lever system (item (*b*)) comprises the main lever with bearings, tie pieces and rocker, the secondary lever with adjusting screws and counterweight, and the cup-and-collar device arranged to engage with the upper lining of the specimen when the test is in progress.

As seen from Figs. 10 and 11, all these parts are erected on a main frame built of riveted channels and gussets. For the tests, this frame was fixed on

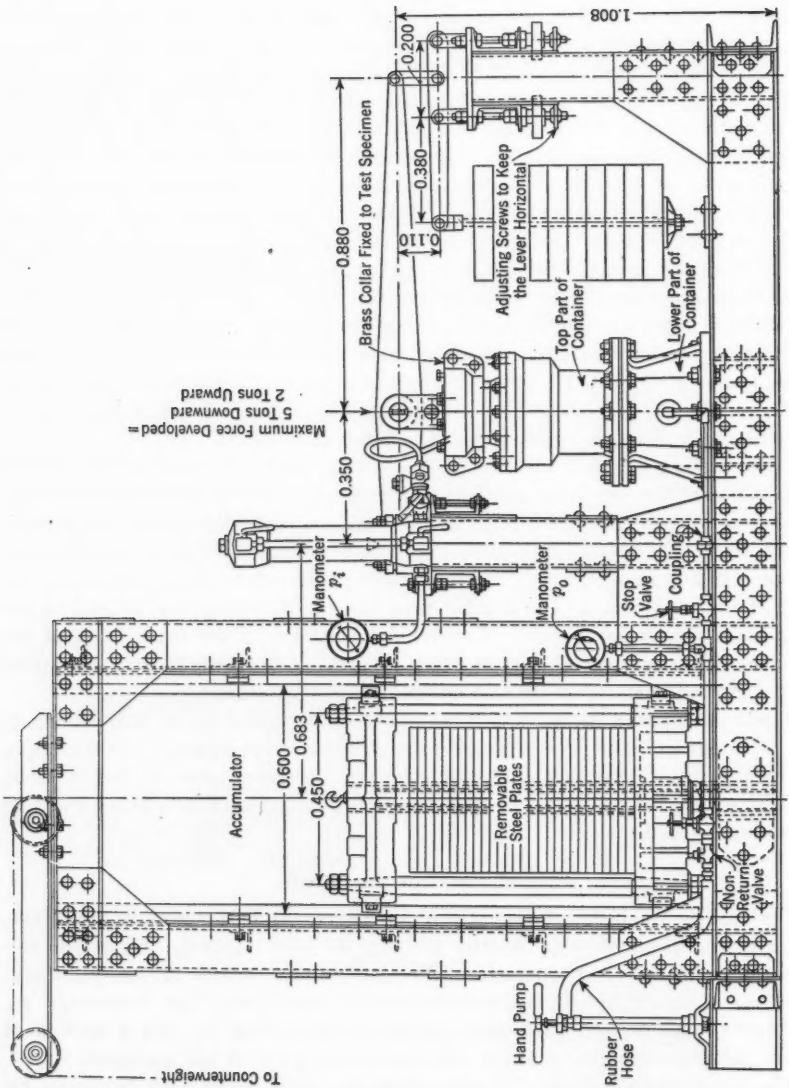

FIG. 10.—GENERAL ARRANGEMENT OF TESTING APPARATUS

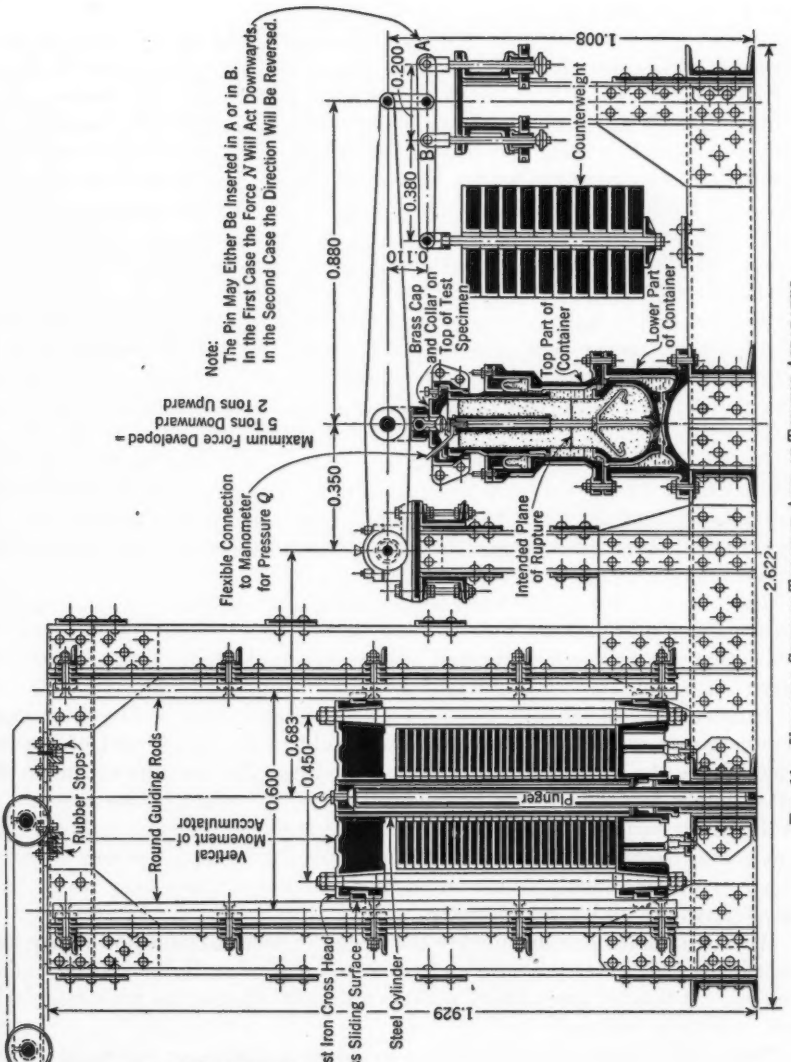

FIG. 11.—VERTICAL SECTION THROUGH AXIS OF TESTING APPARATUS

an independent block of concrete, about ten tons in weight, which was constructed separately from all other foundations of the building, so as to avoid the effect of vibrations. Fig. 12 contains two views showing the machine fully erected in the laboratory.

The supply pipe through which the container is supplied with water is connected at the lower part of the apparatus. This pipe is not shown in Fig. 11 but appears in Fig. 10. It connects the accumulator with the lower part of the container. From this lower part the water passes directly into the top part, and, thence, through the pores in the walls of the specimen, it percolates into the inner space of the latter. A part of the water escapes from the upper surface of the concrete or masonry test piece. During the experiments, it was found necessary to introduce a small sieve in this supply pipe connection, to prevent small particles of the broken concrete from being carried backward by the effect of the pulsations set up when the specimen failed.

The levers are designed in such a way that they can be used to produce, at will, either compression or tension. For that purpose the smaller lever is provided with two bearing pins; depending on which one of them is used, the force transmitted to the test piece is either directed downward or upward.

Had the position of the axles been fixed rigidly, the slope of the levers, due to the deflection of the various parts of the apparatus, would have been so great as to affect, seriously, the precision of the results of the experiment. This was avoided by using the adjusting screws shown on the right side of Figs. 10 and 11—in such a way that the levers were permanently maintained horizontal.

The object of the rocker which transmits the stress from the main lever to the specimen is to prevent horizontal stresses from occurring in the test specimen either during loading (caused by the effect of elastic deformations) or later (caused by temperature variations).

In calculating the force F, in addition to the force transmitted by this rocker, the operator also takes into account the weight of the upper part of the test piece (above the surface of rupture), and the hydraulic pressure acting on the metal linings attached to the specimen; that is, the effect of the pressure p_e on the under surface of the top casting and that of the pressure p_i on the pipe bent connected to the inner space. Both these hydraulic forces can be determined easily since the pressure intensities and the surfaces over which they are effective are all known precisely.

An accumulator was included in the design in order to develop the required intensity of the water pressure and to keep it permanently controlled during the test. It was fed periodically with an ordinary pump of the type commonly used in testing boilers.

The object of the air vessel was to avoid an irregular, or too rapid, rise of the pressure. Its volume was calculated accordingly. It was considered of interest to measure the quantity of water that entered into the air vessel while the test was in progress. Accordingly the vessel was made rather high, as compared with its diameter, and was provided with a glass gage similar to the gages commonly used in boilers.

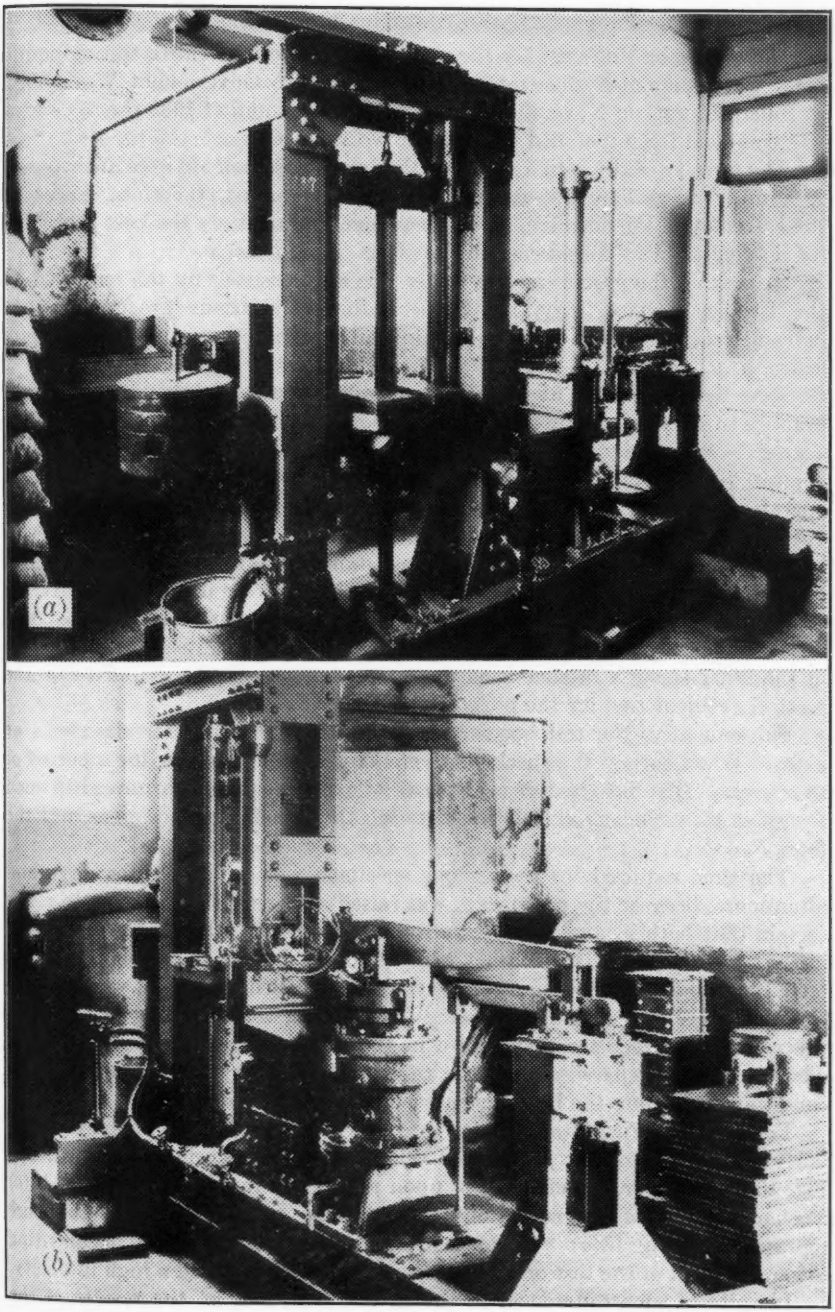

FIG. 12.—VIEWS OF THE LABORATORY WITH TESTING MACHINE FULLY ERECTED

Procedure and Significance of Tests

Detailed shop drawings for the apparatus and for the entire testing equipment were completed and transmitted to the Cairo Government Workshops, at Bulaq, Egypt, on November 2, 1937. In the autumn of 1939 the apparatus was completed and installed in the same workshops.

The novelty of the design was such that some adjustments were anticipated. A number of preliminary experiments were conducted, therefore, to verify the efficiency of the machine, on the one hand, and to study the best procedure for making the test specimens, on the other.

In making the specimens the writer was ably assisted by the engineers of the Bridges Service, Egyptian State Railways. Various procedures were investigated, the object being to obtain uniformity of texture and absence of leaks.

Two methods were finally adopted. The first was based on standard practice in making concrete. In the second method, the particles of the large aggregate were pressed into the layers of mortar after the latter had been deposited in the mold, precisely as in building a masonry dam. The entire operation was completed at such a speed, and with such efficiency, as to form one single, uninterrupted, and continuous process.

After the test, the specimens were left standing on a shelf until the following day, when the upper collar and the steel core were dismantled. At the same time the "skin" was removed from the exposed parts of the tested material. For the outer surface this was done by means of a steel brush, whereas in the inner space a ratchet fixed on a long flexible rod was found to be the most convenient tool for the purpose.

Subsequently, the test specimens were allowed to cure for six weeks or more. While curing, the specimens were kept thoroughly wet, for a period of two weeks. The program of each series of experiments was arranged in such a way as to avoid any correlation between the age of the specimens and the force F.

The time required for testing one specimen was at least three days and often more, because the pressure p_o was raised only very slowly, so as to make certain that both p_o and p_i were truly representative of the pressures existing in the pores in immediate contact with the outer and inner peripheries of the tested material. In this connection attention is called to Fig. 13 which shows three characteristic instances selected from among the diagrams representing the rate of the increase in pressure in the individual experiments. Similar diagrams were prepared for all the tests. They are typical in representing conditions regarding the interdependence between p_o and p_i.

For example, Fig. 13(a) shows a case in which the material appeared to be fairly permeable, so that p_i followed very rapidly after an increase in p_o. In Fig. 13(b), however, the effect of p_o upon p_i was less rapid, whereas Fig. 13(c) is characteristic of the conditions that are the extreme opposite to those represented in Fig. 13(a). In this last experiment, the pressure p_i began rising toward the end of the test only, when p_o had already attained a high intensity.

In spite of such differences in the values of p_o and p_i, the results of the individual experiments were quite consistent with each other. It follows,

therefore, that Eq. 10, which defines the relative effect of p_o and p_i upon p_a, is not only correct theoretically, but is also applicable to the case under review. As will be shown subsequently, the results attained by Rudeloff supply another proof in support of this conclusion.

Attention is also called, in this connection, to the diagrams shown in Fig. 14. The two experiments which they represent were conducted with the special object of verifying Eq. 10, and of ascertaining the effect of variations in the program of loading on the results of the test. These experiments were made generally similar, therefore, but the programs of loading—that is, the rates of increase of the pressure p_o adopted in the two cases—were essentially different. In spite of that, these experiments gave practically the same result. This may be of some importance, as it shows that the program adopted in filling the reservoir does not affect the uplift in the dam.

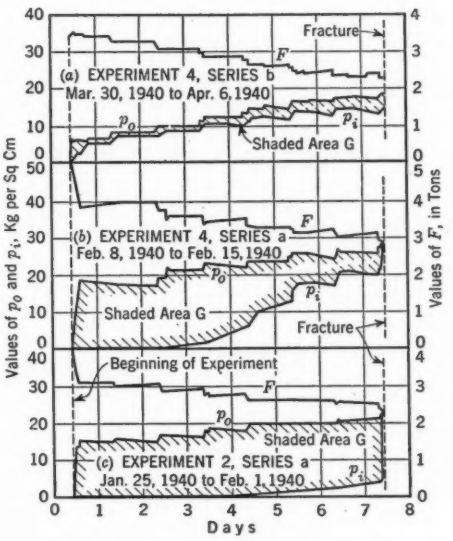
Fracture
F
(a) EXPERIMENT 4, SERIES b
Mar. 30, 1940 to Apr. 6, 1940
p_o
p_i
Shaded Area G
(b) EXPERIMENT 4, SERIES a
Feb. 8, 1940 to Feb. 15, 1940
Beginning of Experiment
(c) EXPERIMENT 2, SERIES a
Jan. 25, 1940 to Feb. 1, 1940
Values of p_o and p_i, Kg per Sq Cm
Values of F, in Tons
Days

FIG. 13.—RATE OF INCREASE IN PRESSURE

Another point, which was also rather important in the tests, was to ascertain the mechanical friction losses in the bearings of the lever systems and in other parts of the apparatus, in order to find the effect of friction on the force F. On several occasions during the experiment the machine was loaded with a special test specimen, which was generally similar to the standard specimen

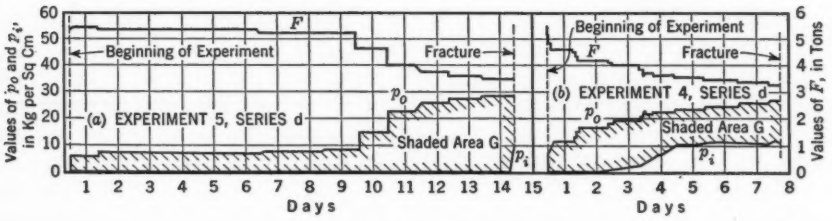

FIG. 14

but was filed across (before being placed in the test vessel) in about the same spot in which failure usually occurred in other specimens. No inner space was provided in this specimen. Consequently, the pressure p became instantly effective over the full section filed, as soon as the accumulator had been loaded with the corresponding number of plates.

It follows, therefore, that in this special experiment water had direct access to every point of the area that had been filed through. Thus, it was possible to compute the unreduced effect of the water pressure precisely. By comparing the resultant pressure so determined to the lever load required to balance it, the friction losses could be found easily.

The results of one of such tests are shown in Fig. 15. The experiments represented by circles are intended to reproduce conditions similar to a standard test in which a certain number of cast-iron weights are placed on the lever and

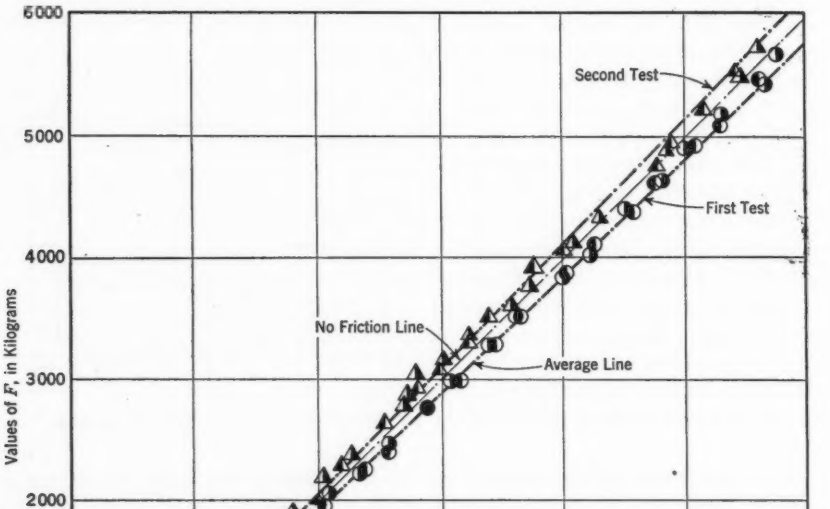

FIG. 15.—TEST TO DETERMINE THE EFFECT OF FRICTION

the pressure p_o is gradually increased until the micrometer shows that the top of the specimen begins moving upward. In this case the friction forces are directed in the same way as in a standard test; that is, they all tend to increase the force F. It is only logical, therefore, that the corresponding points are below the "no-friction line," the recorded pressures $p\,A$ being always greater than the calculated force F. This experiment was repeated many times and for various loads, first in the rising and then in the falling order, the entire set of tests being completed in 48 hr.

The tangent of the angle between the mean line drawn through these points and the vertical is calculated by the formula,

$$\tan \theta = \frac{\Sigma(x\,y)}{\Sigma y^2} \ldots\ldots\ldots\ldots\ldots\ldots\ldots\ldots (12)$$

which is derived from the "least-squares" principle.[28] The symbols y and x appearing in this equation represent the individual values of F, and the corresponding recorded pressures $p\,A$, which are used respectively as ordinates and abscissas in plotting curves in Fig. 15. The slope of the calculated line is 4% less than 1 on 1. Accordingly, a correction of 4% was introduced in all standard tests when calculating the value of F.

Although this might have sufficed for the main object of the tests, it was nevertheless considered of interest, as a matter of general information, to conduct another friction test, similar to the first but with the order of the operations reversed; that is, instead of loading the lever system and then gradually raising the water pressure (applying a load to the accumulator) as was done during the first test, the pressure was kept constant while the lever load was gradually increased, until the top of the test piece began moving downward.

It is clear that, in this case, the friction forces must act in a direction opposite to F. This was actually confirmed by the results, since all the points representing this test (triangles in the diagram) were found to be above the zero-friction line; the slope of the mean line, calculated for these points in the same manner as for the first friction test, was 2% steeper than 1 on 1.

The magnitude of the friction forces is different in this case, as compared with the first test, because the leather collar in the upper part of the container, which is shaped in section as an inverted **U**, is capable of developing different resistances depending on whether the legs of the **U** tend to become opened or closed. This means that the friction must depend on whether the test specimen moves upward or downward, being greater in the first case than in the second.

It was a satisfaction to observe that, in general, the friction forces were reasonably low, as compared with the main forces applied to the specimen; thus the friction correction introduced into the calculation of the force F was more in the nature of a refinement, than a substantial factor that may have influenced the conclusions. It is also of some importance to realize that the consistency of the results of the friction tests supplies another proof of the exactness of the calculation of the force F, because the deviations of the points appearing in Fig. 15, from their average line, give a measure of the precision of the results of this calculation. For example, the standard deviation for 42 points is found to be 41 kg, which is only about 1% of the average value of F. This is an independent confirmation of both the principle and the details of the method applied in calculating this force.

Apart from, and parallel with, the main experiments, a second series of tests were conducted in order to determine the porosity of the tested material. This porosity is required for finding the correction term n_e in Eq. 5.

[28] "Calcul de l'inclinaison des minarets," by S. Leliavsky, *Report on the Reconstruction of the Mosque Mohammed Aly Pasha*, Ministry of Wakfs, Cairo, 1931–1933, p. 95.

All these tests were made in the laboratory of the Bridges Service of the Egyptian State Railways. The specimens were taken from the test pieces used in the uplift experiments, after their failure. In all the cases, the porosity tests were repeated daily with the same specimen, for several months. According to the standard program this period was intended to be subdivided into four sections, as follows: (*a*) Specimen kept in water; (*b*) specimen kept in the room; (*c*) specimen exposed to the effect of wind and sun; and (*d*) specimen placed in the heater. Each operation was continued until the weight of the sample became constant. The results of two cycles, on seven samples, in series d, e, f, and g, are shown in Table 1.

TABLE 1.—RESULTS OF POROSITY TESTS

Sample and series	Critical pressure (kg per sq cm)	Time from failure to first test (hr)	Porosity (%) After Successive Stages of the Test						Total duration of test (days)
			First Cycle			Second Cycle			
			Room temperature	Exposure to sun	Placed in heater	Immersion in water	Room temperature	Placed in heater	
	(1)	(2)	(3)	(4)	(5)	(6)	(7)	(8)	(9)
A, d	27	4	8.2	10.7	15.6	1.3	14.1	....	112
B, d	32	2	6.6	8.7	....	1.5	8.2	14.3	105
C, d	8	2	7.9	8.5	....	0.6	8.5	14.5	100
D, d	16	40	9.6	11.3	18.7	....	....	....	99
E, e	12	11	3.1	3.7	7.0	....	....	....	35
F, f	30	2	8.3	6.1	10.3	....	....	....	114
G, g	15	2	3.5	5.7	12.0	....	....	....	67

In certain cases, it was believed of interest to reimmerse the dried samples. After a period of ten to twenty days in the tank, they absorbed almost the same quantity of water as when subjected to the exceedingly high pressure in the container; there was only 1% to 2% difference in the moisture content corresponding to either case. This result is instructive as it shows that the capacity of absorption is independent of the pressure applied.

The conclusion to be drawn from Table 1 tends to diminish the importance of the porosity on the stress analysis of dam sections—at least in so far as Fillunger's ideas on the subject are concerned. Fillunger believed[14] that the uplift factor was equal to the difference between the porosity of pure cement paste (when set) and the average porosity of the composite material (including cement, sand, and either gravel or stone). These two constants were supposed to represent respectively the coefficients n_a and n_v in Eq. 5. This conclusion was derived theoretically, assuming that the surface of fracture was an ideal plane which passed through the structural joint without intersecting any of the particles of either the fine or the coarse aggregates. In the light of more recent interpretation (which appears to be chiefly due to Hoffman[29]), the surface of rupture, being a surface of least resistance, is itself dependent on the structure of pores. In other words, the percentage area of the voids intersected by this irregular surface is greater than the volumetric porosity

[29] "Permeazioni D'Aqua e loro Effeti nei Muri di Ritenuta," by O. Hoffman, Milan, 1928, p. 28.

of the material. This upsets the Fillunger assumptions, because they are based upon the hypothesis of Delesse[30] according to which the superficial and volumetric porosities are the same (as is actually the case for a plane section). In 1930, Fillunger restated his theory in a paper read before the Second World Power Conference.[31] It is substantially the same theory as in his earlier publications, but instead of the common symbols of Cartesian algebra he introduces the vectorial notation, which makes the discussion rather more general, although this notation is less familiar to the average engineer.

The moisture content under normal conditions appears to be rather high in the writer's tests (see Table 1), leaving a very small margin for additional absorption. This means that when samples of the material destined for use in a dam are being tested in order to find their specific gravity, they already contain such a large percentage of water that their weight is almost the same as when fully saturated. In this connection attention is called to the porosity coefficients appearing in Col. 4, Table 1. It will be observed that these are the values that must be included in the second term of the uplift formula (Eq. 5), as representing the factor n_v. They are found to vary from 3.7% to 11.3%, with an average of about 7%.

These values are very low, corresponding to from only 2% to 4% of the total weight of the material. It appears, therefore, that a 7% effective volumetric porosity can be accepted as a sufficiently close and safe approximation for all cases. Of course, in a large structure the porosity would tend to be slightly greater than in a small block made of the same material; but then the efficiency of evaporation would be higher in the second case, so that a certain compensation must occur. Since the effect of this coefficient on the results of the stress analysis is indeed very small, there is every reason for accepting $n_v = 0.07$ as a sufficiently accurate basis for the calculation of stability. On the other hand, where the construction of a new dam is contemplated, the coefficient n_v can easily be determined experimentally before the profile is designed.

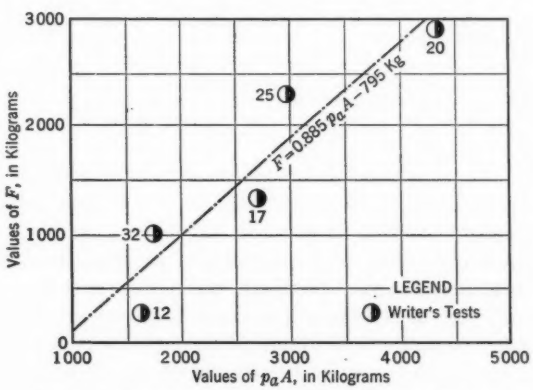

FIG. 16.—SERIES a; CAST DECEMBER 2, 1939, AND TESTED JANUARY 17 TO FEBRUARY 28, 1940 (SEE TABLE 2)

RESULTS

In describing the results of the tests in this section, the writer has followed the chronological order in which the conclusions were revealed. This was found advisable, because the object of and the particular problems to be

[30] "Procédé Mécanique pour Déterminer la Composition des Roches," by M. Delesse, *Annales des Mines*, 4 Série, Tome XIII, 1848, pp. 379-388.

[31] *Transactions*, 2d World Power Conference, Vol. 9, Paper No. 421, Berlin, 1930, p. 323.

solved by some of the later experiments originated from the analysis of the earlier tests.

The results of the first series of tests (referred to as series a) are shown in Fig. 16. The ingredients used in making these test pieces were: Broken Assuan granite and Assuan sand—both taken from the same quarries which were previously used in building and heightening Assuan Dam on the Nile River in Egypt. They were mixed with Portland cement from the Turah Factory, the proportion of cement to sand to stone (by volume of dry material) being 1.0:1.6:1.1. Descriptive data and comparison of results of twelve series of tests are presented in Table 2.

TABLE 2.—RESULTS OF TESTS ON TWELVE SERIES OF SPECIMENS

Series (see Figs. 16 to 27)	Number of tests	Method of preparation[a]	Cement (kg per cu m)	Water-cement ratio (by weight)	Type of coarse aggregate	Average age at test (days)	Uplift Coefficient		At Failure		Probable deviation of a point (tons)	Range of F-values (tons)	Ratio, $\frac{\text{Col. 11}}{\text{Col. 12}}$
							n_a	Probable error	Resistance (tons)	Average stress (kg per sq m)			
	(1)	(2)	(3)	(4)	(5)	(6)	(7)	(8)	(9)	(10)	(11)	(12)	(13)
a	5	C	530	0.40	Granite	70	0.885	0.098	0.795	5.24	0.215	2.597	0.083
b	5	S	290	0.93	Granite	68	0.916	0.030	0.138	0.88	0.069	2.673	0.026
c	5	C	500	0.50	Granite	101	0.954	0.093	0.458	2.91	0.204	2.630	0.078
d	6	S	280	0.72	Granite	137	0.991	0.040	0.474	2.98	0.115	3.611	0.032
e	9	C	300	0.58	Granite	68	0.871	0.038	0.845	5.37	0.173	4.174	0.041
f	7	C	470	0.40	Gravel	82	0.957	0.062	0 929	5.78	0.278	4.232	0.066
g	8	R	435	0.44	....	115	0 853	0.033	0.326	2.14	0.132	3.477	0.038
h	7	C	390	0.40	Fine gravel	218	0.967	0.080	0.978	6.26	0.344	4.030	0.085
i	9	C[b]	325	0.50	Granite	151	1.005	0.034	0.791	5.01	0.136	4.056	0.034
j	8	C	325	0.40	Granite	299	0.900	0.054	0.947	6.02	0.299	4.049	0.074
k	10	S[c]	330	0.68	Granite	179	0.888	0.016	0.404	2.58	0.078	3.500	0.022
l	16	C	300	0.43	Granite	126	0.858	0.017	1.058	6.64	0.111	4.284	0.026
Weighted mean	9.0	..	359	0.52	....	139	0.913	0.043	0.727	4.61	0.171	3.756	0.046

[a] "C" denotes "concrete"; "S" denotes "masonry"; and "R" denotes "mortar." [b] Concrete cast in two days. [c] Dressed masonry work.

The position of the points shown in Fig. 16, both in respect to each other and relative to the axes, leads to two fairly obvious conclusions: (*a*) A definite relation exists between the values of $p_a A$ used as abscissas and the corresponding values of F represented as ordinates, and (*b*) this relation is almost certainly linear. Although one single series of tests would not have been sufficient as a definite proof for these conclusions, the tests of that one series were, nevertheless, found to be corroborated by the results of all other tests, and as such were not devoid of interest—first, because this series confirmed the general principle of the experiments and proved the efficiency of the testing apparatus; and, second, because it showed that the coefficient n_a was constant. It was also apparent from Fig. 16 that the slope of the line representing the coefficient n_a was very steep.

In finding the slope in question (which was the main problem to be solved by these experiments) it was believed advisable, in order to exclude the personal equation, to adopt the same method for all the series tested; and with this object in view the following simple formula embodying the "least-squares"

principle was used:

$$n_a = \frac{N \Sigma(x\,y) - \Sigma x\, \Sigma y}{N \Sigma x^2 - (\Sigma x)^2} \quad \ldots\ldots\ldots\ldots\ldots\ldots (13)$$

in which x and y are the coordinates of the points and N is their total number. Also,

$$z = \frac{\Sigma(x\,y)\, \Sigma x - \Sigma x^2\, \Sigma y}{N \Sigma x^2 - (\Sigma x)^2} \quad \ldots\ldots\ldots\ldots\ldots\ldots (14)$$

The values of the constants defining the average line were calculated by means of Eqs. 12 and 13, applied to each of the series tested. For series a (Fig. 16) the coefficient n_a was found to be equal to 0.885 (see Table 2). This is considerably more than is usually assumed in designing dam profiles (excluding exceptional cases, of course), but it tends to approach the limit suggested by Professor Terzaghi. On the other hand, such a high numerical value completely disproves the Fillunger theory, because the volumetric porosity of the materials tested was only about 0.15.

One other point that Fig. 16 seems to demonstrate is the effect (on the results of the tests) of the ratio of the areas occupied, respectively, by the binding material and the particles of the aggregate appearing on the surface of rupture. In fact, when the average line is taken as a basis of comparison, the points with higher ratios move to the left. Had this been a general rule, it might have been interpreted in two ways—the higher percentage of the stone surface may have meant either a larger uplift factor n_a or a smaller resistance z. In both cases, the primary cause would have lain in the different microstructural characteristics of solid material as compared with a surface of contact between two different substances.

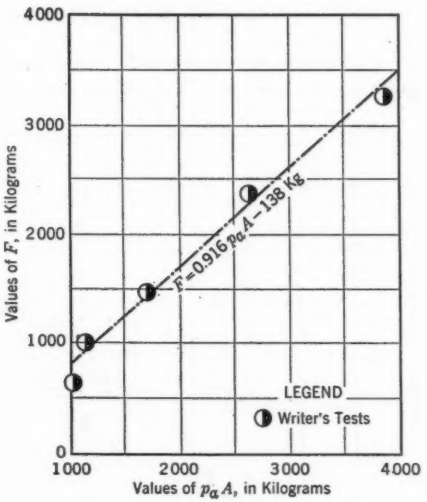

FIG. 17.—SERIES b; CAST JANUARY 17, 1940, AND TESTED MARCH 9 TO APRIL 9, 1940 (SEE TABLE 2)

In order to explore this subject further, two parallel sets of experiments (see series f and g, Table 2) were conducted, with and without coarse aggregate, respectively.

The proportion of cement in the first series of specimens was rather high. It was considered advisable, therefore, to use a relatively small proportion of cement in the second series (1.0:2.7:3.3), the ingredients being the same as in series a. The results are shown in Fig. 17.

The characteristics of the line in Fig. 17 confirm the results of series a; that is, the relation which the data represent is obviously linear and the slope of the line is again very steep. In spite of the difference in the proportion

of cement the factor n_a calculated for series b, the same as in series a, is found to be equal to 0.916, which is only 3% greater than series a (see Table 2).

Apart from that, Fig. 17 is also interesting in that it reveals a case in which the individual points are very close to the calculated line—0.6754 times the standard deviation. (The term "deviation" is used in preference to "error," for in this case the cause of the differences between the observed and theoretical values lies in the irregularities in the texture of the material tested, and not in the inaccuracies of the measurements.) Should the "probable" deviation be taken as a measure of the dispersion of the points, regardless of its physical significance (which, with such a small number of entries, is naturally very limited), the following values may be of interest:

Series	Probable deviation (tons)
a	0.215
b	0.070

For other series, the calculated standard deviation tended to approach the conditions shown in Fig. 16, and therefore Fig. 17 must be considered exceptional. No physical reason is given to explain the exception, the cause being most probably a matter of chance.

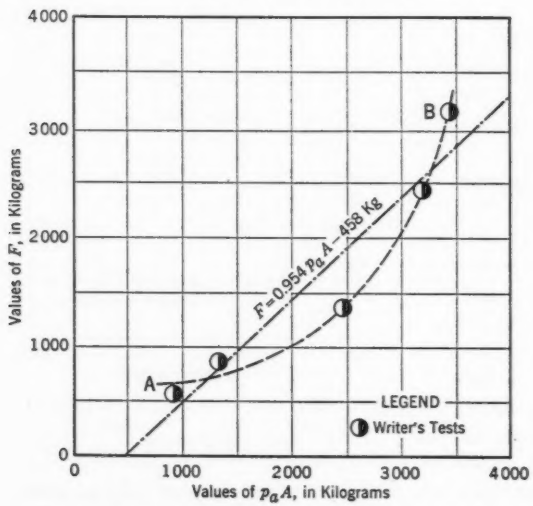

FIG. 18.—SERIES c; CAST MARCH 4, 1940, AND TESTED MAY 22 TO JULY 1, 1940 (SEE TABLE 2)

In series c, Fig. 18, the conditions of the test were the same as series a and b except that the aggregate proportion was 1.0:1.1:2.2. The results are similar to those demonstrated by Figs. 16 and 17 except that these data might also be interpreted as representing a curve, AB. This was the only case in any series in which such a definite curve could have been drawn through the points obtained; but, even here, the curve was absurd because the slope of end B would have been much steeper than 1 on 1 (which was obviously impossible since n_a could not have been greater than 100%).

In series c, as in all other series, the variation was linear and $n_a = 0.954$ was computed as the effective porosity (see Table 2).

In order to avoid conditions such as those that produced Fig. 18, and also to study the effect of extending the data into negative values of F, the number of specimens in all subsequent series was increased. For instance, series d,

Fig. 19, comprised as many as twelve experiments. The larger number of plotted points in Fig. 19 offers a more strict proof of the main conclusions derived from the earlier tests—namely, that there is a systematic relationship between the product $p_a A$ and F, that the relationship is linear, and that the slope of the calculated line is rather steep.

It must be observed, however, that, although this general result was supported by the twelve experiments represented in Fig. 19, the calculation of the average line was based on six records only, because the "weight" of the other six points (shown by dotted circles in Fig. 19) was believed to be less; in other words, the data for these experiments were considered to be less

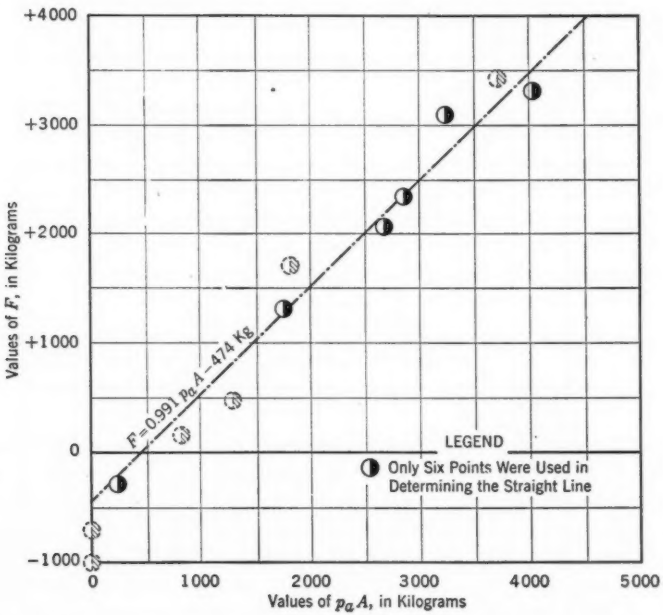

FIG. 19.—SERIES d; CAST APRIL 14 AND 15, 1940, AND TESTED JULY 9 TO SEPTEMBER 23, 1940 (SEE TABLE 2)

certain than those for the other experiments. In regard to the two points in Fig. 19, at $p_a A = 0$ (mechanical tensile tests with no hydraulic pressure, conducted with identical specimens, and using the same machine), it was found that the time factor affected the conditions of failure of the material to a far greater extent than many engineers are inclined to accept. The importance of this factor was discovered almost accidentally during the test run for series d. During one period the machine was stopped with the specimen still in position, with a constant load. After a lapse of about 15 min the specimen failed suddenly. This conclusion concerning the time factor refers chiefly to short periods. If the duration of the test exceeds two or three days, the effect of the rate of loading appears to vanish, or is almost imperceptible.

The next test under similar conditions was conducted more slowly and consequently the breaking tensile limit was found to be lower. Thereafter it was realized that, in order to obtain consistent results, the duration of a purely mechanical tension test must be the same as that of a standard uplift experiment—about three days. This rule was adopted for all subsequent series and the results were found to be quite reliable.

Four other tests in the same series were also considered as being less precise than the remainder, because the specimens broke at night. (Subsequently,

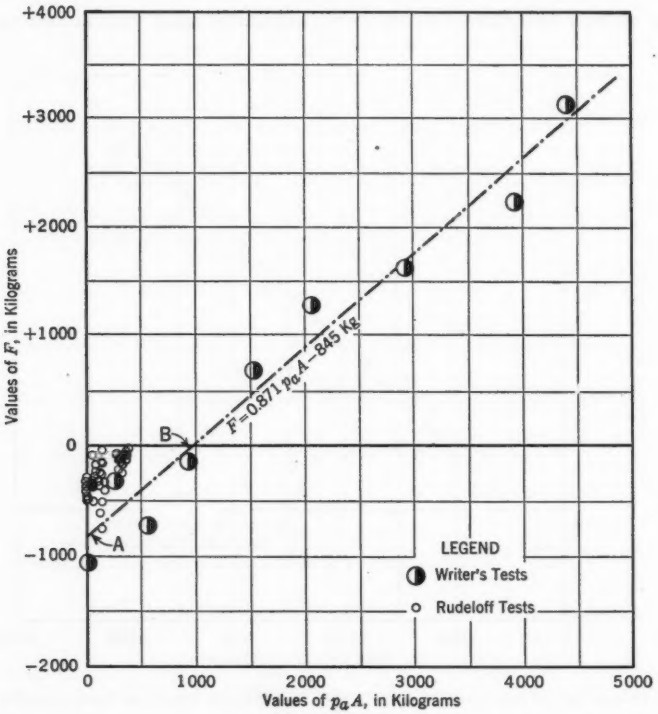

FIG. 20.—SERIES e; CAST AUGUST 7 AND 10, 1940, AND TESTED SEPTEMBER 28 AND NOVEMBER 4, 1940 (SEE TABLE 2)

orders were issued to remove two loads from the accumulator, before closing the room for the night, and to replace them again in the morning. Failures at night were thus avoided.) The four corresponding points were calculated from the last values of p_i recorded in the log book during the day, and were shown by dotted circles in the diagram; but, of course, they were not included in the calculation of the line. Nevertheless, they fell close to the latter.

At this stage of the investigation, in comparing the results determined, the most striking point appeared to lie in the fact that the coefficients n_a calculated for various groups were found to be almost the same. It was decided therefore to alter the ingredients in the new series in such a way as to

ascertain whether the coefficient in question was affected by the nature (if not by the quantities) of the materials used in making the specimens. With this object in view a coarser sand (obtained by washing the sand that had been used before) was used in making the fifth series.

The results of these tests are illustrated in Fig. 20. Although the coefficient n_a is found to be still high (0.871), it is nevertheless slightly lower than the average calculated for the first four groups, which amounts to 0.937 (see Table 2). Thus, by removing the finest particles of the sand it appeared that the uplift was reduced by about 7%, as compared with the average for other series.

To illustrate the importance of the range of conditions under which uplift experiments are to be made, it was decided to plot, on any one of the diagrams representing the writer's experiments, the tests of Rudeloff and Panzerbieter.[13] While Fig. 20 was selected for this purpose, any of the other series might have been used instead with equivalent results.

The coordinates of the small circles, which are used to represent the Rudeloff tests, are computed as follows: The values of the mechanical forces F (which, in these experiments, are all negative) are read off directly from the tables appearing in the published report. The values of $p_a A$ are calculated in accordance with the particular arrangement adopted in each series of these experiments. For the arrangement shown in Fig. 3(a), the formula used is

$$p_a = p_i (1 - \Delta) \ldots\ldots\ldots\ldots\ldots\ldots\ldots (15a)$$

and, for the arrangement in Fig. 3(b), the formula is

$$p_a = p_o \Delta \ldots\ldots\ldots\ldots\ldots\ldots\ldots\ldots (15b)$$

Substituting in Eqs. 15 the breaking values of p_o and p_i published by Rudeloff, the required values of p_a are found in a form that represents his experiments in the writer's graphs. It is obvious from Fig. 20 that the forty-four points so obtained could not have been used for developing empirical formulas or for finding physical constants, because the range of variation of the coordinates was too narrow. The small circles are arranged in a meaningless group, which cannot be defined as a curve or a straight line. In other words, the effect of accidental circumstances that caused the dispersion of points was too large as compared with the range of variation of the main factors; and the entire set of Rudeloff's records was equivalent, in the weight of the information it conveyed, to only one point in Fig. 20.

In the investigation reported herein the conclusions are based on the difference between the individual tests, and not on their average value; and, therefore, in spite of all precautions that had been taken in designing the writer's apparatus and planning his experiments, greatest care and utmost diligence had to be exercised subsequently in making the specimens, and in handling them, in order to reduce the dispersion of the points. Only the most competent, experienced men, fully realizing the importance of regularity in their work, should be employed in such experiments, to insure consistent results. In fact, it was observed that, whenever changes in laboratory assistants occurred, the dispersion of the points immediately became greater, and

two or three series had to be discarded for this reason. The maximum ratio of probable deviation to range of force that can be allowed reasonably in such tests is 1:10. Beyond this ratio the results should be considered as untrustworthy.

Another point, calling for comment in regard to Rudeloff's tests, as they are represented in Fig. 20, is that the ratio of the outer to the inner diameters of the test pieces used in this investigation (the test pieces in question were made hollow as in the writer's tests) was 6.43. When this value is used in Eqs. 15 it will be found that, for Fig. 3(*a*), $p_a = 0.25\, p_i$; and, for Fig. 3(*b*), $p_a = 0.75\, p_o$.

Thus, with equal pressures, the effect in the second case (Fig. 3(*b*)) was three times as much as in the first arrangement (Fig. 3(*a*)), in spite of which the points (which included both arrangements) fell close to each other in Fig. 20. In other words, in order to equalize the conditions that caused failure, the inner pressure had to be raised to an intensity three times as high as that of the outer pressure. In this respect the agreement between test and formula is found to be fully satisfactory.

This goes a long way to show that the formula assesses correctly the relative effect of the two pressures p_o and p_i; and the principle upon which it is based, therefore, is not only correct theoretically, but is also consistent with actual facts.

Another illustration of the importance of a wide range of conditions is afforded by tests reported by Woodard,[12] and by the experiment conducted at Bull Run Dam. The physical interpretation of these experiments was intended to be based on the difference between the conditions that cause the failure of the specimen in the testing machine of the common type (that is, without uplift pressure) and effect of uplift pressure acting alone (without any additional mechanically developed stress). In Fig. 20, these two cases correspond to points A and B, in which the average line intersects, respectively, the vertical and horizontal axes. A glance at Fig. 20 will show that the section of the line defined by these two points is relatively very short. As they are too close to each other, minor errors in determining the position of these two points experimentally must largely affect the slope of the line drawn through them, the calculated value of n_a being uncertain and possibly misleading. Had the same precautions been taken in preparing the test pieces and in conducting the test proper as in the writer's experiments, the ratio of the probable deviation to the range of forces would still have been high. For instance, under conditions similar to those of Fig. 20, this ratio would have been 1:5 (as compared with 1:25 in the writer's test). There is little wonder, therefore, that the results of the earlier uplift tests did not supply the solution to the problem. More precision might have been attained by repeating the test several hundred times, and then taking the averages of the results so obtained; but even so, with two points only, it would have been impossible to obtain a clear picture of the true relation between the variables, and many factors affecting the experiment (such as the predominant effect of time in the mechanical-tension test) might have remained undetected, thus aggravating the inaccuracy of the final calculation.

Fig. 21 includes two series of tests, referred to as groups f and g, respectively. In representing them on the same chart the object was to facilitate comparison because, in this case, the problem was concerned with the difference (if any) in the results obtained with two mixtures. To ascertain the effect of the large particles, these two series were made identical in regard to the composition, except as to one point—the presence in one mixture, and the complete absence in the other, of the coarser aggregate (gravel).

The ingredients were proportioned in such a way as to provide for nearly the same quantity of cement per cubic meter of finished material in both cases.

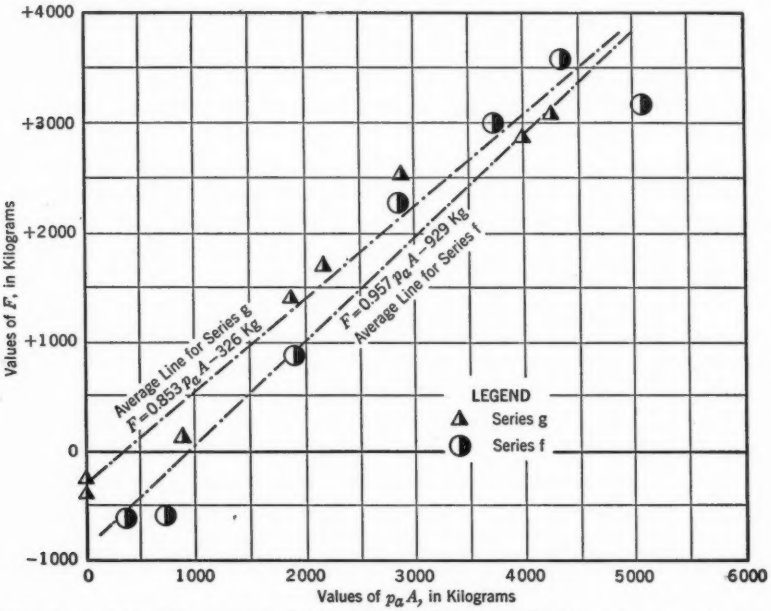

FIG. 21.—SERIES f (CAST OCTOBER 13, 1940, AND TESTED DECEMBER 17, 1940, TO JANUARY 20, 1941) AND SERIES g (CAST OCTOBER 16, 1940, AND TESTED JANUARY 26 TO FEBRUARY 18, 1941) (SEE TABLE 2)

In interpreting Fig. 21 attention is called to what was stated in connection with the first group (Fig. 16), on the possible action of the coarser aggregate, which was supposed to be affecting either the uplift factor (in which case the slope of the two lines in Fig. 21 should have been different) or the resistance of the material against tension. In the latter case the lines would have been parallel, but at some distance from one another.

The results of the tests, as represented in Fig. 21, appear to show that these two effects exist simultaneously, but that they are combined in such a way that they often escape attention because, in a sense, they balance each other. The addition of the aggregate appears to increase the factor of uplift (as one might naturally have expected) but, at the same time, the resistance of the material against tension is also increased, which causes the two groups of the experimental points to be superimposed upon each other.

On the other hand, the differences in the uplift coefficients are found to be so small as to be largely influenced by accidental causes, so that the true conclusion to be derived from Fig. 21 is that the effect of the aggregate is rather of secondary importance.

Another seven specimens were later prepared from fine gravel instead of the coarse gravel that had been used in mixing group f. They were referred to as series h. As the results of these tests were very close to the average conditions, they do not call for any particular remark.

The next series tested (series i) was intended to reveal the effect (if any) of the interruptions in the casting process. Following a special program, nine test pieces were prepared, a lapse of time of twenty-four hours being allowed between the casting of the lower parts of these specimens, and the completion of their top portions. The surface of interruption was located about halfway between the lower and the upper linings fixed to the specimens (middle part of the critical section).

Of all the tests this series gave the highest coefficient. In fact, the value of n_a calculated for this group of specimens, by means of the same formula that had been used before, was found to exceed the theoretical limit—unity. The excess (0.005) was small, however, as compared with the probable error of the coefficient (0.034), and it is interpreted as being the result of the fluctuations of sampling and unavoidable errors. This excess, therefore, seems consistent with the general theory on which the experiments are based.

On the other hand, the fact that the effective area for this particular series was found to be greater than for all other specimens may tend to show that interruptions in the casting of concrete create critical conditions for the uplift pressure, as they do in regard to many other structural characteristics of the material. This conclusion, although based upon relatively small numerical differences, is supported nevertheless by the fact that the surfaces of rupture in these specimens tended to lie closely to the surfaces of interruption. In other groups the surfaces of rupture were irregularly distributed over the height of the critical portion of the broken test pieces.

The eight specimens belonging to series j were intended to supply more information about the effect of the size of the sand particles. With this object in view a sand coarser than that in series e was selected in making them. The reduction in the value of the uplift coefficient that had been observed in series e, and had apparently been due to the removal of the smaller grains in that series, did not seem to have been increased or maintained when the medium particles were also removed and large particles alone were present. The value of such conclusions is very much reduced, however, by the fact that the numerical differences, upon which they are based, are of the same order of magnitude as the probable error.

All the groups thus far described were prepared according to one of the two standard methods ("concrete" or "masonry") discussed under the heading, "Procedure and Significance of Tests" (see also Table 2, Col. 2). On the other hand, the system adopted in making the test pieces of group k differed substantially from all that had been done before. An objective attempt was

made, in this case, to duplicate the methods commonly used in building masonry dams.

The critical sections of these test pieces were built in alternate courses, consisting of three to four pieces of granite laid on approximately horizontal beds. Consequently, the size of the individual stones was larger than in all earlier series, and each stone was dressed roughly so as to reduce the thickness of the joints and to minimize the quantity of mortar per unit volume of the finished material. To make the stones fit more accurately, the critical sections of the test pieces were built before placing the cast-iron collars in position.

Although the value of the coefficient of uplift deduced from these experiments was again very near to the average ($n_a = 0.888$), the points representing the individual tests were closer to the average line than in the earlier series (see Fig. 22).

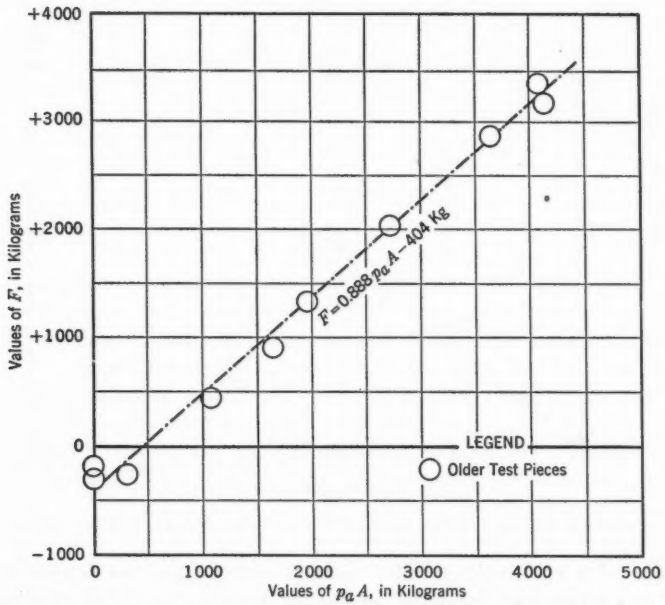

FIG. 22.—SERIES k; CAST FEBRUARY 2 AND 3, 1942, AND TESTED JULY 15 TO AUGUST 25, 1942 (SEE TABLE 2)

Consequently, with this particular method of construction the results of the experiments were more regular and, being less affected by accidental circumstances, conformed more strictly to the theoretical conditions of an ideal case. The reason for the better results obtained with this series might be twofold:

(*a*) The horizontal beds may have presented more uniform conditions for the filtering of water and for the development of the uplift pressure; and

(*b*) The dressing of the stones (such as it was) and the greater regularity in the joints may have resulted in more uniform tensile resistances.

In concluding the program of experiments described in this paper, a set of tests was run with a greater number of specimens. The range of ages of these

specimens was increased in such a way as to accentuate the effect of the time factor, should such effect be actually present. Accordingly, a series of sixteen test pieces was cast from August 8 to August 10, 1942; four of them were tested from September 28 to October 28, 1942; and the remaining twelve were tested from December 15, 1942, to February 12, 1943.

As demonstrated by Fig. 23, no difference whatever can be detected between the earlier and later experiments, and the entire series is fully satisfactory in so far as regularity of results is concerned. The coefficient n_a is equal to 0.858 and the probable error of this factor is 0.024.

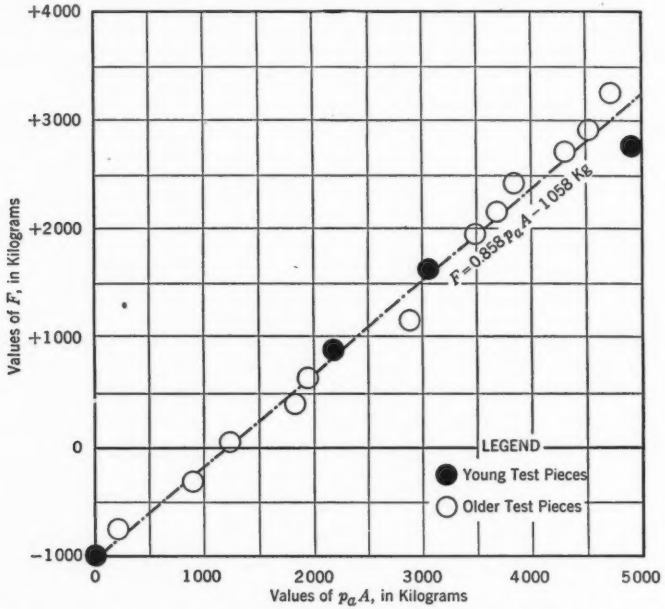

FIG. 23.—SERIES 1; CAST AUGUST 8 AND 10, 1942, AND TESTED SEPTEMBER 28, 1942 TO FEBRUARY 12, 1943.

In spite of a relatively smaller cement percentage, the tensile breaking limit for this series was found to be greater than for all other groups. This was most probably due to the more intensive ramming and to a lower water-cement ratio. Also, the workmen had acquired a greater ability in preparing the test pieces, so that a generally better class of material was obtained.

In addition to the data in Table 2 that have already been discussed, this table also contains information such as the water-cement ratios, which are calculated in the usual way (by weight).

In regard to the values in Col. 11, Table 2 (probable deviations of a point), and Col. 8, Table 2 (probable errors of the coefficient n_a), it should be realized that these terms are used conventionally. Little physical significance can be attributed to statistical parameters based upon so small a number of points as that which is contained in each series taken individually (with the possible exception of series 1 which comprises sixteen tests). These values must be

interpreted as representing results of certain well-known arithmetical operations. As such they are of some interest as a means for comparing the dispersion of the points in the different series, provided the word "probable" is not taken too literally.

Another point to be mentioned in connection with Table 2 concerns the tensile resistances of the material. The average breaking intensity of the tensile unit stress for all the series tested was found to be about 4.6 kg per sq cm, whereas for the experiments in which only mechanical tension was used it was about 3 kg per sq cm. Should individual series be considered, the two values will be found to be very close. For instance, in series 1 the tensile resistance calculated from the average line was 6.6 kg per sq cm, whereas under mechanical tension alone it was found to be 6.5 kg per sq cm.

The fact that the resistance of the material determined under mechanical tension was actually similar to, or less than, that which was indicated by the uplift tests explained much concerning the physical cause of the failure of the test pieces. At the instant when fracture occurred in the uplift tests, the material was still found capable of withstanding considerable tension (at least as much as when tested under mechanical tension only). This is evidence that the specimen had not yet cracked. At that instant the uplift force had already reached its full value, and consequently it was concluded that the channels through which water penetrated into the material were natural "pores"—not failure cracks.

The point may be explained further by reference to the special "friction tests" presented in Fig. 15. In comparing this diagram with the several curves of uplift tests, it will be observed that in Fig. 15 the average line passes through the origin of coordinates, whereas in all other cases it intersects the axes at some distance from the origin. This is due to the fact that the abscissas of the points of the standard uplift tests are always greater than those of the corresponding points of the special "friction tests." In other words, it was always found necessary to raise the pressure to a higher intensity in the uplift tests than with the same force in the "friction tests." The obvious reason for this condition was that in "friction tests" the specimen was filed crosswise beforehand, so that during the experiment its two parts were held together by the application of the force F only. In uplift tests, on the other hand, the two parts formed one solid block, and, therefore, in addition to the force F, there was also the resistance of the material to be overcome by the uplift pressure. Had a crack existed in the "uplift test" the results must have been the same as in the "friction test."

Thus, although the principle of these experiments was compatible with both the old and the new schools of thought, the numerical results tended to show that the modern group of theories supplied the true explanation of the phenomenon (in so far, at least, as the tests themselves were concerned).

Elsewhere, in this paper, the writer has shown that the differences in the values of the uplift factors obtained for various series were surprisingly small. The possibility was also explored that the entire body of tests might not be analyzed as a single composite group of records. This approach would have appeared unorthodox if it had been advanced in the earlier part of the investiga-

tion; but it suggested itself later, as a natural conclusion derived from the numerical results of the tests. (The differences between the individual values of n_a calculated for each series are of the same order of magnitude as the corresponding "probable" errors. This means that these differences may be attributed to accidental circumstances.)

It should be realized, however, that the value of z in the different series (the ultimate resistance of the specimens against tension) is not, and cannot

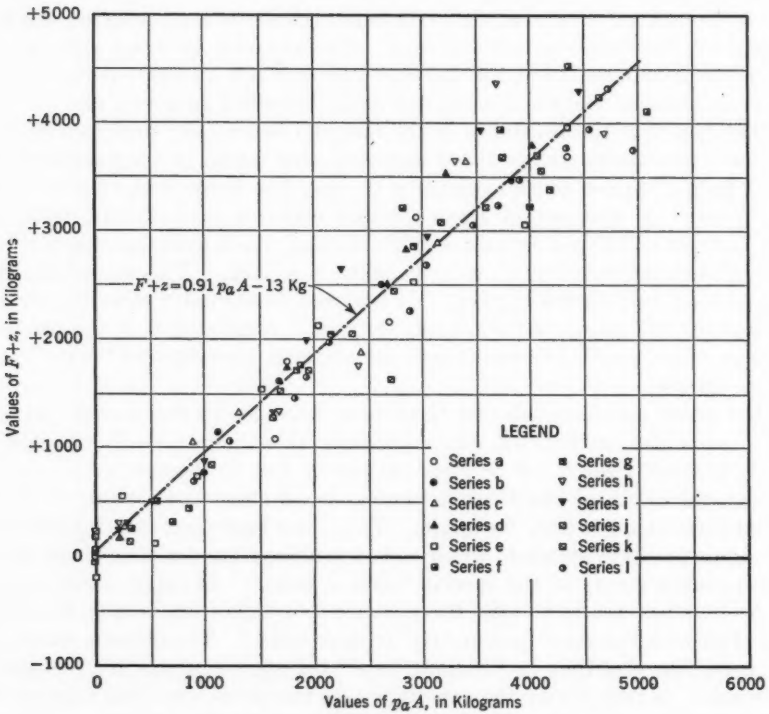

FIG. 24.—COMBINATION OF NINETY-FIVE EXPERIMENTS

be, the same (*a*) for all the various proportions of cement used, (*b*) for the differences in the periods of curing, and (*c*) for differences in the water-cement ratios. Consequently, had the tests relating to different series been superposed upon each other as they occurred, the differences in z would have exaggerated the dispersion of the points and obscured the issue. Therefore, they were removed prior to combining the tests in a single group, and values of $F + z$ were plotted as ordinates instead of F.

The diagram so obtained (Fig. 24) may also be conceived as being derived from Figs. 16 to 23, by using different origins of the vertical scale for different groups in such a way that all the calculated lines intersect at the origin.

The parameters of the new average line calculated for all the ninety-five points taken together, by means of the same formulas as before (Eqs. 13 and

14), are: $z = 0.013$ ton and $n_a = 0.91$. The constant z is so small that, to all intents and purposes, the average line may be assumed to pass through the new origin of coordinates (see Fig. 24). This tends to prove that the principle upon which the adjustment of the ordinates is based is generally reasonable.

The standard deviation for the new combined diagram is 0.305 ton, which is almost the same as the average of the values computed for the individual series (see the line of weighted means in Table 2).

On the other hand, the advantage of the composite diagram, as compared with Figs. 16 to 23, is that, with almost the same standard deviation, it contains a much larger number of observations. From the viewpoint of the statistician a record comprising ninety-five entries may be regarded as very meager, but it represents, nevertheless, a substantial improvement on the individual series which contain only five observations. Thus, it is possible to apply some statistical methods of investigation to the composite group, which can never be applied to the smaller individual groups, considered separately.

The correlation method was adopted for the statistical analysis of the composite data, with the following results:

Description	Correlation	Regression
Coefficient	$r = 0.974$	$b = 0.91$
Probable error	$\Delta r = 0.0035$	$\Delta b = 0.014$
Approximate ratios	$\frac{\Delta r}{r} = 1{:}300$	$\frac{\Delta b}{b} = 1{:}70$

These coefficients appear to be very satisfactory. With the number of experiments available, therefore, the curve in Fig. 24 can be accepted as final, and the value $n_a = 0.91$ can be considered as a fairly reliable average, the corresponding probable error being only about 1.5%. This value of b was checked by the least-squares method. In a preliminary investigation, with seven groups only, the same computation gave $n_a = 0.92$. These seven groups have also been combined without excluding z (that is, using the values of F and $p_a A$ as in the individual diagrams) and almost the same results were obtained.

Fig. 24 has also served as a general basis for detecting the presence of systematic errors, if any. Two main sources of such errors may be anticipated: (*a*) The effect of time; and (*b*) the effect of the difference $p_o - p_i$.

(*a*) *Time.*—Great care was exercised in arranging the test program so as to avoid any apparent or concealed association between the age of the specimens and the main mechanical characteristics of every individual test. Additional evidence was gathered confirming the fact that the time factor had no influence on the test results. The first step in the check analysis was to compute the deviations from the average line, for every test, by the formula:

$$\Delta y = y - n_a x + z \quad \ldots\ldots\ldots\ldots\ldots\ldots (16)$$

in which x and y are the coordinates of the point; and n_a and z are the constants of the average line.

The correlation and regression coefficients between these ninety-five deviations and the age of each of the ninety-five specimens tested were then computed. The result ($r = 0.059$ and $b = 0.00025$ ton per day) is obviously negative. The coefficients are so small as to warrant the conclusion that the tests were not influenced by the time factor.

(*b*) *Difference* $p_o - p_i$.—The effect of the difference $p_o - p_i$ is to create compressive stresses in the material at right angles to the geometrical axis of the specimen and to the main tensile stress that causes its failure. Since the critical breaking value of the tensile stress in question may be influenced by the compressive stress at right angles to it, an effort was made to ascertain whether the results of the experiments were actually affected by the magnitude of the difference $p_o - p_i$.

Messrs. Fillunger and Terzaghi have demonstrated beyond any reasonable doubt that the effect of an interstitial hydraulic pressure upon the resistance of a porous solid is negligible, so long as this pressure is equally distributed over the walls of the pores. Since the existing evidence confirming this statement is conclusive, it follows, in so far as the present tests are concerned, that the ultimate resistance of the test piece is not affected, in all the cases in which $p_o = p_i$. However, the cases in which p_i is smaller than p_o remain to be investigated. When this happens the ring-shaped part of the specimen is subjected to stresses similar to those in a pipe connected to a boiler. Since these stresses are compressive, z could be smaller for higher values of $p_o - p_i$.

The solution of this problem had been attempted previously by Rudeloff who undertook a special set of tests in which an India rubber envelope was placed around the specimen, thereby preventing water from penetrating into the pores. Since in his experiments the pressure was applied on only one face of the wall of the test piece (see Fig. 3) the effect of the ring stresses, in the sense referred to herein, could have been more pronounced than in the tests reported by the writer. In any case, the ring stresses were present and were the same as in the main tests, but there was no water in the pores and, consequently, no interstitial pressure. Hence, the entire effect, had it been found to exist, would have been attributable to the ring stresses alone.

Such special experiments were conducted by Rudeloff for every type of material and testing device used in these experiments; but the present concern is with the apparatus shown in Fig. 3(*b*) because it is mechanically similar to the device used by the writer. Similar to the writer's apparatus, the main stress causing failure in the Rudeloff apparatus is tension, but the secondary ring stress is compression.

The average results obtained by Rudeloff are represented graphically in Fig. 25. The average line is calculated by the least-squares method; its slope (regression coefficient) is found to be 0.034 (or 0.002 ton per atmosphere) which is too small to be detected. Clearly, the effect of compressive ring stresses on the ultimate resistance against tension is negligible.

In the writer's experiments, had the effect of the difference $p_o - p_i$ on z been present, it would have resulted in points with larger values of $p_o - p_i$ tending to move upward, the average line being taken as the basis for com-

parison. Then, the deviations Δy computed by Eq. 16 must have been related to, and affected by, the differences $p_o - p_i$. This possibility was explored analytically, the results being: Correlation coefficient $r = 0.068$; and regression coefficient $b = 0.0016$. (In order to represent the regression coefficient as an absolute number, the deviations Δy were divided by the sectional areas of the specimens.)

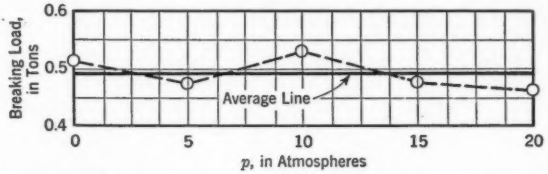

FIG. 25.—RESULTS OF RUDELOFF'S EXPERIMENTS (NO INTERSTITIAL PRESSURE)

Rudeloff's results are thus confirmed. The correlation and regression coefficients are found to be so low that the existence of an interdependence between $p_o - p_i$ and the resistance of the material z is definitely disproved. Although the physical interpretation of this conclusion does not directly concern the subject of the present inquiry, it may be suggested as a most plausible explanation that in Mohr's graphical criterion the lines are curved, as assumed by certain authors, and not straight. This would substantially reduce the effect of the transverse compressive stresses on the resistance against the main tension stresses, particularly in the negative zone, close to the vertical axis of Mohr's diagram.

To complete the description of the writer's tests the following observations should be recorded:

(*a*) The deviations of the ninety-five points from the average line agreed in a general manner with the bell-shaped Gaussian frequency curve.

(*b*) Darcy's coefficient calculated for the various test pieces varied within rather wide limits and did not indicate any correlation with the uplift factor or with any other physical constant. An approximate value of this coefficient can be obtained from the equation

$$K = \frac{\log_e r}{2\pi H} \frac{\int_0^T Q\, dt}{\int_0^T (p_o - p_i)\, dt} \quad \ldots\ldots\ldots\ldots\ldots\ldots (17)$$

in which $\int_0^T Q\, dt$ is the total quantity of water percolating through the specimen during the test and $\int_0^T (p_o - p_i)\, dt$ is found from a diagram in which p_o and p_i are plotted against time (see shaded area G in Figs. 13 and 14).

(*c*) In most cases the failure occurred abruptly, without any warning, but certain specimens suddenly became very leaky an appreciable time before failure occurred. The state of the material during this period (which varied from 2 min to 30 min) could be described as "agony." Although capable of withstanding a large amount of tension, the walls of the specimen allowed water

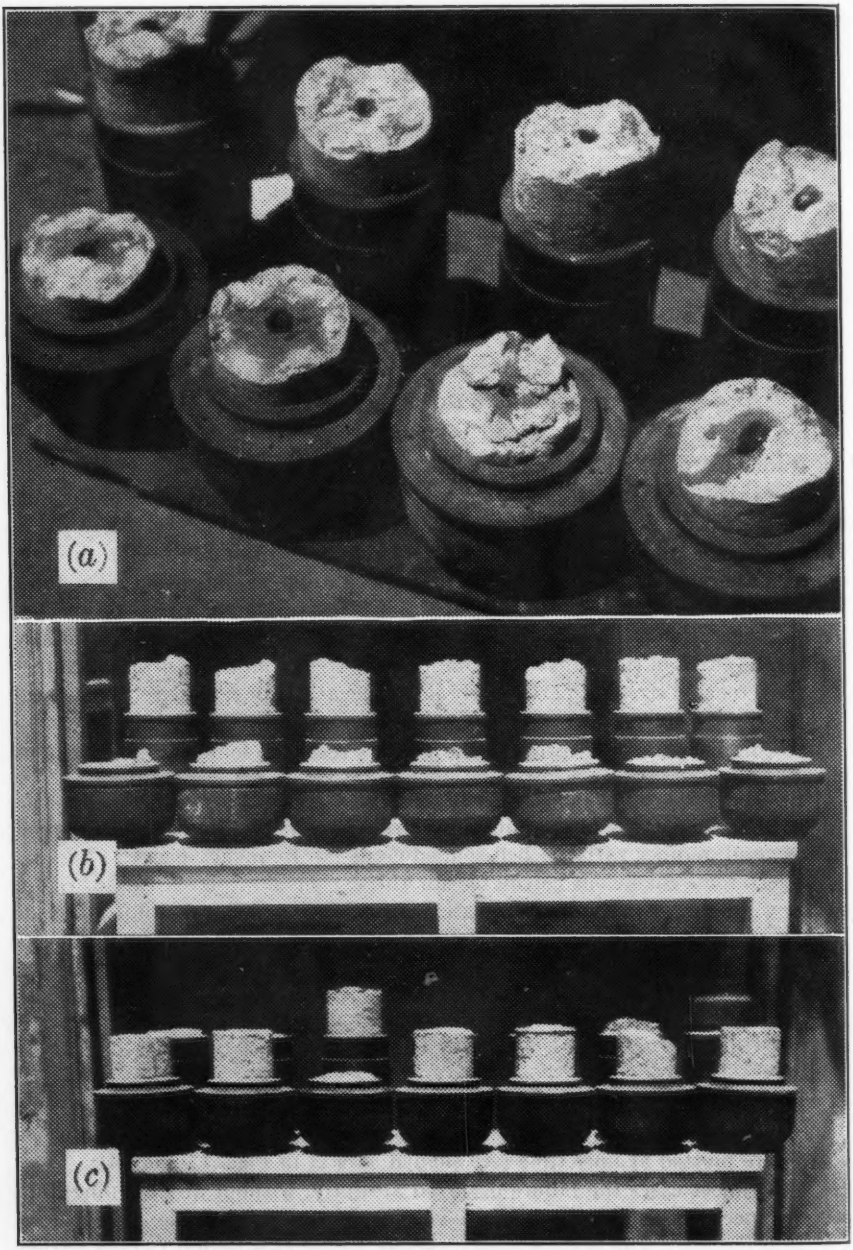

FIG. 26.—VIEWS OF TEST SPECIMENS AFTER FAILURE

to pass freely through them, and the deformations became sometimes excessive. A somewhat similar phenomenon had been observed earlier by Kelen.[16]

Some views of the test pieces after failure are reproduced in Fig. 26.

Conclusions

Although the investigation began with the analysis of individual diagrams, some of which contained five points only, it was later found possible to construct a combined chart having ninety-five points to support the empirical relations which it represented. The conclusions thus derived may be summarized as follows:

(1) Uplift was shown to exist, sufficient to cause failure, by tension, of perfectly solid and sound material. This was true despite the fact that, at the moment this failure occurred, the block was subjected to a mechanically developed compression of variable intensity which tended to oppose the effect of uplift. Sometimes this pressure intensity was as much as 18 kg per sq cm, which is equivalent to a height of superimposed masonry of about eighty meters.

(2) It may be even more important to know that the uplift force was proved to be a measurable quantity, subject to certain laws and capable of analysis by laboratory experimentation—perhaps even more directly measurable than some of the forces that are usually believed to be known, such as the impact effect. This conclusion deserves emphasis since there are many who draw pessimistic comparisons between the alleged "uncertainty" of the uplift effect in dams, as opposed to the precision of the stress analysis in steel framework.

(3) The average value of the "effective superficial porosity" n_a, which was the main unknown to be determined by these experiments, was found to be 0.91, with a probable error equal to 0.014.

(4) Within narrow limits (about three times the standard error) this coefficient appears to be dependent upon certain physical characteristics of the ingredients used in making the material. Such influences must be considered as secondary, however, because the value of the coefficient changes only very slightly, and the causes of such very small changes might be accidental. For practical purposes the coefficient n_a can be assumed to be almost constant.

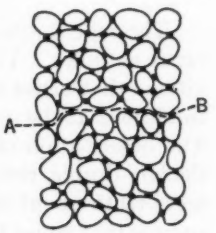

Fig. 27

(5) In general, n_a is much greater than the porosity of the material tested (regardless of the assumption under which the latter may be determined), which completely disproves the ideas of Fillunger, and strongly supports the theory of Terzaghi. According to the latter theory, large values of the coefficient n_a are explained by the fact that the microstructure of a porous solid (see Fig. 27) is an agglomeration of a large number of small blocks, with points of contact so minute as to belong to a still higher order of minuteness. In three series of observations Terzaghi determined values of n_a, respectively, as 0.97, 0.97, and 0.998. The surface of rupture (line AB, Fig. 27) is an irregular surface of "least resistance" which passes almost entirely through the micro-

voids. This seems to supply a possible explanation of the very large difference between n_a and the porosity, observed in the writer's tests.

(6) Although the logic underlying the writer's experiments is compatible with any reasonably evolved theory concerning the characteristics of the uplift pressure, the results derived contain evidence that favors the modern school of thought on this subject.

(7) The factor n_a is found to bear no relation to Darcy's coefficient of filtering, which means that, other things being equal, leakage and sweating cannot serve as evidence that uplift forces are present. It follows that the division of dams into "leaky" and "dry" categories is illusory in so far as uplift is concerned.

(8) On the other hand, if a dam which is known to have been "dry" should suddenly show signs of becoming "leaky," this might be a very strong warning that an "agony period" is impending. Leakage must be prevented or reduced as much as possible in any case, because it may be the cause of the gradual deterioration of the material.

(9) The coefficient n_a is independent of the stress to which the material is subjected (linear relationship between $p_a A$ and F). It is also independent of several other factors which, apparently, might have affected it, such as the cement and water percentages, the temperature, the rate of rise of the pressure, and the consecutive order of loadings and pressures applied.

(10) The increase in the weight of material due to the penetration of water into the pores is less than might have been expected because, in the natural state of the material, the pores are already partly filled with water. The water that may be added, over and above the normal moisture content, represents an average of about 7% of the volume of the materials tested. Therefore, this is the value which, according to the modern views on the subject, must be subtracted from n_a in order to obtain the final, net value of the uplift factor.

(11) It follows that the uplift factor, by Eq. 5, is $0.91 - 0.07 = 0.84$. The writer recommends 85% as a fairly accurate average round figure.

Suggestions for Further Research

The experiments described in this paper should serve as a starting point for further studies. The writer's interpretation of the tests is based upon the conditions that cause the rupture of the specimen, which indeed are the critical conditions to be taken into account in evaluating the safety of a project. The deformation of the test piece could be recorded throughout and, in particular, during the final period before rupture. Such records might reveal more truth about the mechanics of failure and help in explaining the circumstances that cause the "agony" conditions.

To study deformations would require certain alterations in the mechanical details of the apparatus. Had time and money been available, it was the writer's intention to proceed with these additional tests, but under the conditions extant during World War II this was impossible, and some appreciable time will elapse before such results can be obtained and analyzed.

Acknowledgments

The officials of the Egyptian Government have encouraged the experiments described in this paper and have helped in the investigation. In particular the writer is indebted to H. E. Hurst, Director General of the Physical Department, Ministry of Public Works, for valuable assistance and advice, and to the past and present staff in the writer's office, for help with the experiments and computations.

He wishes also to record his admiration for the excellent work done by the Cairo Government Workshops in making the testing machine, according to his drawings, and the expert assistance of the engineers of the Bridges Service, Egyptian State Railways, who helped in preparing the test specimens.

DAMS ON POROUS MEDIA

BY MOHAMED AHMED SELIM,[32] ASSOC. M. ASCE

SYNOPSIS

When a dam or weir is constructed on a porous foundation, some of the water will percolate underneath it toward the downstream side. The purpose of this paper is to present experimental data on the uplift forces, acting on a dam built on porous media, and on the accompanying loss of head. The electric-analogy method of analysis was chosen because of its simplicity, economy, and reliability. Different conditions of substrata and various combinations of simple horizontal floors and cutoff walls are considered.

INTRODUCTION

Two empirical methods have been used in designing dams on porous foundations—the first that proposed by W. G. Bligh[33] and the second that proposed by E. W. Lane,[18] M. ASCE.

The Bligh Theory.—Mr. Bligh[33] treated the course of seepage beneath a dam on the assumption that the water follows a path along the line of contact of the dam foundation (including the cutoff walls) with the foundation material. This contact between dam and foundation is sometimes called the line of creep, and the method may be called the line-of-creep method. The head is assumed to drop along a straight line from the headwater to the tailwater (if there is any) in proportion to the distance along the line-of-creep. According to the Darcy law for a fluid of unit dynamic viscosity,

$$Q = K \frac{h\,A}{L} \ldots\ldots\ldots\ldots\ldots\ldots\ldots\ldots\ldots\ldots (18)$$

in which Q is discharge in cubic feet per second; h is head in feet; A is gross cross-sectional area in square feet; K is a dimensional coefficient; and L is length of path in feet. From continuity, $Q = A\,V$; hence,

$$L = K \frac{h}{V} \ldots\ldots\ldots\ldots\ldots\ldots\ldots\ldots\ldots\ldots (19)$$

For a given size distribution of material, there appears to be a definite maximum velocity, V_m, at which water can emerge below the dam without carrying away the foundation material, thus causing failure of the structure. Combining this value of V_m with K, which also depends on the material, to form a new constant, $c = \frac{K}{V_m}$, Eq. 19 becomes

$$L_m = c\,h \ldots\ldots\ldots\ldots\ldots\ldots\ldots\ldots\ldots\ldots (20)$$

[32] Lecturer "A," Irrig. Dept., Faculty of Eng., Fouad First Univ., Giza, Egypt; formerly Instructor in Mech. Eng., Univ. of California, Berkeley, Calif.

[33] "The Practical Design of Irrigation Works," by W. G. Bligh, D. Van Nostrand Co., New York, N. Y., 1910.

in which L_m is minimum safe length of travel path (length of creep), and c is a constant depending on the foundation material. Mr. Bligh assumed that horizontal length of contact was just as effective as a vertical length. In other words, for a dam with horizontal floor of length b and an upstream cutoff wall of depth d_1:

$$L_m = b + 2\,d_1 = c\,h \ldots\ldots\ldots\ldots\ldots\ldots (21a)$$

For a dam with horizontal floor of length b, and upstream and downstream cutoff walls of depths d_1 and d_2:

$$L_m = b + 2\,d_1 + 2\,d_2 = c\,h \ldots\ldots\ldots\ldots\ldots\ldots (21b)$$

The Lane Theory.—The Bligh theory was accepted widely because of its simplicity until, in 1934, Professor Lane introduced his empirical "weighted-creep" theory. In this theory it is assumed that the line of flow will follow the line of contact between a dam and its foundation; but the vertical contact is considered more effective than the horizontal contact, and the coefficient c is different from that given by Mr. Bligh. After a study of the designs of a large number of dams in the United States and of the failure of some others, Professor Lane recommended that a unit horizontal length of contact be considered to be one third as effective as a unit length of vertical contact.

For a dam with horizontal floor of length b and upstream cutoff wall of depth d_1:

$$L_m = \frac{b}{3} + 2\,d_1 = c_1\,h \ldots\ldots\ldots\ldots\ldots\ldots (22a)$$

For a dam with a horizontal floor of length b and upstream and downstream cutoff walls of depths d_1 and d_2:

$$L_m = \frac{b}{3} + 2\,d_1 + 2\,d_2 = c_1\,h \ldots\ldots\ldots\ldots\ldots\ldots (22b)$$

From Eqs. 22,

$$\frac{\text{Loss of head per unit length of vertical}}{\text{Loss of head per unit length of horizontal}} = 6 \ldots\ldots\ldots (23)$$

Throughout this paper, this ratio has been called the "efficiency of the vertical."

R. B. Khosla has developed quite an ingenious method of solving problems in this field. For comparison, some of his results are mentioned in this paper; but, because of limited space, the reader is referred to the original source[34] for more complete information.

Theory of the Flow of Water Through Homogeneous Porous Media

Flow may be either laminar or turbulent depending for the most part upon the resistance offered by the material through which the liquid is flowing. The resistance of a porous medium composed largely of grains smaller than gravel is sufficient to prevent turbulent flow if natural channels are prevented

[34] "Design of Weirs on Permeable Foundations," by R. B. Khosla, N. K. Bose, and E. Taylor, *Publication No. 12*, Central Board of Irrig., Simla, India, September, 1936.

from enlarging. Hence, for ordinary practical purposes, only laminar flow need be considered.

For two-dimensional flow, the general differential formula for the steady flow of water through homogeneous materials has the form of a LaPlace equation:

$$\frac{\partial^2 p}{\partial x^2} + \frac{\partial^2 p}{\partial y^2} = 0 \ldots\ldots\ldots\ldots\ldots\ldots\ldots\ldots (24)$$

Eq. 24 is obtained by substituting the Darcy law of flow—

$$u = k\frac{dp}{dx} \quad \text{and} \quad v = k\frac{dp}{dy} \ldots\ldots\ldots\ldots\ldots\ldots (25)$$

—into the equation of continuity

$$\frac{\partial u}{\partial x} + \frac{\partial v}{\partial y} = 0 \ldots\ldots\ldots\ldots\ldots\ldots\ldots\ldots (26)$$

in which p is the pressure, k is a permeability coefficient which includes the effect of viscosity, and u and v are the two components of the discharge per unit gross area in the directions x and y, respectively. Eq. 26 is dependent on the following conditions: (1) The voids are completely filled with water; (2) the porous medium is uniform in all directions; (3) the quantity of flow entering any small element of volume is equal to the quantity flowing out of this element of volume during any given time; and (4) both water and material are incompressible.

Eq. 24 represents two families of curves, intersecting at right angles, which are usually referred to as the flow lines and equipotential lines (or lines of equal head loss). Four methods are in common use for the solution of Eq. 24; namely—(*a*) the mathematical method, (*b*) the graphical method, (*c*) the method of model experiments, and (*d*) the electric-analogy method. The writer's paper is confined to the electric-analogy method. For treatment of the other methods, beyond the scope of the present paper, the reader is referred to the work of W. Weaver;[19] A. Casagrande,[35] M. ASCE; E. W. Lane and F. B. Campbell, Members, ASCE, and W. H. Price;[36] R. Rhoades and M. N. Sinacori,[37] Assoc. M. ASCE; M. G. Ionides;[38] and B. F. Reltov.[39]

Electric-Analogy Method

The method introduced by N. N. Pavlovsky[40] in 1920 is more advantageous than other methods because: (1) It is simple, economical, and rapid; (2) it

[35] "Seepage Through Dams," by A. Casagrande, *Journal*, New England Waterworks Assn., June, 1937, pp. 131–172; see also *Bulletin No. 209*, Harvard Univ., Cambridge, Mass.

[36] "The Flow Net and the Electric Analogy," by E. W. Lane, F. B. Campbell, and W. H. Price, *Civil Engineering*, October, 1934, pp. 510–514.

[37] "Pattern of Ground-Water Flow and Solution," by Roger Rhoades and M. N. Sinacori, *The Journal of Geology*, November-December, 1941, pp. 785–794.

[38] "A Method of Determining the Flow-Net in Soil Seepage," by M. G. Ionides, *Engineering*, August 30, 1935, pp. 211–212.

[39] "Electrical Analogy Applied to Three-Dimensional Study of Percolation Under Dams Built on Pervious Heterogeneous Dams," by B. F. Reltov, *Transactions*, 2d Cong. on Large Dams, Washington, D. C., Vol. V, 1936, pp. 73–85.

[40] "Motion of Water Under Dams," by N. N. Pavlovsky, *Transactions*, 1st Cong. on Large Dams, Stockholm, Sweden, 1933, Vol. 4, pp. 179–192.

gives results that correspond to the exact theoretical solution, even in complicated examples where the theoretical solution is very difficult or even unreliable; and (3) it can be used in certain instances to investigate cases of nonhomogenous media. Development of this method was possible because of the analogy between the Ohm law for flow of electricity and the Darcy law for the flow of water in granular material. Thus, if the components of the current are i_x and i_y, in the x-direction and y-direction, respectively, the equation of continuity is

$$\frac{\partial i_x}{\partial x} + \frac{\partial i_y}{\partial y} = 0 \ldots\ldots\ldots\ldots\ldots\ldots\ldots\ldots (27)$$

but, according to the Ohm law,

$$i_x = C\frac{\partial E}{\partial x} \quad \text{and} \quad i_y = C\frac{\partial E}{\partial y} \ldots\ldots\ldots\ldots\ldots\ldots (28)$$

in which C is a coefficient and $\partial E/\partial x$ and $\partial E/\partial y$ are the components of voltage gradient in the x-direction and the y-direction, respectively. Hence, substitution of Eq. 28 into Eq. 27 gives the following LaPlace equation:

$$\frac{\partial^2 E}{\partial x^2} + \frac{\partial^2 E}{\partial y^2} = 0 \ldots\ldots\ldots\ldots\ldots\ldots\ldots\ldots (29)$$

The similarity of Eqs. 24 and 29 is the basic principle by which the electric-analogy method is applied. Thus, if an electrolyte is placed in a shallow tank in which a set of boundary conditions are introduced which are analogous to a certain hydraulic system, the flow lines of electricity and the equipotential lines can be plotted. The details of this procedure have been described previously by L. F. Harza,[41] engineers of the Bureau of Reclamation,[42] and many others. A complete description of the general methods used need not be repeated. Certain improvements in the technique of the experimental equipment have been developed, however, and are described in the section to follow.

Experimental Equipment and Technique

In the study reported herein, all experiments were conducted in a wooden tank (40½ in. by 31 in. by 2½ in. deep) coated inside with a waterproof nonconductive paint. In most electric-analogy experiments made in the past, a Wheatstone bridge and earphones have been used to detect the equipotential lines. When these experiments were conducted for a considerable time, however, the experimenter often experienced difficulty in recognizing the null points. Instead of using the Wheatstone bridge and earphones in the present experiments a vacuum-tube voltmeter was used. This instrument was equipped with six accurately calibrated scales covering various ranges to a maximum of 16 v. It was also equipped with a 10,000-ohm resistance and could be used to measure the voltage at any point in the tank without using an appreciable amount of current. During an experiment the various equi-

[41] "Uplift and Seepage Under Dams on Sand," by L. F. Harza, *Transactions*, ASCE, Vol. 100 (1935), pp. 1352–1385.

[42] "Model Studies of Penstocks and Outlet Works," *Bulletin No. 2*, U. S. Bureau of Reclamation, Denver, Colo., 1938, pp. 107–118.

potential lines were detected by means of a probe attached to a pantograph. For example, if the 90% line was to be plotted, the voltmeter was maintained at 10 v, and the probe was moved along that potential curve to various closely spaced points corresponding to a voltmeter reading of 9 v.

Fig. 28(*a*) shows the arrangement of the pantograph, equipped with probe and pencil, and the experimental tank. As an illustration, the setup for mapping the equipotential lines under a dam with only a horizontal floor is shown. In this example, the sides of the tank upstream and downstream from the base of the dam were covered with copper plates. Therefore, current flows through the electrolyte from one plate to the other in a manner analogous to that of the flow of water from the upstream bed to the downstream bed.

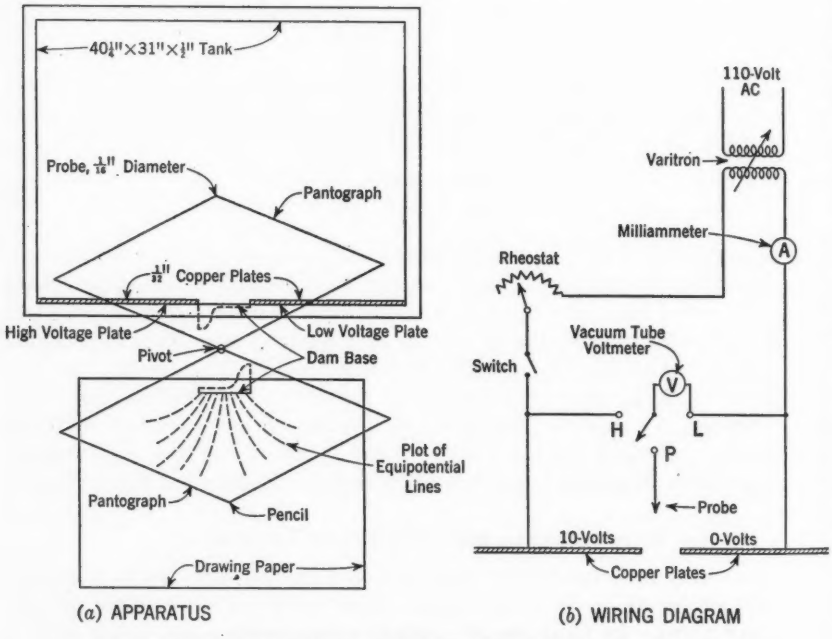

FIG. 28.—EXPERIMENTAL SETUP FOR PLOTTING EQUIPOTENTIAL LINES FOR A DAM WITH A HORIZONTAL FLOOR AND NO CUTOFF WALLS

In mapping the flow lines for the dam shown in Fig. 28(*a*), the position of the copper plates and that of the nonconductive surfaces was reversed—that is, the base of the dam was constructed of copper plate and the entire perimeter of the tank was covered with copper, with the exception of that part of the sides which represented the upstream bed and downstream bed of the stream. The equipotential lines which are mapped with this latter arrangement then represent the flow lines of the system.

Fig. 28(*b*) shows the general wiring diagram of the apparatus. Alternating current (120 v, 60 cycles) was used in the experiments to avoid polarizing effects of the electrodes. Using a variable-potential transformer, a potential of only

10 v could be maintained on the circuit. The supply of current was regulated by a rheostat and measured by a 200 milliammeter. The control switch shown in Fig. 28(*b*) was set on "L" (low) when "zeroing" the voltmeter, set on "H" (high) when the over-all voltage between high and low was selected, and set on "P" (probe) while mapping the equipotential lines. The over-all voltage for determining the potential distribution was measured by placing the probe very near the high voltage plate. This latter step was necessary to eliminate oxidizing effects on the plate.

The base length of all model dams was maintained at 6 in. The model floor and cutoff walls were constructed of $\frac{1}{32}$-in. copper plates when the flow lines were mapped and of $\frac{1}{32}$-in. bakelite plates when the potential lines were mapped. The electrolyte, $\frac{3}{4}$ in. deep, was a solution of copper sulfate in distilled water acidulated with sulfuric acid (50 g of copper sulfate and 25 cc of sulfuric acid per 5 gal of water). In plotting the flow lines, the large current required by the relatively large copper area necessitated a dilution of the solution to half the foregoing concentration.

Probable Sources of Error

The sides of the tank represent streamlines for the flow system. Consequently, the ends of the tanks should be semicircular, since it can be proved mathematically that the streamlines approach semicircles at a relatively large distance from the dam. However, the influence of the sides of the tank was very small for the uplift and head losses considered. Also, the experimental results with this tank, whose breadth was 5.2 times the dam width, approached very closely the results calculated mathematically for a dam on a homogeneous material of infinite depth. The possible errors may be summarized as follows: Boundary effects, copper plates not flush with the surface at the tank sides, difference in thickness between bakelite and copper plates, evaporation of the electrolyte, and possible defects in the electric instruments.

Experimental Results of Studies on Loss of Head

Dams on Permeable Strata of Infinite Depth.—Four cases were investigated in this category: (I) Horizontal floor and upstream cutoff wall, (II) horizontal floor and upstream cutoff wall at one twelfth of the base width from the upstream toe, (III) horizontal floor and sheet-pile cutoff walls at both upstream and downstream toes, and (IV) horizontal floor only.

Case I. Dam with a Horizontal Floor and Upstream Cutoff Wall.—Fig. 29(*a*) shows a typical example of the plot of flow lines and equipotential lines for the set of experiments in which the depth of cutoff wall d_1 was varied to give values of the ratio, b/d_1, between 1 and 6. These data are summarized in Table 3. The reading at point A, Col. 2 (see Fig. 29(*a*)), represents the percentage of head remaining to be lost after subtracting the percentage lost along the upstream face of the sheet piling. Similarly, the reading at point B (Cols. 3 and 4) represents the percentage of head remaining to be lost by the horizontal floor. Subtraction of the reading at point B from 100 gives the percentage of head that is lost because of the cutoff wall (that is, lost in the

length $2\,d_1$). Losses of head per unit length of path, expressed as percentages of h, are given in Cols. 5 and 6, subscripts v denoting the depth of cutoff wall, or vertical path and subscript b denoting the horizontal path. In other words, h_v (Col. 5) $= \dfrac{100 - \text{Col. } 3}{d_1}$; and h_b (Col. 6) $= \dfrac{\text{Col. } 3}{b}$. In Cols. 7 and 8, Table 3, the efficiency of the vertical is computed as the ratio $\dfrac{\text{Col. } 5}{\text{Col. } 6}$.

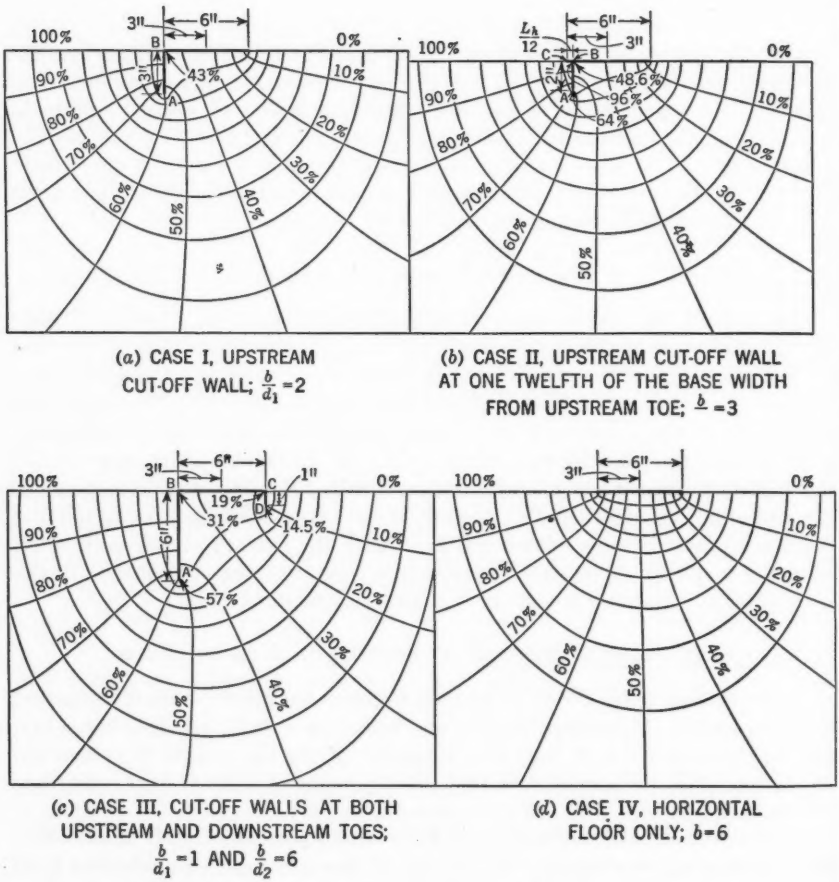

(*a*) CASE I, UPSTREAM CUT-OFF WALL; $\frac{b}{d_1}=2$

(*b*) CASE II, UPSTREAM CUT-OFF WALL AT ONE TWELFTH OF THE BASE WIDTH FROM UPSTREAM TOE; $\frac{b}{}=3$

(*c*) CASE III, CUT-OFF WALLS AT BOTH UPSTREAM AND DOWNSTREAM TOES; $\frac{b}{d_1}=1$ AND $\frac{b}{d_2}=6$

(*d*) CASE IV, HORIZONTAL FLOOR ONLY; $b=6$

FIG. 29.—FLOW LINES AND EQUIPOTENTIAL LINES. DAM WITH HORIZONTAL FLOOR ON PERMEABLE MATERIAL OF INFINITE DEPTH

Case II. Dam with Horizontal Floor and Upstream Cutoff Wall at One Twelfth of the Base Width from the Upstream Toe.—A typical example of a plot of the flow line and equipotential lines is shown in Fig. 29(*b*), and the data are summarized in Table 4. Similarly to Table 3, the reading in Col. 2, Table 4, is that part of the head which remains to be lost by the cutoff wall

and the remainder of the horizontal floor. The loss of head along the upstream part of the horizontal floor ($b/12$ in this case) is 100—Col. 2.

From Table 4(b) it is obvious that the efficiency of the vertical cutoff wall is decreased by moving the wall slightly toward the downstream toe. From an

TABLE 3.—READINGS FOR CASE I (SEE FIG. 29(a)), PERMEABLE STRATUM OF INFINITE DEPTH
(Expressed as Percentages of h)

$\frac{b}{d_1}$	(a) Loss of Head			(b) Comparative Loss Between Vertical and Horizontal Lengths			
	Point A	Point B		Loss Per Unit Length of Path		Efficiency of the Vertical	
		Selim	Khosla	h_a	h_b	Selim	Lane
(1)	(2)	(3)	(4)	(5)	(6)	(7)	(8)
6	76	68.5	64	31.5	11.42	2.75	6.0
3	68.5	49.5	51	25 25	8.25	3.06	6.0
2	60	43	42	19 0	7.16	2.65	6.0
1.5	60	35	....	16.25	5.84	2 79	6.0
1.2	60	33.7	....	13.30	5 61	2.38	6.0
1.0	60.2	31.6	....	11.40	5.27	2.17	6.0

economical point of view, the cutoff wall should be as close as possible to the upstream toe of the dam.

Case III. Dam with Horizontal Floor and Sheet-Pile Cutoff Walls at Both Upstream and Downstream Toes.—A typical example of a plot at the flow

TABLE 4.—READINGS FOR CASE II (SEE FIG. 29(b)), PERMEABLE STRATUM OF INFINITE DEPTH

$\frac{b}{d_1}$	(a) Loss of Head[a]			(b) Comparative Loss Between Vertical and Horizontal Lengths		
	Point C	Point A	Point[b] B	Loss per Unit Length of Path[a]		Efficiency[c]
				h_a	h_b	h_a/h_b
(1)	(2)	(3)	(4)	(5)	(6)	(7)
6	92	72	62.8	29.2	11.8	2.47
3	96	64	48.6	23.7	8.77	2.70
2	96.5	59	38.5	19.33	7.0	2.76

[a] Expressed as percentages of h. [b] Compare with Col. 3, Table 3. [c] Efficiency of the vertical, h_a/h_b; compare these values with Col. 7, Table 3.

lines and equipotential lines is shown in Fig. 29(c). A relatively large number of combinations of b/d_1 and b/d_2 were investigated and the data summarized in Table 5.

The general effect of the downstream cutoff wall on the readings at points A and B for a particular b/d_1-ratio can be found quickly by comparing the top line where $b/d_2 = \infty$ with the other b/d_2-ratios. In an effort to summarize these data for the designer, Col. 11, Table 5, was computed to give the efficiency

of the cutoff wall under various values of b/d_2 and b/d_1. These values show the fallacy of using excessive lengths of downstream cutoff wall, because in such cases the horizontal length of the floor has relatively little effect as part of the so-called path of percolation.

TABLE 5.—READINGS FOR CASE III (SEE FIG. 29(*c*)) PERMEABLE STRATUM OF INFINITE DEPTH

$\frac{b}{d_2}$	(*a*) Loss of Head[a]				(*b*) Comparative Loss Between Vertical and Horizontal Lengths					
					Loss per Unit Length of Path[a]			Efficiencies h_v/h_b		
	Point A	Point B	Point C	Point D	h_v upstream	h_v downstream	h_b	Upstream[b]	Downstream[b]	Total[c]
(1)	(2)	(3)	(4)	(5)	(6)	(7)	(8)	(9)	(10)	(11)
					(*a*) $b/d_1 = 1.0$					
∞	60.2	31.6	0	0	11.40	0	5.27	2.17	0	....
6	57.0	31.0	19.0	14.5	11.50	19.00	2.0	5.75	9.50	7.0
3	57.8	35.0	25.0	19.6	10.82	12.50	1.67	6.50	7.50	7.0
2	59.5	39.5	35.0	25.0	10.08	11.67	0.75	14.40	15.50	15.0
1.5	59.5	43.0	39.5	29.5	9.50	9.875	0.584	16.40	16.90	15.0
1.2	62.0	47.0	44.0	32.0	8.84	8.80	0.50	17.68	17.60	15.0
1.0	64.0	51.0	49.0	37.0	8.16	8.19	0.33	24.7	24.7	25.0
					(*b*) $b/d_1 = 1.2$					
∞	60.0	33.7	0	0	13.30	0	5.61	2.38	0	....
6	57.0	34.5	17.0	15.0	13.10	17.00	2.92	4.50	5.83	5.0
3	58.4	39.0	31.0	23.0	12.20	15.50	1.34	9.10	11.57	10.0
2	65.0	44.0	39.0	28.0	11.20	13.00	0.834	13.42	15.60	14.0
					(*c*) $b/d_1 = 2.0$					
∞	60.0	43.0	0	0	19.00	0	7.16	2.65	0	....
6	70.0	47.0	26.0	16.0	17.70	26.00	3.50	5.05	7.43	6.0
3	67.0	52.0	39.0	27.0	16.00	19.50	2.17	7.38	9.00	8.0
2	69.0	55.0	45.0	31.0	15.00	15.00	1.67	9.00	9.00	9.0
					(*d*) $b/d_1 = 3.0$					
∞	63.5	49.5	0	0	25.25	0	8.25	3.06	0	....
6	70.0	54.5	30.0	20.0	22.75	30.00	4.08	5.57	7.34	6.0

[a] Expressed as percentages of h. [b] Efficiency h_v/h_b of the upstream and downstream cutoff walls. [c] Efficiency h_v/h_b of the total path; that is, both cutoff walls and the horizontal floor. E. W. Lane, M. ASCE, reported this value as 6 in all cases.

Case IV. Dam with Horizontal Floor Only.—The plot of the flow lines and equipotential lines for this case is shown in Fig. 29(*d*). Data from this plot are discussed subsequently in the section on uplift diagrams.

Dams on Permeable Stratum of Finite Depth H.—Only three cases were investigated in this category, Case II being omitted. Experiments were conducted on two depths (H) of permeable stratum—namely, with $H = 2\,b$ and $H = b$.

Case I. Dam with Horizontal Floor and Upstream Cutoff Wall.—A typical example of a plot of the flow lines and equipotential lines is shown in

Fig. 30(*a*). Comparing Cols. 3 and 4, Table 6, with Cols. 2 and 3, Table 3, it is evident that a finite depth of permeable layer has only a small effect on the head-loss readings. The effect of the finite depth of porous material in reducing the efficiency of the vertical lengths as compared with that for an

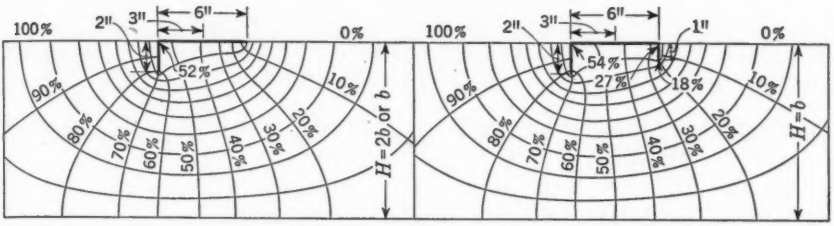

(*a*) CASE I, UPSTREAM CUT-OFF WALL

(*b*) CASE III, CUT-OFF WALLS AT THE UPSTREAM AND DOWNSTREAM TOES; $\frac{b}{d_2}=6$

FIG. 30.—FLOW LINES AND EQUIPOTENTIAL LINES, DAM WITH HORIZONTAL FLOOR ON PERMEABLE STRATUM OF FINITE DEPTH $H = 2\,b$ $(b/d_1 = 3)$

TABLE 6.—READINGS FOR CASE I (SEE FIG. 30(*a*)) PERMEABLE STRATUM OF FINITE DEPTH *H*

Depth, *H*, of permeable stratum	$\frac{b}{d_1}$	(*a*) Loss of Head[a]		(*b*) Comparative Loss Between Vertical and Horizontal Lengths		
		Point[b] A	Point[c] B	Loss per Unit Length of Path[a]		Efficiency[d] h_v/h_b
				h_v	h_b	
(1)	(2)	(3)	(4)	(5)	(6)	(7)
2 *b*	6	80.0	69.5	30.5	11.59	2.63
	3	70.0	52.0	24.0	8.67	2.77
	1	56.0	32.0	11.25	5.41	2.08
b	2	62.0	60.0	19.68	6.84	2.88

[a] Expressed as percentages of *h*. [b] Compare Col. 2, Table 3. [c] Compare Col. 3, Table 3. [d] Efficiency of the vertical, h_v/h_b; compare Col. 7, Table 3.

TABLE 7.—READINGS FOR CASE III (SEE FIG. 30(*b*)), PERMEABLE STRATUM OF FINITE DEPTH *H*

$\frac{b}{d_1}$	$\frac{b}{d_2}$	(*a*) Loss of Head (Percentages of *h*)[a]				(*b*) Comparative Loss Between Vertical and Horizontal Lengths				
		Point A	Point B	Point C	Point D	Loss Per Unit Length of Path[b]			Efficiency h_v/h_b	
						h_v upstream	h_v downstream	h_b	Upstream[c]	Downstream[c]
(1)	(2)	(3)	(4)	(5)	(6)	(7)	(8)	(9)	(10)	(11)
2	2	70.0	55.5	44.5	30.0	14.85	14.85	1.67	8.9	8.9
3	6	70.0	54.0	27.0	20.0	23.0	27.0	4.5	5.12	6.0

[a] Compare values in Cols. 3, 4, 5, and 6 with appropriate lines of Table 5—Cols. 2, 3, 4, and 5, respectively. [b] Expressed as percentages of *h*. [c] Compare values in Cols. 10 and 11 with appropriate lines of Table 5—Cols. 9 and 10, respectively.

infinite depth of material is demonstrated by comparing Col. 7, Table 6, with Col. 7, Table 3.

Case III. Dam with Horizontal Floor and Sheet-Pile Cutoff Walls at Both Upstream and Downstream Toes.—For this arrangement of floor and cutoff walls, only the case in which $H = 2\,b$ was investigated. A typical plot is shown in Fig. 30(*b*), and the data are summarized in Table 7.

Case IV. Dam with Horizontal Floor Only.—The data from these plots are discussed subsequently in the section on uplift diagrams.

Permeable Strata Under the Dam Composed of Two Materials with Different Permeabilities and the Depth of the Upper Layer is Finite

A dam with horizontal floor only was investigated for this condition. Because of the difficulty of adapting the upper plates to the various positions of the glass false bottom, only the equipotential lines were drawn (see Fig. 31). At the boundary between isotropic soils of different permeability, the equipotential lines are deflected in such a manner that the angles α and β and the permeabilities as defined by Eq. 18 or 25 are related as follows (see Fig. 31):

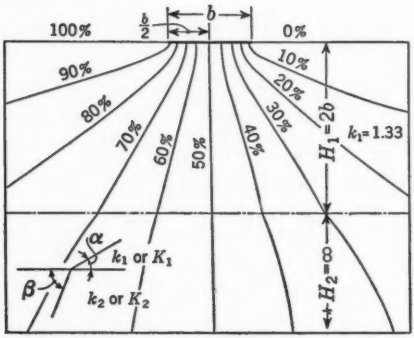

Fig. 31.—Dam with Horizontal Floor on Two Types of Permeable Strata ($H_1 = 2\,b$ and $H_2 = \infty$)

$$\frac{\tan \beta}{\tan \alpha} = \frac{k_1}{k_2} = \frac{K_1}{K_2} \quad \ldots\ldots (30)$$

Eq. 30 states merely that the deflection of the equipotential lines occurs in such a manner that the tangent of the intersecting angle with the boundary is inversely proportional to the coefficient of permeability.

Uplift Diagrams

The distribution of uplift force on the base of a dam may be conveniently represented in the form of a diagram. In the present investigation, uplift diagrams were prepared from the various graphs of equipotential lines by plotting, as ordinates, the values of head at the intersection of the potential lines with the base of the dam. The maximum ordinate of 100% h will be that at the upstream toe and the minimum ordinate at 0% h will be at the downstream toe. The following definitions are useful in discussing uplift diagrams: A_F is the area of diagram expressed in terms of the base width b and the head h (representing the total uplift force); $\bar{X}$ is the distance at the center of gravity of the uplift diagram from the downstream toe of the dam; and M is the moment of uplift force about the downstream toe of the dam. "Bligh's uplift diagram" is a triangle with the maximum ordinate at the upstream toe and the zero ordinate at the downstream toe. This diagram is for

a dam with a horizontal floor only and zero depth at the downstream toe. "Theoretical uplift (horizontal floor only)" is the uplift calculated by the formula:[19]

$$P = \frac{h}{\pi} \cos^{-1}\left(\frac{2x}{b}\right) \ldots\ldots\ldots\ldots\ldots\ldots\ldots\ldots (31)$$

in which the origin is at the midpoint of the floor and P is the value of the force in percentage of the total head, h, acting on the dam.

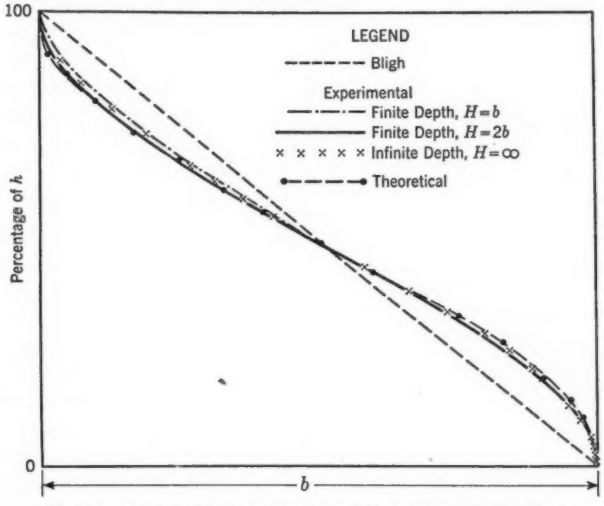

FIG. 32.—UPLIFT DIAGRAM, DAM WITH HORIZONTAL FLOOR ONLY

Dam with Horizontal Floor Only.—Fig. 32 shows the uplift diagram according to Mr. Bligh, the Weaver theoretical formula, and the author's experiments for a dam with a horizontal floor only. A comparison of uplift forces and the resulting moments for the various conditions of thickness of permeable strata are given in Table 8. The coincidence between the theoretical (that is, mathematical) and experimental results is evident. The effect of finite depth of permeable layer is very small and the results still approach the theoretical values. In connection with Table 8, as well as in the data to follow, the values of moment are given only for comparative purposes, because the type of dam to which this information would be applied nearly always has such a wide base that overturning is no problem.

TABLE 8.—COMPARISON OF RESULTS, DAM WITH HORIZONTAL FLOOR ONLY

H	AF	$\bar{X}$	M
	(*a*) THEORETICAL		
∞	$0.5\,b\,h$	$0.625\,b$	$0.3125\,b^2\,h$
	(*b*) EXPERIMENTAL		
∞	$0.504\,b\,h$	$0.626\,b$	$0.313\,b^2\,h$
b	$0.496\,b\,h$	$0.629\,b$	$0.312\,b^2\,h$
$2\,b$	$0.492\,b\,h$	$0.630\,b$	$0.310\,b^2\,h$

Dam with Horizontal Floor and Upstream Cutoff Walls (Permeable Strata of Infinite Thickness).—Uplift diagrams for the cutoff wall at the upstream toe are shown in Fig. 33(*b*) and in Fig. 33(*c*) when the sheet piling is one twelfth of the base width from the upstream toe. Data from these diagrams are summarized in Table 9, which also shows the effect of the upstream cutoff wall in reducing the uplift force and its moment about the downstream toe. Table 10(*a*) offers a comparison between the two cases (Tables 9(*a*) and 9(*b*)), taking into consideration the experimental value of uplift force for a dam on horizontal floor ($H = \infty$) only as a basis. It is obvious that the cutoff wall is more effective at the upstream toe than if it is moved back from the toe toward the downstream toe.

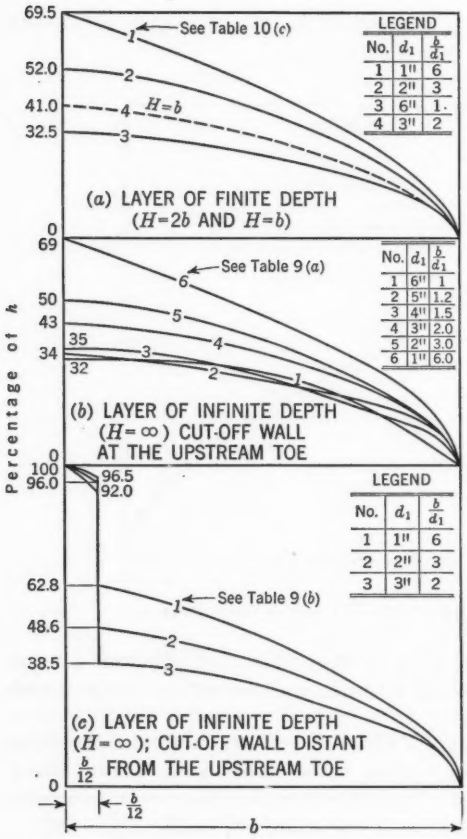

FIG. 33.—UPLIFT DIAGRAMS, DAM ON A PERVIOUS FOUNDATION, WITH HORIZONTAL FLOOR AND UPSTREAM CUTOFF WALL (b = 6 IN.)

Dam with Horizontal Floor and Upstream Cutoff Wall (Permeable Strata at Finite Depth).—The uplift diagrams and values of moment are shown in Fig. 33(*a*) for the cases of finite thickness, $H = b$ and $H = 2b$. The effect of the upstream cutoff wall on the uplift force for various thicknesses of the substratum can be noted in Table 10 by comparing Col. 2 ($H = \infty$) with Cols. 6 and 7 and Col. 4 ($H = \infty$) with Cols. 8 and 9. The basis of comparison is the uplift force obtained experimentally for a dam with horizontal floor only, on a very deep permeable layer.

Dam with Horizontal Floor with Upstream and Downstream Cutoff Walls (Permeable Strata of Infinite Depth).—The uplift diagrams for various lengths of the downstream cutoff wall for a length of upstream cutoff wall (d_1) equal to the base width (b) are shown in Fig. 34(*a*). A summary of data for several arrangements of upstream and downstream cutoff walls is shown in Table 11. Clearly, the effectiveness of the upstream cutoff wall, in reducing both the uplift force and its moment about the downstream toe, is offset by the use of a downstream cutoff wall. This effect is heightened by increasing the depth of the downstream cutoff wall. Consequently, a cutoff wall at the upstream

toe only is better for design as far as the uplift force on the dam and the moment about the downstream toe are concerned. The downstream cutoff wall may be valuable, however, in reducing the exit gradient to such a value that material will not be disturbed by the outflow from under the dam.

TABLE 9.—UPLIFT FORCE AND ITS MOMENT ABOUT THE DOWNSTREAM TOE, DAM ON A PERVIOUS FOUNDATION OF INFINITE DEPTH, WITH HORIZONTAL FLOOR AND AN UPSTREAM CUTOFF WALL

$\frac{b}{d_1}$	Curve	(*a*) CUTOFF WALL AT UPSTREAM TOE (b = 6 IN., SEE FIG. 33(*b*))				(*b*) CUTOFF WALL DISTANT $b/12$ FROM UPSTREAM TOE (SEE FIG. 33(*c*))		
		d_1	A_F	$\bar{X}$	M	A_F	$\bar{X}$	M
∞	....	....	$0.5\ b\,h$	$0.626\ b$	$0.313\ b^2\,h$	$0.5\ b\,h$	$0.626\ b$	$0.313\ b^2\,h$
6	6	1	$0.44\ b\,h$	$0.604\ b$	$0.266\ b^2\,h$	$0.453\ b\,h$	$0.627\ b$	$0.283\ b^2\,h$
3	5	2	$0.336\ b\,h$	$0.564\ b$	$0.189\ b^2\,h$	$0.393\ b\,h$	$0.623\ b$	$0.245\ b^2\,h$
2	4	3	$0.304\ b\,h$	$0.559\ b$	$0.17\ b^2\,h$	$0.324\ b\,h$	$0.663\ b$	$0.214\ b^2\,h$
1.5	3	4	$0.244\ b\,h$	$0.480\ b$	$0.117\ b^2\,h$	....	....	....
1.2	2	5	$0.238\ b\,h$	$0.552\ b$	$0.132\ b^2\,h$	....	....	....
1.0	1	6	$0.236\ b\,h$	$0.567\ b$	$0.134\ b^2\,h$	....	....	....

Dam with Horizontal Floor with Upstream and Downstream Cutoff Walls (Permeable Strata of Finite Depth).—Experiments on this arrangement of cutoff walls were made with a thickness of permeable stratum equal to twice the base width and with only two combinations of floor and depth of cutoff walls.

TABLE 10.—COMPARISON BETWEEN THE EFFECTS OF AN UPSTREAM CUTOFF WALL IN DIFFERENT DEPTHS OF PERVIOUS STRATA

$\frac{b}{d_1}$	(*a*) CUTOFF WALL IN RELATION TO UPSTREAM TOE[a] ($H = \infty$)				(*b*) VARIATION IN FINITE DEPTH OF PERVIOUS LAYER[a] (FIG. 33(*a*))				(*c*) UPLIFT DIAGRAM (FIG. 33(*a*))			
	At the toe	Not at the toe	At the toe	Not at the toe	$H = b$	$H = 2\,b$	$H = b$	$H = 2\,b$	d_1 (in.)	A_F	$\bar{X}$	M
	Uplift force		Moment		Uplift force		Moment					
(1)	(2)	(3)	(4)	(5)	(6)	(7)	(8)	(9)	(10)	(11)	(12)	(13)
6	12.0	9.4	15.0	9.6	....	14	....	14.4	1	$0.43\ b\,h$	$0.622\ b$	$0.268\ b^2\,h$
3	32.8	21.4	39.6	21.7	....	31.2	....	31.4	2	$0.349\ b\,h$	$0.616\ b$	$0.215\ b^2\,h$
1	....	....	....	....	....	....	....	....	6	$0.225\ b\,h$	$0.611\ b$	$0.137\ b^2\,h$
2	39.2	35.2	45.7	31.7	44	55	42.8	56.1	3	$0.28\ b\,h$	$0.64\ b$	$0.179\ b^2\,h$

[a] Percentage reduction in uplift forces and moments about the downstream toe.

The uplift diagrams from these experiments are shown in Fig. 34(*b*). A comparison of these results with those for similar arrangements of floor and cutoff walls for an infinite thickness of permeable stratum is given in Table 12. The same conclusions appear to apply for the case of finite depth of permeable layer (Table 12) as for that of infinite depth (Table 11).

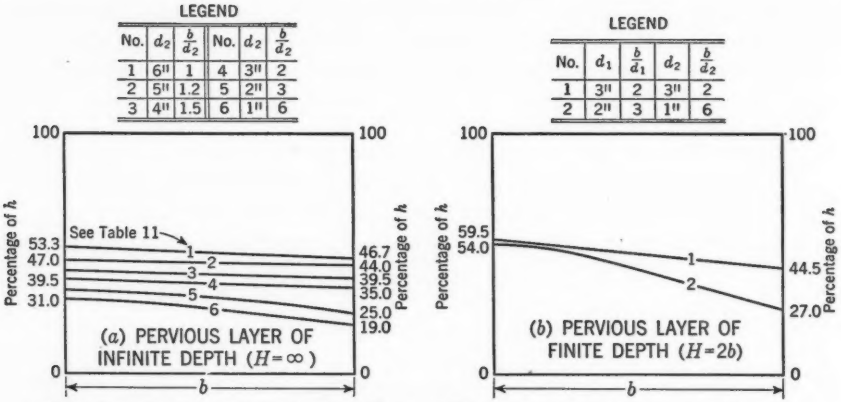

FIG. 34.—UPLIFT DIAGRAMS, DAM ON A PERVIOUS FOUNDATION WITH HORIZONTAL FLOOR AND BOTH DOWNSTREAM AND UPSTREAM CUTOFF WALLS (b = 6 IN.)

TABLE 11.—SUMMARY OF DATA, DAM WITH HORIZONTAL FLOOR ON AN INFINITELY DEEP STRATUM OF IMPERVIOUS MATERIAL ($H = \infty$) AND WITH CUTOFF WALLS AT THE UPSTREAM AND DOWNSTREAM TOES ($d_1 = b$)

$\frac{b}{d_2}$	Uplift Force (See Fig. 34(a))		$\overline{x}$	Moment about Downstream Toe	
	Area A_F	Reduction (%)		M	Reduction (%)
(1)	(2)	(3)	(4)	(5)	(6)
			(a) $b/d_1 = \infty$		
∞	0.5 $b\,h$	0	0.626 b	0.313 $b^2\,h$	0
			(b) $b/d_1 = 1$		
∞	0.236 $b\,h$	52.8	0.567 b	0.134 $b^2\,h$	57.1
6	0.256 $b\,h$	48.8	0.555 b	0.140 $b^2\,h$	55.2
3	0.305 $b\,h$	39.0	0.5444 b	0.1659 $b^2\,h$	47.0
2	0.373 $b\,h$	25.4	0.51 b	0.1903 $b^2\,h$	39.3
1.5	0.406 $b\,h$	18.6	0.515 b	0.2094 $b^2\,h$	33.2
1.2	0.455 $b\,h$	9.0	0.505 b	0.2299 $b^2\,h$	26.5
1	0.50 $b\,h$	0	0.51 b	0.2554 $b^2\,h$	18.5
			(c) $b/d_1 = 1.2$		
∞	0.238 $b\,h$	52.4	0.552 b	0.132 $b^2\,h$	57.8
6	0.276 $b\,h$	44.8	0.56 b	0.154 $b^2\,h$	50.8
3	0.350 $b\,h$	30.0	0.516 b	0.181 $b^2\,h$	42.2
2	0.412 $b\,h$	17.6	0.526 b	0.217 $b^2\,h$	30.7
			(d) $b/d_1 = 2$		
∞	0.304 $b\,h$	39.2	0.559 b	0.17 $b^2\,h$	45.7
6	0.382 $b\,h$	23.6	0.533 b	0.204 $b^2\,h$	34.8
3	0.461 $b\,h$	7.8	0.518 b	0.239 $b^2\,h$	23.6
2	0.50 $b\,h$	0	0.516 b	0.258 $b^2\,h$	17.6
			(e) $b/d_1 = 3$		
∞	0.336 $b\,h$	32.8	0.664 b	0.189 $b^2\,h$	39.6
6	0.425 $b\,h$	15.0	0.622 b	0.251 $b^2\,h$	15.7

TABLE 12.—SUMMARY OF DATA, DAM WITH HORIZONTAL FLOOR ON A FINITE LAYER ($H = 2\,b$) OF IMPERVIOUS MATERIAL AND WITH CUTOFF WALLS AT THE UPSTREAM AND DOWNSTREAM TOES

$\frac{b}{d_2}$	UPLIFT FORCE (SEE FIG. 34(b))		$\overline{X}$	MOMENT ABOUT DOWNSTREAM TOE	
	Area A_F	Reduction (%)		M	Reduction (%)
(1)	(2)	(3)	(4)	(5)	(6)
(d) $b/d_1 = 2$ (CORRESPONDS WITH TABLE 11(d))					
∞	$0.50\,b\,h$	55	$0.512\,b$	$0.256\,b^2\,h$	56.1
2		0			18.3
(e) $b/d_1 = 3$ (CORRESPONDS WITH TABLE 11(e))					
∞	$0.424\,b\,h$	31.2	$0.58\,b$	$0.246\,b^2\,h$	31.4
6		15.2			21.4

Effect of Layers of Different Permeability on the Uplift Diagram of a Dam with Horizontal Floor Only.—These experiments were made to show the effect on the uplift force and the resulting moment about the downstream toe when adjacent layers with different permeabilities are present. The depth of the upper stratum was changed from $H = b$ to $H = 2\,b$; and the ratio of permeabilities, k_1/k_2, had values of 1.33 and 1.5. The uplift diagram for one such experimental condition is shown in Fig. 35 along with the comparable curve by Mr. Bligh and the theoretical curve by Mr. Weaver. The difference between the theoretical and experimental curves appears to be negligible. Data from the various diagrams for dams with horizontal floors only are summarized in Table 13. The change in uplift force and moments did not exceed $\pm 2\%$ for $k_1/k_2 = 1.33$ or $\pm 3\%$ for $k_1/k_2 = 1.50$. However, because of the limited number of experiments, a general conclusion cannot be reached.

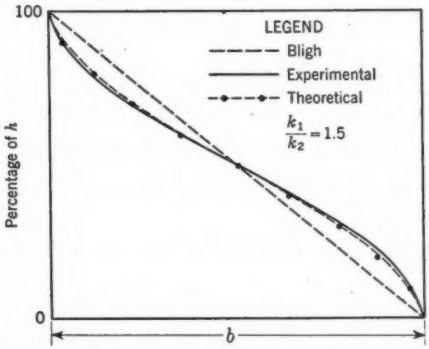

FIG. 35.—UPLIFT DIAGRAM, DAM ON A FINITE PERVIOUS LAYER ($H_1 = b$ and $k_1 = 1.50$) OVERLYING AN INFINITELY DEEP PERVIOUS LAYER ($H_2 = \infty$ AND $k_2 = 1.0$)

APPLICATION OF EXPERIMENTAL RESULTS TO PRACTICAL EXAMPLE

Example 1.—A weir 10 ft high, with a horizontal floor ($b = 60$ ft) and with a cutoff wall ($d_1 = 20$ ft) at the upstream toe rests on an impervious foundation as shown in Fig. 36. The ratio b/d_1, therefore, has a value of 3; and, according to the data in Table 3(a), the loss of head due to the sheet piling is 50.5% at the head, h, and the loss of head due to the horizontal floor is 49.5% of h.

From Table 3(*b*), the ratio of the loss of head per unit of vertical length to the loss of head per unit of horizontal length is 3.06. If γ is the weight per cubic ft of water, the uplift force on this dam (see Table 9) is $0.336\ b\ h\ \gamma = 201.6$ lb and the moment of this force about the downstream toe is $0.189\ b^2\ h\ \gamma = 6{,}804\ \gamma$ ft-lb.

TABLE 13.—COMPARISON OF RESULTS, DAM WITH HORIZONTAL FLOOR AND WITHOUT CUTOFF WALLS, ON STRATA OF VARIOUS DEPTHS

$\frac{k_1}{k_2(=1)}$	Condition of substratum	Uplift Force		Moment about Downstream Toe	
		A_F	Change (%)	M	Change (%)
(1)	(2)	(3)	(4)	(5)	(6)
		(*a*) $H = \infty$			
1.0	Uniform	$0.5\ \ b\ h$	0	$0.313\ b^2\ h$	0
		(*b*) $H = b$			
1.33	Stratified	$0.492\ b\ h$	−1.6	$0.310\ b^2\ h$	−0.96
1.50	Stratified	$0.491\ b\ h$	−1.8	$0.319\ b^2\ h$	+1.92
∞	Impermeable	$0.496\ b\ h$	−0.8	$0.312\ b^2\ h$	−0.32
		(*c*) $H = 2\ b$			
1.33	Stratified	$0.496\ b\ h$	−0.8	$0.316\ b^2\ h$	+0.96
1.50	Stratified	$0.486\ b\ h$	−2.8	$0.322\ b^2\ h$	+2.78
∞	Impermeable	$0.492\ b\ h$	−1.6	$0.310\ b^2\ h$	−0.96

These results differ markedly from those determined by the weighted-creep method.[18] For example, the length of the path of percolation is $L_m = \frac{b}{3} + 2\ d_1 = \frac{60}{3} + 40 = 60$ ft and, by the weighted-creep method, the loss at head due to the sheet piling is $\frac{20}{60}\ h\ 100 = 66.66\%$ of h; but the loss of head due to the horizontal floor is 33.4% of h (Fig. 36(*b*)); and the uplift force on the dam

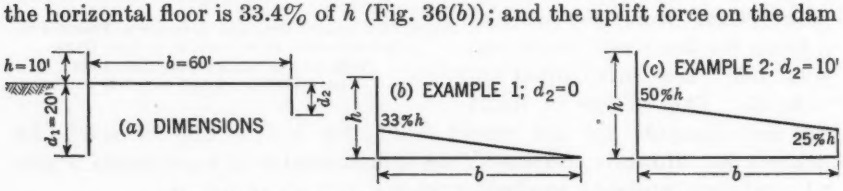

FIG. 36.—PRACTICAL APPLICATION OF EXPERIMENTAL RESULTS

is $0.167\ b\ h\ \gamma = 100.2\ \gamma$ lb. Finally, the moment of this force about the downstream toe is $0.111\ b^2\ h\ \gamma = 3{,}996\ \gamma$ ft-lb.

Example 2.—For a weir with both upstream and downstream cutoff walls, assume the same weir as in Example 1, except that a 10-ft downstream cutoff wall is added ($d_2 = 10$ ft). According to Table 5(*a*), for the case of $b/d_1 = 3$ and $b/d_2 = 6$:

Path	Loss (percentage of h)
d_1	45.5
d_2	30.0
b	24.5

These data give a ratio of head loss per unit vertical length to head loss per unit horizontal length of 5.57 for the upstream cutoff wall and 7.34 for the downstream cutoff wall (see Table 5(b)). The uplift force from Table 11 is $0.425\ b\ h\ \gamma = 255\ \gamma$ lb; and the moment of this force is $0.251\ b^2\ h\ \gamma = 8{,}835\ \gamma$ ft-lb.

In comparison, the weighted-creep analysis yields a length of the path of percolation equal to $L_m = 2\ d_1 + \frac{b}{3} + 2\ d_2 = 40 + 20 + 20 = 80$ ft and the losses of head are:

Path	Loss (percentage of h)
d_1	50
d_2	25
b	25

The ratio of loss of head per unit of vertical path to the loss per unit of horizontal floor is assumed to have a value of 6. The pressure distribution is assumed to be that shown in Fig. 36(c); and the uplift force then is $0.375\ b\ h\ \gamma = 225\ \gamma$ lb and the moment of this force about the downstream toe is $0.208\ b^2\ h\gamma = 7{,}488\ \gamma$ ft-lb.

Summary and Conclusions

A new experimental technique is presented in this paper. A vacuum-tube voltmeter is used instead of earphones and a Wheatstone bridge to detect the lines of equal voltage, and a pantograph is used for the direct plotting of the points.

The advantage of an upstream cutoff wall in reducing the uplift force is demonstrated. A downstream cutoff wall tends to increase the uplift force and hence to offset the value of the upstream cutoff wall. The downstream cutoff wall may be necessary, however, to prevent the formation of channels beneath the dam. It is recommended that only a relatively short downstream cutoff wall be used in connection with a relatively deep upstream wall.

When the thickness of the stratum of porous material under a dam is greater than the base width, the uplift force and moment are essentially the same as when the porous media is of infinite depth.

Acknowledgment

The data on which this paper is based are included in an academic thesis by the writer, entitled "Underflow and Uplift Pressure for Dams and Weirs on Porous Media by Electric Analogy." It was presented to the University of California at Berkeley in May, 1941, in partial fulfilment of the requirements for the degree of Doctor of Philosophy in Irrigation Engineering. Copies of the thesis are filed at the University of California and at Engineering Societies Library in New York, N. Y.[42a]

[42a] 29 West 39th St., New York 18, N. Y.

AMERICAN SOCIETY OF CIVIL ENGINEERS

Founded November 5, 1852

DISCUSSIONS

DETERMINATION OF PRESSURES WITHIN A SIPHON SPILLWAY

Discussion

BY A. SHUKRY

A. SHUKRY,[3] ESQ.[3a]—The main assumptions on which the author has based the formulas for pressures within the sections at the summit and near the outlet of a siphon spillway are: (*a*) The flow around the siphon bends obeys the free vortex law; and (*b*) the elevation of the mean hydraulic and energy gradients at any point can be determined by adding the head losses of the individual elements from the inlet to the point under consideration.

As given by Eq. 7, the second assumption really was made because the given formulas must depend on a foreknowledge of the elevation of the mean water gradient at the point concerned.

The writer would like to discuss the foregoing two assumptions in the light of experiments conducted in 1942[4] on siphon models in the irrigation research laboratory of Fouad I University, Gîza, Egypt. Under the direction of Prof. H. Hefny, the writer measured the pressure and the velocity distribution across different sections of siphon models to study the behavior of the siphonic flow and to determine the extent to which the flow obeys the laws of pipe flow. Fig. 2(*a*) illustrates a view of one of the models, and Fig. 2(*b*) the arrangement of the laboratory. The identity of the various points marked by letters in Fig. 2(*b*) is as follows:

Point	Description
A	Adjustable copper gate shown in Fig. 2(*a*)
B	Side scales for the air vent
C	Lip of the siphon
D	Glass side for observing the action of priming
E	Pitometer tube for measuring velocity distribution
F	Differential gage for measuring velocity heads
G	Suction pump
H	Rubber tube connections with the pressure gages

NOTE.—This paper by I. M. Nelidov was published in March, 1945, *Proceedings*.

[3] Lecturer, Irrig. Dept., Faculty of Eng., Fouad I Univ., Gîza, Egypt.

[3a] Received by the Secretary June 22, 1945.

[4] "The Flow of Water Through Siphon Spillways," by A. Shukry, thesis presented to the Faculty of Engineering, Fouad I Univ., Gîza, Egypt, in 1942, in partial fulfilment of the requirements for the degree of Master of Science in Civil Engineering.

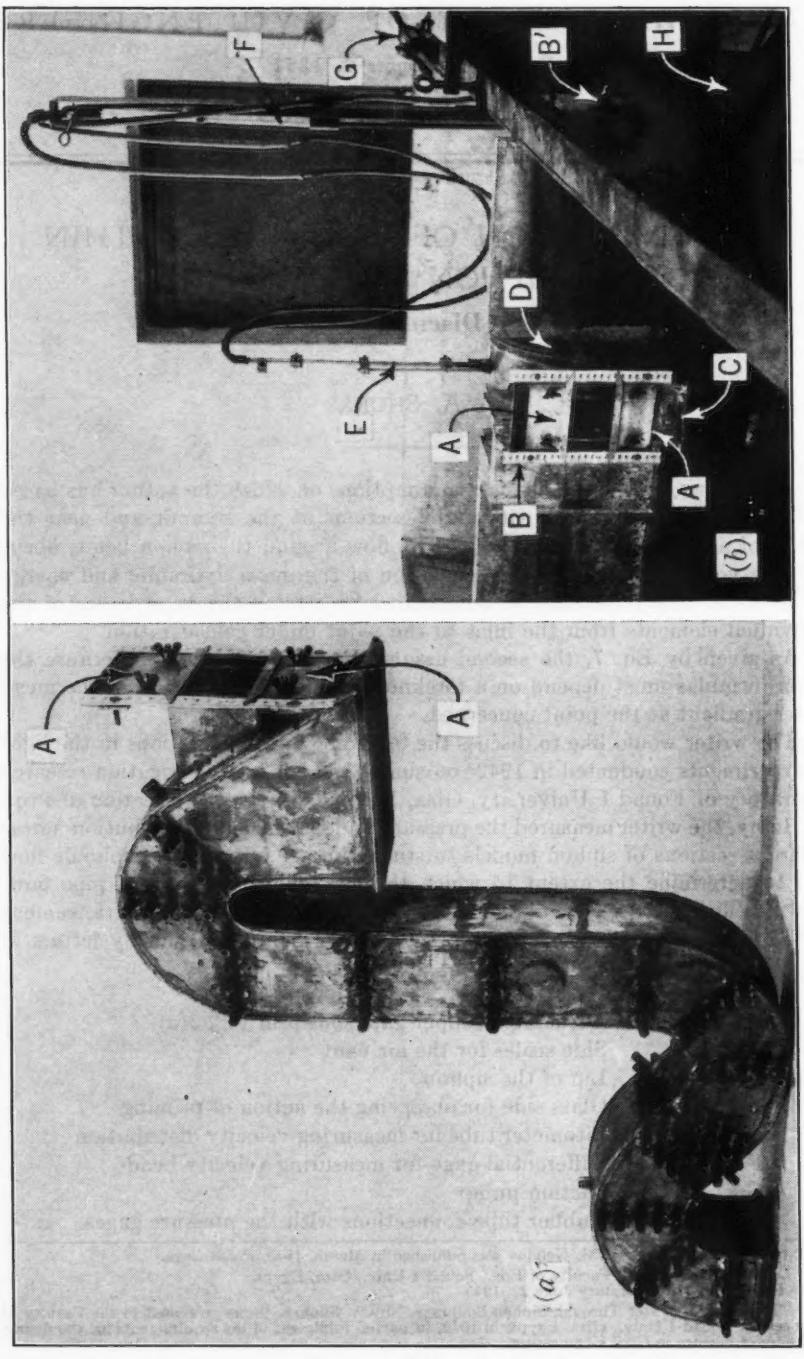

FIG. 2.—MODEL OF SIPHON, AND LABORATORY ARRANGEMENT

Regarding assumption (*a*), the theoretical velocity distribution based on a free vortex flow at the summit and outlet bends of a siphon was derived by integrating a discharge element of depth dr. If the working head on the siphon is designated by H, then, according to Fig. 3,

$$Q = \int_{r_i}^{r_c} dQ = b\int_{r_i}^{r_c} V\,dr = b\int_{r_i}^{r_c} \frac{V_i\,r_i}{r}\,dr = b\,V_i\,r_i\int_{r_i}^{r_c}\frac{dr}{r}$$

$$= b\sqrt{2\,g\,H}\,r_i\log_e\frac{r_c}{r_i} \qquad (28)$$

The velocity at any point distant r from the center would then be:

$$V = \frac{V_i\,r_i}{r} = \frac{Q}{b\,r\log_e\dfrac{r_c}{r_i}} \qquad (29)$$

The working head H considered in Eq. 28 should not exceed 24.0 ft of water, which is the practical limit of partial vacuum, however high the working head

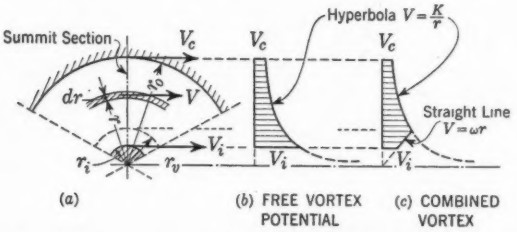

FIG. 3.—VELOCITY DISTRIBUTION AT THE SUMMIT SECTION OF A SIPHON SPILLWAY

may be.[5] The mean percentage difference (ΔV) between the theoretical and the actual velocity distribution curves was calculated at any section by the formula:

$$\Delta V = \frac{\displaystyle\int_{r_i}^{r_c}[V\text{ (theoretical)} - V\text{ (actual)}]\,dr}{\displaystyle\int_{r_i}^{r_c} V\text{ (actual)}\,dr} \times 100 \qquad (30)$$

The following three types of sections were considered: (1) All sections at the bends of the siphon when operated under a constant working head (Fig. 4); (2) the summit section of the siphon when operated under different working heads (Table 3); and (3) the summit section of the siphon for various shapes of outlet, operated under the same working head (Fig. 5).

The results showed that similarity between the actual and the theoretical flow distribution was closer for smaller than for larger ratios of $r_c : r_i$, and that the velocity distribution at the summit bend did not appreciably change within the possible range of the working head or with different shapes of outlets.

[5] "Design of a High-Head Siphon Spillway," by Elmer Rock, *Transactions*, Am. Soc. C. E., Vol. 105 (1940), p. 1050.

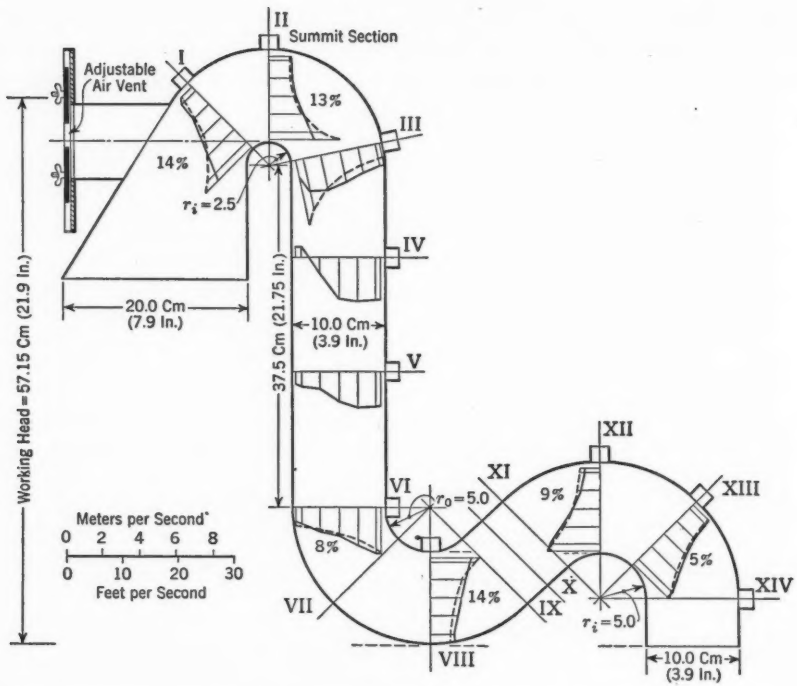

FIG. 4.—THEORETICAL AND ACTUAL VELOCITY DISTRIBUTION ACROSS A SIPHON WITH AN OUTLET A AS IN FIG. 2 (Q = 16.41 LITERS PER SEC OR 260 GAL PER MIN)

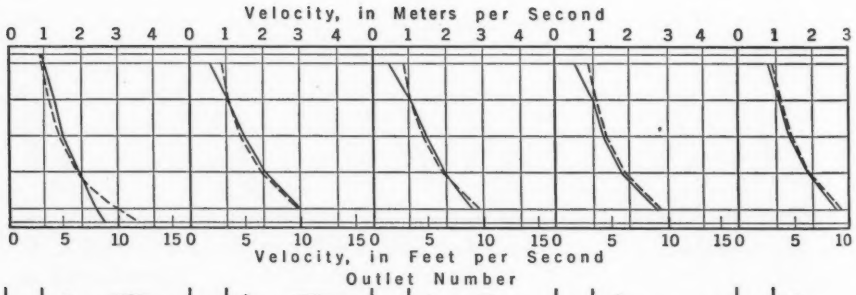
Velocity, in Meters per Second
0 1 2 3 4 0 1 2 3 4 0 1 2 3 4 0 1 2 3 4 0 1 2 3
0 5 10 15 0 5 10 15 0 5 10 15 0 5 10 15 0 5 10
Velocity, in Feet per Second
Outlet Number
a
b
c
d
e
Outlet Shape
13 10 12 12 8
Percentage Difference, ΔV

FIG. 5.—THEORETICAL AND ACTUAL VELOCITY DISTRIBUTION AT THE SUMMIT SECTION FOR VARIOUS OUTLETS AND CONSTANT DISCHARGE (Q = 17 LITERS PER SEC OR 269 GAL PER MIN)

To study the applicability of the free vortex law in predetermining the discharge passing through any siphon spillway, the theoretical and the actual discharges of seven different types of siphon spillways were compared. As seen in Table 4, the theoretical discharges are always less than the actual discharges. The percentage difference can thus be considered as a factor of

TABLE 3.—THEORETICAL AND ACTUAL VELOCITY DISTRIBUTION AT THE SUMMIT SECTION FOR VARIABLE WORKING HEADS ON A SIPHON WITH AN OUTLET A AS IN FIG. 2

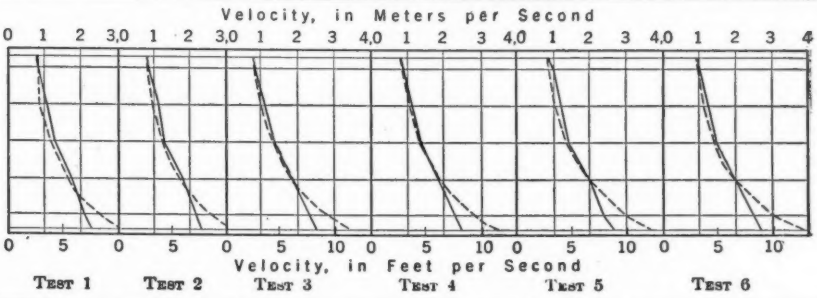
Velocity, in Meters per Second
0 1 2 3,0 1 2 3,0 1 2 3 4,0 1 2 3 4,0 1 2 3 4,0 1 2 3 4
0 5 0 5 0 5 10 0 5 10 0 5 10 0 5 10
Velocity, in Feet per Second
TEST 1
TEST 2
TEST 3
TEST 4
TEST 5
TEST 6

Description	Test 1	Test 2	Test 3	Test 4	Test 5	Test 6
Discharge:						
Liters per second	14.69	15.38	15 94	16.41	17.06	17.82
Gallons per minute	232.8	243.8	252.7	260.1	270.4	282.5
Working Head:						
Centimeters	43.50	48.00	51.70	53 70	57.15	60 92
Inches	17.1	18.9	20.4	21.2	22 5	24.0
Percentage difference[a]	....	14	14	13	14	13

[a] Percentage difference between the theoretical and the actual distribution.

safety; but, beyond a ratio of $r_c/r_i = 3.0$, the design, according to a free vortex assumption, may become uneconomic.

The reason for a departure of the actual flow from the ideal free vortex is explained by the fact that the free vortex law, when applied to bends of closed or open conduits, should be limited with respect to the pressure induced at the inner wall of the bend. According to this law the velocity at any point in the bend is inversely proportional to its radius. Consequently, as r_i approaches the value zero in very sharp curves, V_i approaches infinity and P_i/γ approaches a negative infinity. Since the negative pressure in closed conduits cannot exceed 24.0 ft of water, this pressure condition actually limits the radius at which the flow follows the theoretical free vortex law. Calling this radius r_v, the inner portion of the fluid behaves as a separate vortex filament, all particles of which have a constant rate of rotation ω, similar to conditions in a forced vortex where $V = \omega r$. The velocity distribution in this combined potential, generally known as the Rankine vortex, is shown diagrammatically in Fig. 3. It is obvious that the energy of flow in this vortex filament cannot be considered a constant because of its rotational motion. If r_i is greater than r_v, the flow in the bend will obey the free vortex law. On the other hand,

if r_i is smaller than r_v the flow will obey the combined vortex potential. The value of r_v for any bend can be determined in terms of the dimensions and the flow conditions of the bend.

TABLE 4.—COMPARISON BETWEEN THEORETICAL AND ACTUAL RATES OF DISCHARGES FOR SOME OF THE EXISTING SIPHON SPILLWAYS[a]

Item	Description	Leaburg[b]		Laggan[c]		Inglis[d]		Alpine[e]		Ocoee[f]		Walterville[g]		Ferro[h]	
		Q_{th}	(%)	Q_{th}	(%)	Q_{th}	(%)	Q_{th}	(%)	Q_{th}	(%)	Q_{th}	(%)	Q_{th}	(%)
	(1)	(2)	(3)	(4)	(5)	(6)	(7)	(8)	(9)	(10)	(11)	(12)	(13)	(14)	(15)
1	Ratio r_c/r_1 for the summit section	2.375		1.500		2.670		2.750		2.330		2.835		5.500	
2	Working head (H) on the siphon, in feet	28.4		66.0		23.0		31.0		27.2		45.9		13.1	
	Flow in the Siphon:														
3	Actual, Q_a, in cu ft per sec	470	...	650	...	501	...	667	...	220	...	700	...	353	...
	Theoretical,[i] with Head Losses as Computed by the Methods of:														
4	W. P. Creager and J. D. Justin	468	0	590	−9	494	−1	667	+1	202	−8	700	0	299	−16
5	J. Williamson	630	+34	670	+3	546	+9	770	+15	251	+14	890	+27	357	+ 1
6	Theoretical; free vortex[j]	407	−13	650	0	453	−10	595	−11	200	− 9	587	−16	192	−46

[a] The headings of this table are abbreviated considerably for compactness, the full significance of each being described in footnotes ([b]) to ([h]). The heading Q_{th} denotes the theoretical rate of flow in the siphon, in cubic feet per second, as applied to values in lines 4, 5, and 6; and (%) denotes the percentage difference, $\frac{Q_a - Q_{th}}{Q_a} \times 100$, for these three lines.

[b] The behavior of the siphons of the Leaburg Hydro-Electric Plant, Eugene, Ore.; as reported by J. C. Stevens, President, Am. Soc. C. E. (*Transactions*, Am. Soc. C. E., Vol. 99 (1934), p. 986).

[c] Siphon, Battery No. 2, at the Laggan Dam in England, as reported by A. H. Naylor ("Siphon Spillways," Edward Arnold & Co., 1935, London).

[d] The Inglis Siphon reported by A. H. Gibson, Thomas H. Aspey, and Fred Tattersall (*Minutes of Proceedings*, Inst. C. E., London, England, Vol. 231, 1931, p. 203).

[e] The Siphon at Alpine Dam in Marin County, California ("Construction of Dams," by Edward Wegmann, 8th Ed., p. 430).

[f] See "Design and Tests of Wasteway of Large Flume Connected with Tennessee Power Company's Second Ocoee River Development," by W. P. Creager, *Engineering Record*, Vol. 69, 1914, p. 567.

[g] The behavior of the siphons of the Walterville Hydro-Electric Plant, Eugene, Ore., as reported by Mr. Stevens (*Transactions*, Am. Soc. C. E., Vol. 104, 1939, p. 1787).

[h] The siphon type developed by Cavicini and Masini, as reported by G. Ferro (*Engineering*, London, Vol. 121, 1926, p. 5).

[i] Theoretical rate of flow (Q_{th}) in the siphon, based on the total sum of head losses, in cubic feet per second.

[j] Theoretical rate of flow (Q_{th}) in the siphon, based on a theoretical free vortex at the summit section

As regards the second assumption made by Mr. Nelidov, it should be mentioned that there has been considerable discussion as to whether the siphonic flow obeys the laws of flow in pipes—in other words, whether it is possible to divide the total length of the siphon into a number of bends and straight sections and to apply the existing coefficients and formulas for the individual parts so as to obtain the progressive net losses in friction and eddies. Most of this discussion[6,7,8,9,10] was based on pressure measurements at some sections

[6] "Experiments on Siphon Spillways," by A. H. Gibson, Thomas H. Aspey, and Fred Tattersall, *Minutes of Proceedings*, Inst. C. E., London, England, Vol. 231, 1931, p. 203.

[7] "The Laws of Siphon Flow," by P. Davies, *ibid.*, London, England, Vol. 235, 1932–1933, p. 352.

[8] "The Flow of Water through Rectangular-Pipe Bends," by P. Davies and S. V. Puranik, *Journal*, Inst. C. E., London, England, Vol. 2, 1935–1936, p. 83.

[9] "Experiments on Pipe Bends," by H. Addison, *Selected Paper No. 5084*, Inst. C. E., London, England, 1936.

[10] "Considerations on Flow in Large Pipes, Conduits, Tunnels, Bends, and Siphons," by James Williamson, *Journal*, Inst. C. E., London, England, Vol. 11, 1938–1939, p. 451.

of siphon models. The pressure head at any section was considered as the mean reading of the pressure gages, and the total head was calculated by adding to the pressure head the velocity head h_{vm}. Through the omission of the head-correction factors resulting from the nonuniform distribution of velocities and pressures, serious discrepancies in the energy lines were encountered, especially at the *vena contracta* downstream from the summit bend. Investigators found the same phenomena when analyzing the energy losses from the recorded pressures in some existing siphon spillways.[11,12]

For the purpose of determining the correct analysis, the energy method was followed in deriving the mean values of the pressure, velocity, position, and total heads at any section. This was accomplished by integrating the energy curves (instead of the head curves) with respect to the area of the section, as given by the following: Mean pressure head,

$$h_{pm} = \frac{1}{V_m A} \int_0^A \frac{p}{\gamma} V \, dA \ldots\ldots\ldots\ldots\ldots\ldots (31a)$$

mean velocity head,

$$h_{vm} = \frac{1}{V_m A} \int_0^A \frac{V^3}{2g} dA \ldots\ldots\ldots\ldots\ldots\ldots (31b)$$

mean position head,

$$h_{sm} = \frac{1}{V_m A} \int_0^A y \, V \, dA \ldots\ldots\ldots\ldots\ldots\ldots (31c)$$

and mean total head,

$$h_{tm} = \frac{1}{V_m A} \int_0^A \left(\frac{p}{\gamma} + \frac{V^2}{2g} + y \right) V \, dA \ldots\ldots\ldots\ldots (31d)$$

In the writer's investigation, the aforementioned energy process eliminated the apparent discrepancies in the energy line of a siphon. The siphon was then divided into three parts—the summit bend, the straight leg, and the outlet bend. The coefficient K expressing the loss of head in terms of h_{vm} was obtained for each part and compared with the value given in the existing published data. The loss of head due to wall friction was calculated according to the modified Chézy formula (in foot-second units):

$$h_l = \frac{V^2_m \, n^2}{R^{1.333}} \ldots\ldots\ldots\ldots\ldots\ldots\ldots\ldots (32)$$

in which h_l is loss of head per unit length; n is Kutter's coefficient of roughness equal to 0.009 for the model walls; V_m is mean velocity in the section, and R is the hydraulic radius. The loss of head due to a bend, which is the head in excess of that which would occur in a straight conduit of equal length, has been obtained by at least two investigators: (*a*) William P. Creager and Joel D. Justin, Members, Am. Soc. C. E., determined coefficients based on the mean results of most of the tests which had been conducted on pipe bends;[13] and

[11] "On the Behavior of Siphons," by J. C. Stevens, *Transactions*, Am. Soc. C. E., Vol. 99 (1934), p. 986.

[12] "Siphons as Water-Level Regulators," by J. C. Stevens, *ibid.*, Vol. 104 (1939), p. 1787.

[13] "Hydro-Electric Handbook," by W. P. Creager and J. D. Justin, John Wiley & Sons, Inc., New York and Chapman Hall, London, 1927, p. 118.

(*b*) James Williamson derived coefficients[10] in which the effect of the wall material of the bend was taken into consideration.

Comparison of the two revealed that the actual losses in the siphon elements were totally different from the losses of these elements when tested separately, as may be noted in Table 5. It was found, however, that the various elements of the siphon seemed to have a counterbalancing effect on each other. A reduction of the loss at one part was offset by an increase of the loss at another, so that the total sum of the energy losses appeared to be practically unchanged. This may help to compute the rate of discharge passing through any type of siphon spillway with a reasonable degree of accuracy, as shown in Tables 4 and 5, but fails to give any correct indication for the pressures that may be induced at some sections of a siphon or the elevation of the energy line.

TABLE 5.—COMPARISON BETWEEN EXPERIMENTAL (K_a) AND COMPUTED (K_c) VALUES OF THE ENERGY LOSS COEFFICIENTS (BASED ON THE MEAN VELOCITY AT THE SUMMIT SECTION) AND THE RATE OF FLOW IN A SIPHON MODEL

Item	Sources of energy loss	Experimental values K_a	Computed Values, K_c	
			Creager and Justin[a]	J. Williamson[a]
1	Entry plus friction between inlet and outlet	1.448	0.416	0.416
2	Summit bend	0.400	1.308	1.122
3	Outlet bend	1.175	2.030	1.020
4	Outlet	1.150	1.150	1.150
5	Total	4.173	4.904	3.708
6	Percentage difference $(\Sigma K_a - \Sigma K_c)100/\Sigma K_a$	....	+17.5	−11.1
	Working Head H:			
7	In meters	0.5500	0.5500	0.5500
8	In feet	1.805	1.805	1.805
	Mean Velocity V_m at the Summit Section $(\sqrt{2gH/\Sigma K})$:			
9	In meters per second	1.605	1.485	1.700
10	In feet per second	5.266	4.872	5.577
	Experimental Rate of Discharge Q_a:			
11	In liters per second	16.22	....	....
12	In gallons per minute	259	....	....
	Computed Rate of Discharge Q_c:			
13	In liters per second	....	15.00	17.15
14	In gallons per minute	....	238	272
15	Percentage difference $(Q_c - Q_a)100/Q_a$	....	−8	+6

[a] Computed value of the energy loss coefficient K_c, with bend losses as determined by the methods of W. P Creager and J. D. Justin, and by J. Williamson, respectively.

Mr. Nelidov has shown clearly the relatively high pressures within the summit and near the outlet bends of a siphon, and the importance of providing good reinforcement for these unbalanced pressures, due to which failure of the siphon may occur. It may be added that a good factor of safety in the structural design should also be provided to withstand the intermittent violent shocks and serious vibrations during the actions of priming and de-priming, especially if the siphon is to be operated under high heads.

AMERICAN SOCIETY OF CIVIL ENGINEERS

Founded November 5, 1852

DISCUSSIONS

MATHEMATICAL EXAMINATION OF THE HIGHWAY TRANSITION SPIRAL

Discussion

BY MAX C. KOEHLER

MAX C. KOEHLER,[11] ASSOC. M. AM. SOC. C. E.[11a]—With the nation returning to a normal economy, reconstruction of existing highways and the construction of new superhighways will be one of the major programs of the postwar period, and a discussion of the spiral easement curve is timely. Prior to World War II this refinement of design was going through its "growing pains"; it is still in that process and will possibly continue so for ten years or more. It has followed, and will follow, the same processes of development as the railroad easement curves in the nineteenth century; wherein every one from roadmaster to college professor advanced his pet idea on how to make the transition from a tangent to a circular curve without throwing the locomotive off the track or the passengers in the aisles. The smooth gliding ride of the modern "streamliners" at from 70 to 100 miles per hr has forced the passengers again to rely on the weather as a topic of conversation. A short history of this period may reveal the pattern that will be followed in highway design.

Writing at the University of Glasgow in Glasgow, Scotland, in 1862, W. J. M. Rankine (60)[11b] stated that a Mr. Gravatt, in 1828, was using the sine curve for railroads in England. This curve was transitional throughout, but was objected to by many because there was no simple curve. Rankine recommended the use of a transition curve developed by William Froude in 1841. Froude made "short shift" of curve staking as follows:

(1) Locate the center of the railroad, using simple curves and tangents.

(2) Determine the length for the "curve of adjustment" by the formula $L = 300\,x$ the greatest change of cant (superelevation) in feet.

NOTE.—This paper by John Oran Eichler and Howard W. Eves was published in May, 1945, *Proceedings*. Discussion on this paper has appeared in *Proceedings*, as follows: November, 1945, by Joseph Barnett, Ralph W. Stewart, Donald Thompson, T. F. Hickerson, Allen H. Brownfield, René S. Pulido y Morales, and C. C. Wiley.

[11] Engr. P-3, U. S. Engr. Office, Seattle, Wash.

[11a] Received by the Secretary September 28, 1945.

[11b] Numerals in parentheses, thus: (60), refer to corresponding items in the Bibliography (see Appendix of the paper), and at the end of discussion in this issue.

(3) Compute the shift b, in terms of the length L and the radius R, as follows:

$$b = \frac{L^2 R}{24} \quad \ldots\ldots (79)$$

(4) Set out the curve by use of formula (a cubic parabola):

$$y = 4\, b\, \frac{l^3}{L^3} \quad \ldots\ldots (80)$$

in which l is the distance measured on the circular arc and y is the ordinate. For further information, Rankine refers to a technical article (61) published in 1860 and 1861. Rankine also advised raising the outer rail above the center line for one half the cant, and depressing the inner rail an equal amount. Happily, the outer rail is now adjusted for the full cant and "grade" is carried on the inner rail. The highways passed through this same experience, complicated by parabolic crowns and extra widening on the inside. It is now fairly uniform practice to omit the crown as soon as the superelevation begins, carry the grade on the inside edge of the pavement, and "throw" all the superelevation to the outside of the curve. Where the curve is located on a "ruling grade" the grade is "compensated"; that is, it is reduced so that the grade of the high edge does not exceed the "ruling grade."

In the United States the late Elliot Holbrook, M. Am. Soc. C. E. (41), seems to have been the first to publish a comprehensive article on the transition spiral. It contains a rigorous proof that the spiral angle θ, when the ratio of degree of curve to length L is unity, is:

$$\theta = \frac{L^2}{200} \quad \ldots\ldots (81)$$

This is the first published account the writer has been able to find of the "American Spiral," in which the degree of curve varies directly as the distance along the curve. The editor remarks at the end of Holbrook's article, that "In Germany, and on some roads in France, the tangent is connected with the curve proper, or circular curve by what is called a 'connecting-curve,' which in Germany is made parabolic." However, the late William Cain, M. Am. Soc. C. E. (50), claims that the late A. M. Wellington, M. Am. Soc. C. E. (62), was the first man to define the true transition spiral. Wellington himself refers to it as a cubic parabola in which the length is proportional to the square root of the offset.

Holbrook prepared a table for a spiral increasing 10 min in degree of curve for every 10 ft of length along the spiral up to 210 ft where $\theta = 3° 30'$. This same table contains a column for deflection angles from the beginning of the spiral. For lengths as great as 50 ft, d (deflection) seems to be $\frac{\theta}{2}$; but after that $d = \frac{\theta}{3}$ which has since been proved true for any deflection, using a slight correction when θ exceeds 15°. A short but rigorous proof of the intrinsic equation of the spiral has been presented by the late D. E. Hughes, M. Am.

Soc. C. E. (63), as follows: Referring to Fig. 9, R varies as $\frac{1}{L}$; that is, $R = \frac{K}{L}$. Also, $R = \frac{dL}{d\theta}$, from which $\frac{dL}{d\theta} = \frac{K}{L}$, or

$$L\,dL = K\,d\theta \ldots\ldots\ldots\ldots (82)$$

Integrating Eq. 82, $\frac{1}{2}L^2 = K\theta$; or

$$L = \sqrt{2K\theta} \ldots\ldots\ldots\ldots (83)$$

In other words, θ varies as L^2 (see Eq. 83) and $L = 2R\theta$, or twice a circular arc of the same radius and angle. Hughes then expands the sine and cosine series of $d\theta$ to derive:

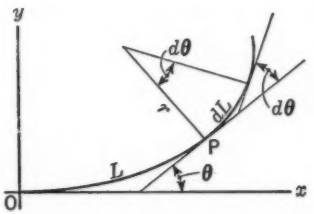

FIG. 9

$$x = \sqrt{2K\theta}\left(1 - \frac{\theta^2}{5^2} + \frac{\theta^4}{9^4} - \frac{\theta^6}{13^6} + \cdots\right) \ldots\ldots\ldots\ldots (84a)$$

and

$$y = \sqrt{2K\theta}\left(\frac{\theta}{3^1} - \frac{\theta^3}{7^3} + \frac{\theta^5}{11^5} - \frac{\theta^7}{15^7} + \cdots\right) \ldots\ldots\ldots\ldots (84b)$$

suggesting that a table be prepared for values of x and y. It is to be noted that Hughes does not use the degree of curve. Messrs. Eichler and Eves prefer this same reasoning. They call K a constant of proportionality which is equal to $\sqrt{2RL}$.

In 1901 the late Arthur N. Talbot, Past-President and Hon. M. Am. Soc. C. E. (29), gave the definition of this spiral as: "The Transition Spiral is a curve whose degree-of-curve increases directly as the distance along the curve from the point of spiral," which is expressed mathematically as

$$D = a\,L \ldots\ldots\ldots\ldots (85)$$

in which D = degree of curve = $\frac{5{,}730}{R}$; a is the constant ratio $\frac{D}{L}$; and L is the length of the spiral in 100-ft stations. Eq. 85 is the same expression as $\frac{1}{R} = K\,S$ "dressed in different clothing."

In computing and staking curves it is always necessary to know how much central angle has been consumed by any given length of curve. In the simple curve it is the degree of curve times the length of arc in stations, since, by definition, 100 ft of arc subtends 1° of central angle. All other arcs are directly proportional, and therefore their degree is an expression of the number of times their radius will divide into the unit radius of 5,730 ft. For convenience, these values are usually in simple whole numbers. In the spiral curve, since one starts from a tangent and progresses at a uniform rate of change of curvature a until the desired degree of curve is reached, the amount of central angle consumed is exactly half that of the simple curve of the same length. This is the application of the law of averages.

Since $R = \frac{dL}{d\theta} = \frac{5{,}730}{D}$,

$$d\theta = \frac{D\,dL}{5{,}730} \quad \ldots\ldots (86a)$$

From Eq. 85, $D = a\,L$; but L is in stations, and

$$d\theta = \frac{a\,L\,dL}{57.30} \quad \ldots\ldots (86b)$$

Also,

$$\theta = \int \frac{a\,L\,dL}{57.30} = \frac{a\,L^2}{114.6}\ (\text{radians}) = \frac{a\,L^2}{2}\ (\text{degrees}) \quad \ldots\ldots (87)$$

The 100-ft arc was chosen to subtend 1° of central angle because the radius of such a circle is 5,730 ft (nearly) and is not, by coincidence, the number of degrees in one radian. Eq. 87 is exact, even though two incommensurable numbers appear in the solution. They are the same and divide equally into each other.

Talbot seems to have been the first to recognize that "A spiral diverges from its osculating circle, at any point, at the same rate that the spiral deflects from the initial tangent" and as a result devised the best method of computing the backward and forward deflections to any point on a spiral from any other point in the spiral. This is such a valuable tool, to the locating engineer, when moving up along the line in heavy timber or brush, that it is worth repeating:

> "The deflection angle between the local tangent, at any point on the spiral, to any other point on the spiral is the sum or difference of the deflection angle of the osculating circle for a length equal to the distance between the two points and the deflection angle for the spiral from the P.S. for a length equal to the distance between the two points."

Referring to Fig. 10, PP′ = PC = AB; $\phi = \frac{\theta_1}{3}$; and $\delta = \frac{i}{2}$. According to the rule, the forward deflection is $(\delta + \phi)$ and the backward deflection is $(\delta - \phi)$. A more comprehensive treatment of this rule has been published by T. F. Hickerson, M. Am. Soc. C. E. (13).

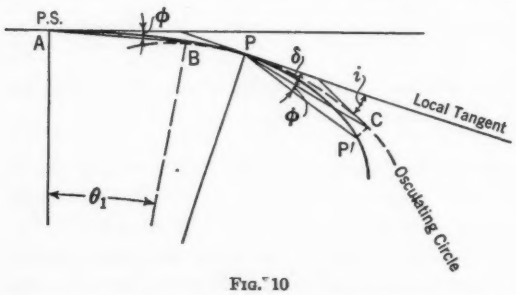

FIG. 10

Orville Kofoid, Assoc. M. Am. Soc. C. E., computed the deflection angle from any point back on the spiral to any point forward without reference to the local tangent by the following formula (15):

$$(L_1 + L_2 + L_3)\,(L_3 - L_1)\,\frac{\theta}{3\,(L)^2} \quad \ldots\ldots (88)$$

in which L_1 is the distance from point of spiral PS to backsight; L_2 is the

distance from PS to transit point; L_3 is the distance from PS to foresight; L is the total length of spiral; and θ is the total spiral angle. Although it is useful, Eq. 88 is not well suited for field work because of the multiplication and division involved; and the use of logarithms by field men is becoming a lost art since the introduction of the computing machine.

Most field men prefer the "ten-chord spiral" because of available tables in which all ten deflections from the PS may be read directly. "Moving up along the spiral" is accomplished simply by multiplying the first deflection by a suitable coefficient which is also selected from a table. Since the coefficients are mostly two-digit numbers, and the first deflection $\left(\frac{\theta}{300} \text{ in all cases}\right)$ is also a small number, the multiplication is not involved (25). The writer once edited a table (not published) for staking a "ten-chord spiral" backward—that is, from the sharp end toward the tangent. The table was prepared by several of the field engineers in the Portland (Ore.) office of the U. S. Public Roads Administration so that staking could proceed along the spiral in the direction of the stationing at all times. The objection to the "ten-chord spiral" is the tendency of the field men to omit staking the "breaks" unless they happen to fall at a chord point.

It seems fairly certain that the type of spiral to be used on highway work is finally accepted as a curve whose degree of curvature or radius varies as the distance along the curve, and that sine curves, series of compound curves, lemniscates, logarithmic and Archimedes spirals, etc., have been tested and found wanting in one respect or another. The tempest in the teapot now raging is whether to abandon the degree of curve in favor of the even-radius curves, such as 1,000 ft, 2,000 ft, etc. One argument in favor of the latter is that the radius of the curve could be posted on the highway and would be understood readily by the layman, whereas the degree of curve means nothing to him. Time alone will decide that issue.

In applying the spiral to highway design, the present tendency is to combine it with superelevation, since both begin at the PS and both progress uniformly until the central circular curve is reached where both curvature and superelevation become some predetermined constant. The degree of curve is determined by the designing engineer to fit the topography of the ground; the superelevation is determined by the "design speed" of the highway and varies with the degree of curve. These conditions are usually set by the county, state, or bureau doing the design. L. I. Hewes, M. Am. Soc. C. E., has prepared a useful table (11*a*) which also recommends the length of spiral to be used for each combination of "design speed" and degree of curve.

It is evident from the foregoing data that the question of whether a curve is transitional throughout will be self-determined by the various restrictions of design.

At the conclusion of the paper by Messrs. Eichler and Eves, the authors raise several questions for further study and discussion. While studying the locus of the center of radius of the spiral, the writer seemingly stumbled on a conclusion that the spiral is restricted to 90° of central angle. It would be interesting to discover if this theory can be either proved or disproved.

The question was raised as to how to improve upon existing methods of describing right of ways, a subject that the writer has treated in some detail elsewhere (64).

Attention is invited to the fact that, in Eq. 7, the correction C is subtracted from $\frac{\phi}{3}$ when ϕ exceeds 15°.

Bibliography.—

(11) **"American Highway Practice,"** by L. I. Hewes, John Wiley & Sons, Inc., New York and London, 1942. (*a*) Vol. I, Table 15.

(13) **"Highway Surveying and Planning,"** by T. F. Hickerson, McGraw-Hill Book Co., Inc., New York, N. Y., 2d Ed., 1936. (*a*) Table 10. (*b*) Table 11. (*c*) Tables 1, 7, and 8.

(15) **"A Solution for Laying Out Spiral Curves for Highways,"** by Orville Kofoid, *Western Construction News*, June, 1939, pp. 196–197 (gives a convenient formula for moving up along the spiral).

(25) **"Field Engineering,"** by W. H. Searles, revised and enlarged by H. C. Ives, John Wiley & Sons, Inc., New York, N. Y., 21st Ed., 1936.

(29) **"The Railway Transition Spiral,"** by A. N. Talbot, 6th Ed., Eng. News Publishing Co., 1927. (*a*) p. 93.

(41) **"Railroad Alignment,"** by Elliot Holbrook, *Railroad Gazette*, December 3, 1880, p. 639.

(50) *Transactions*, Am. Soc. C. E., Vol. XXVI (January–June, 1892), p. 473.

(60) **"A Manual of Civil Engineering,"** by W. J. M. Rankine, Griffin, Bohn, & Company, London, 20th Ed., 1898, p. 651.

(61) *Transactions*, Inst. of Engrs. in Scotland, Vol. IV, 1860–1861.

(62) **"Economic Theory of the Location of Railways,"** by Arthur M. Wellington, John Wiley & Sons, Inc., New York, N. Y., 1900.

(63) *Engineering News*, Vol. 28, December 29, 1892, p. 610.

(64) **"Method of Computing the Intersection of a Line with a Spiral and Any Curves Parallel to the Spiral,"** by M. C. Koehler, *Public Roads*, Vol. 22, No. 3, May, 1941, p. 63.

AMERICAN SOCIETY OF CIVIL ENGINEERS

Founded November 5, 1852

DISCUSSIONS

STRESSES IN THE LININGS OF SHIELD-DRIVEN TUNNELS

Discussion

BY LOUIS BALOG

LOUIS BALOG,[40] ESQ.[40a]—In the design of underground cylindrical structures the analysis can often be limited to a ring of unit length under the action of transverse forces. The method of ring analysis applied to the solution of this problem by Mr. Bull was developed for structures of circular section with concentrated supports. Inasmuch as the support conditions of the tunnel ring are continuous and elastic, it would be advantageous to begin the analysis by the theory of curved beams on continuous elastic support.

The first step in the solution of this problem by this approach—the formulation of a differential equation of the elastic line of the circular ring—was published in 1883.[41] The general solution of this differential equation for the circular beam on continuous elastic support (inverted foundation arch) was published in 1900;[42] another solution appeared in 1921;[43] and the solution of the author's problem (equations of influence lines for stresses in an elastic ring embedded in an elastic medium) was published by Adolf Voellmy in 1936.[44] Mr. Voellmy's work, including experimental verification, was completed in 1934.[45]

The carrying capacity of an elastic cylinder embedded in the soil is greatly influenced by the deformations. "Safe" design assumptions which disregard this important fact may result in weaker structures at considerably increased

NOTE.—This paper by Anders Bull was published in November, 1944, *Proceedings*. Discussion on this paper has appeared in *Proceedings*, as follows: January, 1945, by J. A. Van den Broek; February, 1945, by Nathan D. Brodkin, M. A. Drucker, and Sigvald Johannesson; May, 1945, by Jacob Feld; June, 1945, by Leon Beskin, and D. P. Krynine; September, 1945, by A. A. Eremin; and November, 1945, by G. N. Alexander.

[40] Cons. Engr., New York, N. Y.

[40a] Received by the Secretary November 2, 1945.

[41] "Résistance d'un anneau à la flexion, quand sa surface extérieure support une pression normale constante par unité de longueur de sa fibre moyenne," by J. Boussinesq, *Comptes Rendus*, Vol. 97, Paris, 1883, pp. 843 and 1131.

[42] "Einiges über Grundbögen," by A. Francke, *Schweizerische Bauzeitung*, Vol. 36, 1900, p. 71.

[43] "Theorie des Trägers auf elastischer Underlage," by Keiichi Hayashi, Julius Springer, Berlin, 1921, p. 145.

[44] "Erddruck auf elastisch eingebettete Rohre," by A. Voellmy, *Publications*, Vol. IV, International Assn. for Bridge and Structural Eng., Zürich, 1936, pp. 591–611.

[45] "Eingebettete Rohre," by Adolf Voellmy, Leemann & Co., Zürich, 1937, p. 151.

expense. Since the thinner cylinder is able to undergo larger deformations without failure, such deformations advantageously modify the pressure distribution on the cylinder surface. Thus, the internal stresses will be smaller than those in a structure with thicker walls. This explains the great carrying capacity of thin ductile metal cylinders and shows the importance of designing underground cylindrical structures as flexible as practicable. Therefore, a basic distinction should be made between pressures and stresses derived with or without considering the effect of deformations in the ring and the surrounding medium. The segregated determination of these two kinds of pressure and stress distributions facilitates clear visualization of the behavior of the structure as influenced by deformability characteristics—a great advantage in judging the effect of the various factors that enter into the design and in selecting the proper solution. From the design point of view, the inseparable consideration of these effects impairs the practical value of the author's method.

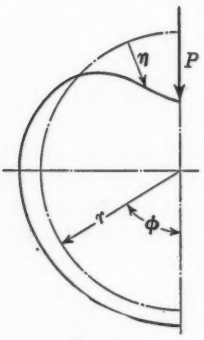

FIG. 29

As is the case for the analysis of suspension bridges, the difference between the stresses that refer to the original shape of the structure, and those that refer to the deformed shape, will be small if the ring is rigid. In designing suspension bridges, the continuous change of the deformability characteristics along the span generally makes it impracticable to use the principle of superposition, whereas the constant deformability characteristic of a circular ring facilitates design by superposition. In the latter case superposition is also best suited to the nature of the design problem under consideration. Two kinds of influence lines are required, therefore, for design purposes: (*a*) Influence lines which are generally valid for a circular ring and (*b*) one influence line for the consideration of the effects of the deformations of a given ring.

The differential equation of the elastic line of the circular ring on elastic support (see Fig. 29) is:[44]

$$\eta'''' + \eta'' + \left(1 + \frac{r^4 K}{B}\right)\eta = \frac{C_1 r^2}{B} \quad \ldots\ldots\ldots\ldots\ldots (66)$$

and the general solution of Eq. 66 is:

$$\eta = \frac{C_1 r^3}{B a^2} + (C_2 \sinh v_1 \phi + C_3 \cosh v_1 \phi) \sin v_2 \phi + (C_4 \sinh v_1 \phi + C_5 \cosh v_1 \phi) \cos v_2 \phi \quad \ldots\ldots\ldots\ldots\ldots (67)$$

For the case of a radial load at $\phi = \pi$ (see Fig. 29), constants C_1 to C_5 are determined by the following five conditions: (*a*) $\eta' = 0$ for $\phi = 0$; (*b*) $\eta' = 0$ for $\phi = \pi$; (*c*) $V = -\frac{B}{r^3}(\eta' + \eta''') = 0$ for $\phi = 0$; (*d*) $V = -\frac{B}{r^3}(\eta' + \eta''') = -\frac{p}{2}$ for $\phi = \pi$; and (*e*) $\frac{1}{B}\int_0^{\pi} M\, d\phi = -\frac{1}{r^2}\int_0^{\pi} (\eta + \eta'')\, d\phi = 0$. Introducing the derivatives of Eq. 67 into conditions (*a*) to (*e*), the following values

are obtained for the constants C_1 to C_5: From conditions (a) and (c), $C_3 = C_4 = 0$; from conditions (b) and (d), $C_2 = \frac{p\,r^3}{4\,B\,v_1\,v_2}\Phi$ and $C_5 = -\frac{p\,r^3}{4\,B\,v_1\,v_2}\Psi$; and, from condition ($e$), $C_1 = \frac{p}{2\,\pi}$. Introducing these values of the constants in Eq. 67, the influence line of the radial deflections in section $\phi = \pi$ becomes:

$$\eta_1 = \frac{r^3}{4\,B\,v_1\,v_2}\left(\frac{2\,v_1\,v_2}{a^2\,\pi} + \Phi \sinh v_1\,\phi \sin v_2\,\phi - \Psi \cosh v_1\,\phi \cos v_2\,\phi\right) \ldots (68)$$

in which

$$a = \sqrt{1 + \frac{r^4\,K}{B}}; \qquad B = \frac{m^2}{m^2 - 1}\,E\,I; \qquad v_1 = \sqrt{\frac{a-1}{2}};$$

$$\text{and} \qquad v_2 = \sqrt{\frac{a+1}{2}} \ldots\ldots\ldots\ldots\ldots\ldots (69)$$

Furthermore,

$$\Phi = \frac{v_1 \sinh v_1\,\pi \cos v_2\,\pi - v_2 \cosh v_1\,\pi \sin v_2\,\pi}{a\,(\sinh^2 v_1\,\pi + \sin^2 v_2\,\pi)} \ldots\ldots\ldots (70a)$$

and

$$\Psi = \frac{v_1 \cosh v_1\,\pi \sin v_2\,\pi + v_2 \sinh v_1\,\pi \cos v_2\,\pi}{a\,(\sinh^2 v_1\,\pi + \sin^2 v_2\,\pi)} \ldots\ldots\ldots (70b)$$

In Eq. 69 m is Poisson's number (10/3 for metals). If m is neglected, $B = E\,I$. Because the deflections and pressures are assumed to be proportional (Eq. 15), the expression for the influence line of passive pressures becomes:

$$p_1 = K\,\eta = \sqrt{\frac{a^2 - 1}{2\,r}}\left(\frac{2\,v_1\,v_2}{a^2\,\pi} + \Phi \sinh v_1\,\phi \sin v_2\,\phi - \Psi \cosh v_1\,\phi \cos v_2\,\phi\right) \ldots\ldots\ldots\ldots (71)$$

The evaluation of this influence line for the pressures and reactions acting on the ring, assumed to be rigid, gives the passive pressures on the elastic ring. The algebraic summation of the values thus obtained and of the pressures and reactions producing them constitutes the actual load distribution on the deformed ring. The actual stresses in the deformed ring are obtained by applying this actual load distribution to influence lines which are generally valid for a rigid circular ring. The generally valid influence lines are the boundary values of Eqs. 68 and 71 and of the expressions for moment, shear, and thrust that are similar to them. These stresses refer to the conditions: $K = 0$, $B = \infty$, $a = 1$, $v_1 = 0$, and $v_2 = 1$; and, for radial loads, they become

$$M = \frac{r}{2\,\pi}\left(\phi \sin \phi + \frac{\cos \phi}{2} - 1\right) \ldots\ldots\ldots\ldots (72a)$$

$$V = \frac{1}{2\,\pi}\left(\phi \cos \phi + \frac{\sin \phi}{2}\right) \ldots\ldots\ldots\ldots (72b)$$

and

$$T = \frac{1}{2\pi}\left(\phi \sin \phi + \frac{\cos \phi}{2}\right) \ldots\ldots\ldots\ldots\ldots\ldots (72c)$$

In Section 28, Mr. Bull states that the critical stresses and cross-sectional areas indicated in Fig. 13 are in good agreement with actual sections used in large corrugated steel culverts.[6] This agreement is due only to the circumstance that the reduction of the stresses by the deformations of the culverts received consideration in the design. The support and loading conditions as well as the deformations of, and the moment distribution in, these culverts are different from those on which Figs. 12 and 13 are based. The culverts are cradled in a firm bed of soil, and the backfill around their sides is compacted to a desired density. The maximum moment in the culverts occurs at the invert and not at the crown; and it is opposite in sign to that indicated in Fig. 12.

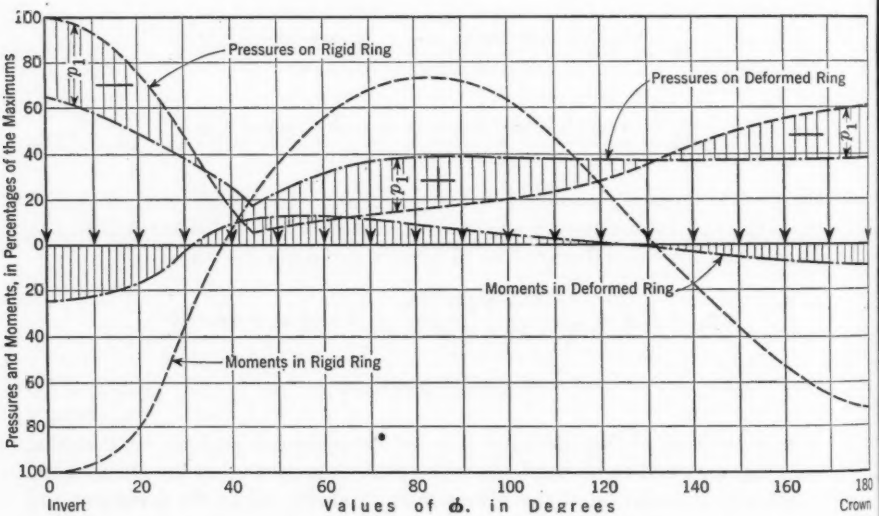

FIG. 30.—PRESSURE AND MOMENT DISTRIBUTION OF RIGID AND DEFORMED RING (FOR DEFINITION OF ϕ, SEE FIG. 29)

In Fig. 30 the pressures on, and the corresponding moments in, a ring that was first assumed to be rigid and the modification of the pressures by the deformations of the ring and of the actual pressures on, and moments in, the deformed ring are indicated in percentages of the maximum values. This diagram facilitates the visualization of the effect of the deformations. The wide-shaded areas between the pressure diagrams indicate the deformations of the ring and the pressure modifications resulting from these deformations. The close-shaded areas indicate the actual moments. The distribution of the

[6] *Engineering News-Record*, November 7, 1940, p. 74.

pressures on the deformed ring, as obtained by the use of Eq. 71, is identical with the experimental results of M. G. Spangler,[7] M. Am. Soc. C. E.

The functional relations between the forces acting and internal stresses of an elastic ring embedded in an elastic medium are thus shown to be well established. Although he approaches the problem indirectly, Mr. Bull contributes to this knowledge. However, the paper does not help to dispel the uncertainties concerning the magnitude and variation of the forces acting on the tunnel ring. Until methods are found by which these forces can be determined or controlled as reliably as in the case of the culvert type of structure, claims for the rational design of the shield-driven tunnel lining are not warranted.

[7] "The Structural Design of Flexible Pipe Culverts," by M. G. Spangler, *Bulletin No. 153*, Eng. Experiment Station, Iowa State College, Ames, 1941.

AMERICAN SOCIETY OF CIVIL ENGINEERS

Founded November 5, 1852

DISCUSSIONS

DETERIORATION OF CONCRETE DAMS DUE TO ALKALI-AGGREGATE REACTION

Discussion

BY J. C. WITT

J. C. WITT,[10] M. AM. SOC. C. E.[10a]—For convenience in discussion, the writer has divided the title of this paper into three sections, each of which refers to a section of the paper:

1	2	3
"Deterioration of Concrete Dams	Due to	Alkali-Aggregate Reaction."

The first section of the paper consists largely of a rather general account of deteriorated concrete, together with descriptions and illustrations of some examples. Many papers have appeared in which the deterioration of various types of building materials has been discussed, and examples almost without limit could be listed. In the third section, chemical reactions between compounds of alkalies and compounds of silicon are mentioned. These reactions have been known for a long time.

The tying together of the two groups of phenomena by the second section of the title suggests that the relation of the two is to be demonstrated in the paper. This relation is not demonstrated. In fact, if, by the reading of previous papers, one had been convinced that an increase of a few tenths of one per cent of alkali compounds in a cement would cause concrete to deteriorate, some statements in this paper might weaken his belief materially. Some of the statements that suggest this conclusion are:

(*a*) "The problem is extremely complicated, however, and many questions, practical and technical, remain to be answered satisfactorily" (see heading, "Synopsis").

(*b*) "It is suspected that, under some conditions, restraint is sufficient to prevent most of the expansion that would normally occur if the concrete was

NOTE.—This paper by R. F. Blanks and H. S. Meissner was published in January, 1945, *Proceedings*. Discussion on this paper has appeared in *Proceedings*, as follows: September, 1945, by Ralph R. Proctor, Milton D. Burris, H. A. Kammer, Thomas E. Stanton, R. W. Spencer, and W. L. Chadwick.

[10] Tech. Director, Marquette Cement Mfg. Co., Chicago, Ill.

[10a] Received by the Secretary September 27, 1945.

not restrained" (see heading, "Symptoms and Diagnosis of Alkali-Aggregate Deterioration in Concrete Dams"). Statement (*b*) implies that even in concrete free from cracks reactions tending to cause deterioration may be in progress.

(*c*) "Chemical analyses of the gels show them to be composed essentially of sodium and potassium silicates" (see paragraph that introduces Table 1). The analyses in Table 1 indicate that the gels contain sodium, potassium, and silicon; but they do not indicate how these elements are combined.

(*d*) "Hand specimen and microscopic study of core samples from affected concrete also invariably reveal what appear to be zones of chemical reactivity, alteration, or infiltration around certain aggregate particles, as shown in Fig. 5."

The authors have cited a number of references in support of their statements, and they could have cited additional ones. Many statements in opposition could also be made. For example, in discussing the expansion of mortar bars made with 106 cements varying in alkali content, W. C. Hanna (15)[10b] states:

> "At the age of 2 months the expansions of these bars, with few exceptions, were observed to be definitely related to the alkali content of the cements. At 6 months many exceptions were observed in this relation, and at the age of 18 months nearly all of the bars had expanded excessively. In many instances bars of low alkali content expanded to a greater extent than those of higher alkali content. * * * Some bars to which a deliberate addition of sodium hydroxide was made showed lower expansions than companion bars made without addition."

No one should accept the relation between the deterioration of concrete and the alkali content of cement expressed, and implied, in the paper without familiarizing himself with the great mass of information on this subject that is available in literature.

Under the heading, "Corrective and Preventive Measures," the following statements are made:

(*e*) "Experience to date indicates that reactive aggregates can be used without danger of destructive reaction, provided that low-alkali cement (less than 0.60% $Na_2O + K_2O$) is employed (see Fig. 7)."

(*f*) "Specification of low-alkali cement for all important hydraulic structures is strongly recommended regardless of what may or may not be known about the reactive tendencies of the aggregates to be used." If the deterioration of concrete may be caused by internal alkali compounds, and if there is a preventive measure, surely this preventive measure (statements (*e*) and (*f*)) is not so simple as to be merely a matter of reducing the percentage of alkali compounds in the cement. Many factors are involved, some of which are the total sodium and potassium in the concrete (not in the cement only), and the nature of their compounds.

(*g*) "Such a precautionary measure [reduction in alkali content] not only provides insurance against possible eventual deterioration due to alkali-

[10b] Numerals in parentheses, thus: (15), refer to corresponding items in the Bibliography (see Appendix of the paper), and at the end of discussion in this issue.

aggregate reactions, but limits undesirable constituents of Portland cements and usually improves the quality in several other ways." Some examples are mentioned in which, "the reduction in alkali content has been accompanied by marked reductions in C_4AF (tetracalcium alumino-ferrite), which is a fluxing material having little cementing value in itself, and lower C_3A (tricalcium aluminate), which is generally considered to be an undesirable compound. Coincidentally the principal cementing compounds, C_3S (tricalcium silicate) and C_2S (dicalcium silicate), have been increased as much as 9%." There is no fixed relation between the alkali content of a cement and the percentages of the principal clinker minerals. This applies to the succeeding paragraph also.

(*h*) "It seems evident that the additional cost of low-alkali cement, which may range from nothing to about 20¢ per bbl, is more than repaid by the improvement in quality alone." If the authors mean the manufacturing cost, such a general statement is not warranted.

The lag between research accomplishments and their application is one of the most serious retarders of industry. Also serious, although far less common, is the lag between application and research accomplishments.

Bibliography.—

(15) **"Notes on the 'Effect of Alkalies in Portland Cement on the Durability of Concrete,'"** by W. C. Hanna, *Proceedings*, A.S.T.M., Vol. 43, 1943, p. 210.

AMERICAN SOCIETY OF CIVIL ENGINEERS

Founded November 5, 1852

DISCUSSIONS

COMPUTING COAGULANT REQUIREMENTS IN SLUDGE CONDITIONING

Discussion

BY WALTER H. BROWN, JR.

WALTER H. BROWN, JR.,[23] ESQ.[23a]—The purpose of this discussion is to show that, through the use of the equation recommended by Mr. Genter, material savings were made in the use of ferric chloride at the Cranston sewage treatment works. The writer is not a chemist and will therefore limit his remarks to the mechanical results obtained.

By substituting Eqs. 2*a* and 4*b* into Eq. 5 in place of Y_1 and Y_2, an equation for the total dose of ferric chloride for elutriated sludge is evolved, as follows—

$$\text{Total dose } FeCl_3\ (\%) = \frac{H_2O\ (\%)}{\text{Solids}\ (\%)} \times 0.0001 \times \text{alkalinity (ppm)} \times 1.08 + \frac{\text{Volatile matter}\ (\%)}{\text{Ash}\ (\%)} \times 1.6 \quad \ldots\ldots\ldots\ldots\ldots\ldots (11)$$

By using Eq. 11, Buechner funnel tests were performed in the laboratory at Cranston, the results of which checked closely the dosage as determined theoretically. However, when such dosage was applied to the elutriated sludge in actual practice, the sludge was absolutely unmanageable. It was found that almost an 80% increase above the theoretical was required. This fact led to a suspicion that the ferric feeders or mixing tank, or both, were not functioning as efficiently as possible.

Examination proved that the ferric feeders were very erratic in their operation. They were subsequently discarded and a volumetric type feeder was designed by the writer. After a period of adjustment and refinement, the actual dose was found to be approaching the theoretical. Further investigation showed that the mixing tank at Cranston was short-circuited; and, after that was remedied, Eq. 11 yielded the actual as well as the theoretical dosage.

Table 7 contains the data that led to a check of the equipment at the Cranston works. In the period reported a fairly wet filter cake (77.8% H_2O)

NOTE.—This paper by A. L. Genter was published in March, 1945, *Proceedings*. Discussion on this paper has appeared in *Proceedings*, as follows: June, 1945, by Paul D. McNamee; and October, 1945, by D. L. McLean, and K. Fraschina.

[23] Supt. Sewage Treatment, Dept. of Public Works, City of Cranston, Cranston, R. I.

[23a] Received by the Secretary August 6, 1945.

was being produced with an average excess ferric dose of approximately 74%. For the months of May through September, 1945, the overdose was only about 8% and the filter cake had been reduced to about 76.5% H_2O. This resulted in a substantial saving in the use of ferric chloride. Furthermore, the digested

TABLE 7.—CHECK TESTS ON FERRIC FEEDERS, SEWAGE TREATMENT WORKS AT CRANSTON, R. I.

(Units Are Percentages Except as Indicated)

Month	Primary Sludge		Digested Sludge			Elutriated Sludge			Filter Cake		$FeCl_3$ (lb)	$FeCl_3$ (Percentage of Dry Solids)		
	Solids	Volatile	Solids	Volatile	Alkalinity[a]	Solids	Volatile	Alkalinity[a]	H_2O	Dry solids[b]		Actual	Theoretical	Excess[c]
	(1)	(2)	(3)	(4)	(5)	(6)	(7)	(8)	(9)	(10)	(11)	(12)	(13)	(14)
(a) Original Feeders														
1944:														
July	4.60	77.8	4.58	61.1	4,745	4.12	60.5	415	78.2	58,930	3,771	6.40	3.4	88
August	4.61	78.4	4.49	60.1	4,714	4.36	59.8	416	77.3	56,930	3,043	5.34	3.4	56
September	4.92	78.3	5.21	59.7	5,675	4.52	59.2	431	77.4	51,590	3,395	6.58	3.3	100
October	4.75	80.3	5.62	59.0	6,125	4.03	58.9	413	78.2	40,100	2,323	5.80	3.4	71
November	5.11	76.3	...	...	...	3.89	59.3	374	78.8	39,360	2,050	5.21	3.3	58
December	4.58	75.8	7.38	44.1	5,360	4.08	51.1	553	76.7	45,364	2,325	5.12	3.1	64
1945:														
January	4.51	80.8	5.50	53.6	5,312	4.37	54.4	613	78.3	31,508	1,909	6.06	3.4	79
February	4.80	78.3	6.42	52.9	6,350	4.24	57.7	760	79.7	5,420	317	5.84	4.1	41
(b) New Feeder														
1945:														
March	4.77	80.3	6.74	53.4	6,425	4.37	55.7	586	78.6	37,980	1,844	4.86	3.4	44
April	5.43	80.1	5.57	54.2	5,815	4.45	56.1	553	78.1	25,800	1,100	4.26	3.3	30
May	4.83	76.3	6.08	55.1	5,400	4.47	56.2	362	77.1	31,770	1,092	3.43	3.0	13
June	5.80	74.9	6.00	54.0	6,083	4.83	54.5	411	76.8	44,580	1,506	3.38	2.8	21
July	6.02	71.8	7.01	52.9	6,250	5.63	51.7	559	76.0	50,450	1,628	3.23	2.8	14
August	5.48	76.9	7.44	53.1	6,500	5.12	51.4	583	76.0	59,220	1,684	2.85	2.8	4
September	5.60	79.2	6.47	52.1	6,080	4.85	54.4	609	76.3	44,220	1,259	2.84	3.2	−12

[a] Parts per million. [b] Total dry solids, in pounds. [c] Percentage excess (Col. 12 − Col. 13)/Col. 13.

sludge at the Cranston works now contains, on the average, less volatile matter and much more alkalinity than shown in Table 2. Due to the relatively large quantities of brewery waste discharged into the sewers and treated at the Cranston plant, sludge digestion is particularly turbulent (gas production, 1.7 cu ft per capita per day) and the resulting alkalinity of the digested sludge is notably high. As will be seen from comparison of Cols. 2, 4, and 7, showing the volatile contents of the digested and elutriated sludges, the latter is frequently higher than the former. This is due to the accumulation of top, or less completely digested, solids sent to elutriation.

In view of the effects of such industrial wastes on the treatment at Cranston, for some time the writer doubted the applicability of Mr. Genter's equation to the sludge treated at Cranston; but subsequent tests and investigations have demonstrated that this basic equation undoubtedly holds.

AMERICAN SOCIETY OF CIVIL ENGINEERS

Founded November 5, 1852

DISCUSSIONS

DESIGN OF ROADBEDS

Discussion

BY DELBERT L. LACEY

DELBERT L. LACEY,[33] ESQ.[33a]—Among highway engineers there are two schools of thought regarding the proper density to which soils in roadbeds should be compacted. One group contends that an extremely high soil density with a resultant low void space is necessary to provide adequate permanent support for traffic loads. The other group contends that each soil has some "natural" density or range of "natural" density, and although placed outside the density range, either above or below it, when exposed to cycles of freezing and thawing and moisture changes, the soil will, return to its "natural" density state. Therefore, it is the contention of the second group that it is useless and a waste of effort to compact fine-grained plastic soils to a density greater than the "natural" density as such soils will eventually return to that density.

The contention of the second group of engineers is largely based on observations made on plastic soils that were compacted at low moisture contents and fairly high densities. Pavements placed on such soils become distorted as the soil beneath the edges of the pavement and beneath expansion joints absorbs moisture from the surface—causing the soil to undergo a considerable volume increase and to exert sufficient force to lift sections of the pavement above the original position. Since not all the subgrade soil has access to this moisture increase, the part of the soil under the center of the pavement and for some distance back of the joints does not undergo any volume change, and the remaining pavement stays in its original position. The result is a very disagreeable riding surface.

However, laboratory research conducted by the Kansas Highway Department[34] to determine the expansive properties of soils indicates that the moisture content at which a soil is compacted has more influence on volume increase (while the soil absorbs moisture) than does the density to which it was com-

NOTE.—This paper by Ira B. Mullis was published in April, 1945, *Proceedings*. Discussion on this paper has appeared in *Proceedings*, as follows: October, 1945, by Charles W. Britzius, J. T. L. McNew, and Gustavo Pérez Guerra; and November, 1945, by Jacob Feld, and Jasper L. Stuckey.

[33] Field Soils Engr., State Highway Comm. of Kansas, Topeka, Kans.

[33a] Received by the Secretary October 26, 1945.

[34] "The Results of Tests to Determine the Expansive Properties of Soils," by Harold Allen and A. W. Johnson, *Proceedings*, Highway Research Board, National Research Council, 1936, p. 220.

pacted. During this research, specimens of a soil were compacted at a number of different moisture contents and to various degrees of compaction. A load equivalent to the weight of a concrete pavement was placed on each specimen, and each specimen was permitted to absorb water until all vertical movement of the soil ceased. The vertical movement was measured and the volume increase of the specimen, based on original volume, was calculated. The results of a series of these tests conducted on a silty clay loam soil to determine percentage of volume increase are shown in Table 8. The volume change of a soil definitely decreases as the initial moisture content at which the soil was compacted is increased. At any given moisture content, on the other hand, there is very little decrease in the soil swell if the density to which the soil was compacted is increased.

TABLE 8.—THE PERCENTAGE INCREASE IN THE VOLUME OF SOIL AS AFFECTED BY THE COMPACTED DENSITY AND THE PERCENTAGE MOISTURE CONTENT AT WHICH THE SOIL WAS COMPACTED

Compacted density (lb per cu ft)	Percentage Moisture When Compacted				
	10	12	14	16	18
94	1.0	3.2	2.6	1.6	....
100	5.5	3.6	2.6	1.8	1.2
106	5.7	4.4	2.6	1.6	0.7
112	5.6	4.1	2.5	1.4	0.0
115	5.5	3.6	1.5	0.8	....

Therefore, had the plastic soils that caused pavement distortion been compacted to the same high densities, but at higher moisture contents, the volume change would not have been large enough to cause any appreciable change in the pavement elevation. This conclusion is logical when it is considered that, under an impervious surface that retards evaporation, soils tend to absorb moisture until their void space is nearly filled. Therefore, if sufficient moisture is present in the soil during compaction nearly to fill the void space and to satisfy the colloidal requirements, there will not be space for enough additional moisture to cause detrimental soil swell. In the light of the foregoing information and line of reasoning, there seems to be very little danger of overcompacting a soil if it contains sufficient moisture to fill the voids when compaction is completed.

In further support of the author's contention that high soil densities are essential to a durable roadbed, it should be emphasized that the deflection of the surface of a soil caused by a given wheel load is directly dependent upon the existing density of the soil. Thus, a loose, poorly compacted soil might deflect enough under a wheel load to rupture the wearing surface. This deflection would be due to an increase in the soil density; whereas if the soil had been compacted to a high density before the surface was constructed, this surface deflection due to density change would have been eliminated and all deflection would have been due to the plastic flow of the soil. Since resistance to plastic flow is largely dependent upon friction between the soil particles and since these particles are in more intimate contact when the soil exists at a high density, the resistance of the soil to plastic flow is increased, and consequently a stronger roadbed results.

Additional evidence to substantiate the author's contention that a high

state of compaction provides additional soil strength or bearing power is presented in Table 9. These data are the results of triaxial shear tests conducted on a number of soils, largely from the central and western semiarid areas of Kansas. The values in Cols. 9 and 12, Table 9, are the moduli of deformation of the soil tested, for a depth below the point of load application equal to the

TABLE 9.—SUBGRADE MODULUS FOR SOILS TESTED AT VARIOUS DENSITIES (TRIAXIAL SHEAR TESTS)

Sample No.	Class	Plastic index	Sand (%)	Clay (%)	Specific gravity	Test 1, Density Lower			Test 2, Density Higher		
						Density[a]	Moisture[b]	Modulus[c]	Density[a]	Moisture[b]	Modulus[c]
(1)	(2)	(3)	(4)	(5)	(6)	(7)	(8)	(9)	(10)	(11)	(12)
216	SiL	20	20	19	2.55	100	22	905	108	20	2,345
9	SiL	11	36	8	2.55	81	16	645	89	17	1,285
12	SiL	11	26	14	2.60	100	20	810	112	18	1,155
231	SiL	13	32	14	2.55	93	20	540	106	20	4,600
212	SiL	13	31	13	2.59	88	16	550	100	16	2,300
18	SiL	10	20	15	2.54	82	10	335	103	16	1,025
21[d]	SiL	4	23	6	2.55	96	17	470	108	4	4,755
44	SiL	15	18	18	2.51	98	23	660	113	18	1,135
44[d]	SiL	15	18	18	2.51	105	18	445	115	14	1,657
64	SiL	13	25	17	2.51	109	18	1,400	117	15	2,480
64[d]	SiL	13	25	17	2.51	105	17	1,990	121	11	3,195
72	SiL	16	22	13	2.45	91	16	600	101	20	2,655
84	SiL	9	20	8	2.55	83	19	611	97	21	2,680
2A[d]	SiC	14	13	34	2.51	94	21	820	99	23	1,530
130	SiC	18	16	21	2.58	97	19	1,095	104	19	1,385
138	SiCL	25	14	27	2.58	103	23	745	112	18	4,310
146	SiL	14	17	17	2.55	88	20	336	101	20	2,300
153	SiL	11	32	15	2.54	101	20	940	110	19	1,570
160	SiCL	13	18	21	2.56	94	17	1,280	98	13	3,720
164	SiL	14	19	18	2.55	100	19	2,415	109	19	6,040

[a] Initial density (before saturation) in pounds per cubic foot. [b] Initial moisture content (before saturation), expressed as percentage of dry weight. [c] Modulus of deformation, in pounds per square inch, for a depth below the point of load application equal to the thickness of the flexible surface required. [d] The four samples indicated in Col. 1 were remolded in the laboratory. The remaining sixteen were obtained in an undisturbed condition from the existing roadbed.

thickness of flexible surface required. Thus, a soil having a high modulus would require a thinner base course to support a given load than would a soil having a low modulus.

The results of triaxial shear tests conducted on two types of samples are summarized in Table 9. One type is obtained by cutting out an undisturbed section of an existing roadbed and trimming it to proper size for testing, with a minimum of particle disturbance. The second type of sample is prepared for testing by compacting loose, moist soil into a mold of proper size. After the samples are either cut or molded to proper size, they are saturated by admitting a supply of water to the lower part of the sample and applying a vacuum to the upper part until free water is drawn through. Therefore, the two specimens prepared from each sample were treated in the same manner, the only difference being that one specimen existed at a lower density prior to saturation than the other. In each case, regardless of whether undisturbed or molded samples were tested, an increase in density resulted in an appreciable increase in the subgrade modulus value.

One specimen of each undisturbed sample was obtained from the extreme upper section of the roadway, representing a high-density stratum condition

developed by the action of traffic. The density of such a sample is usually higher than standard density for the soil, and is always considerably higher than the density of the material below that stratum. Some of these crust-density values were so high that it was not possible to duplicate them in the laboratory using a large static load applied by a hydraulic compression machine.

A large proportion of the undisturbed samples was obtained from beneath flexible bituminous wearing surfaces that had been in place for several years. However, the high density condition in the crust, developed by traffic before the surface was constructed, still existed. Thus, soils similar to those in Table 9 do not undergo any appreciable loss of density with the passage of time if they have reasonable protection from surface moisture.

The data presented by Mr. Mullis and the limited quantity of data included in this discussion indicate definitely that high compaction of roadbeds is essential if the best possible use is to be made of materials that exist within the right-of-way limits. Although most of the data presented in this discussion have been within the present working range of densities (that is, those commonly obtained during construction), they indicate the need for research to determine the increase in durability and bearing power obtained by compacting soils to much greater densities than can be obtained with present compaction equipment. Such a research program might show that it would be more economical to spend more effort and money during construction to compact the soils that comprise the upper section of the road structure to an extremely high density than to spend the same amount of effort and money on expensive road surfaces.

AMERICAN SOCIETY OF CIVIL ENGINEERS

Founded November 5, 1852

DISCUSSIONS

ECONOMICS OF PHOTOGRAMMETRY

Discussion

BY W. J. RYAN

W. J. RYAN,[10] M. AM. SOC. C. E.[10a]—The difficulties involved in mapping heavily wooded areas are worthy of note in any discussion of photogrammetry. These difficulties are much more serious in the Pacific Northwest than in other parts of the United States. The Corps of Engineers, U. S. Army, has mapped a large part of the Pacific Coast area on the scale of 1 : 62,500 with 100-ft contours. Although these maps have great value, they are not entirely dependable because the actual position of the ground cannot be determined through a cover of dense coniferous forest. The method most generally used is: First, mapping the tree tops and then correcting for the height of the timber (which may vary from 25 ft to 250 ft, resulting in large errors).

Photogrammetric mapping is also under a heavy handicap because of the small number of suitable flying days. Forests are frequently covered with smoke during the late summer and fall, and the days or hours of bright weather during the spring are limited. In the latitude of Oregon and Washington the winter months do not provide satisfactory light.

Heavy forest areas also make suitable ground control difficult. In many cases, it is impossible to identify picture points without artificial marking, which sometimes involves climbing and topping trees. Some controls have been established by building towers of trees topped 100 ft or more from the ground. These factors make aerial mapping less satisfactory, because they may delay a project a full year beyond the planned time for completion.

If a map is to be of practical value to the logging industry, it must necessarily have the section corner positions as established by the General Land Office (GLO). The proper location of these corners on the map is one of the most difficult factors in mapping. The original surveys were frequently made with little care, and the accepted plat often does not represent the position of the corners on the ground. For commercial use, a map with a scale of any-

NOTE.—This paper by Leon T. Eliel was published in March, 1945, *Proceedings*. Discussion on this paper has appeared in *Proceedings*, as follows: June, 1945, by Raymond A. Hill, Raymond L. Moore and Ralph S. Pearse; and October, 1945, by George D. Whitmore, Benjamin A. Wasil, Charles H. Davey, and Robert H. Randall.

[10] Chf. Engr., Weyerhaeuser Timber Co., Tacoma, Wash.

[10a] Received by Secretary October 30, 1945.

thing less than 1 in. equals 400 ft is more valuable for representing the positions of the section corners with relation to geographical points than for providing extreme accuracy in the actual distances on the map. It has been found possible to place section corners on these aerial maps on the basis of the information available from ground surveys and from stream crossings shown on the GLO plat, thus preparing maps of value for reconnaissance work. Such maps must give the drainage and the shape of the terrain, but extreme accuracy in elevation or position are not necessary. The specifications for such work could be much less rigid than those adopted as a standard by mapping agencies of the U. S. Government, if methods were offered for doing the work more rapidly and economically. The U. S. Geological Survey is using a combination of aerial and ground methods that seems to be the most practical answer to the problem if federal requirements for map accuracy are to be maintained. This process is slow and expensive.

If the vast area still unmapped could be covered by another system, and if maps could be made available for this generation instead of the next, it would be a genuine economic accomplishment.

In forest surveys, the preparation of mosaics seldom seems worth the effort, as individual pictures, properly indexed on a planimetric map, are usually more serviceable. For any larger scale than that used for a purely reconnaissance map, the study of the individual prints through a stereoscope is frequently more satisfactory than the contour map that can be made in a heavily timbered area.

In the case of actual working maps for locating roads, railroads, logging plans, and forestry developments, it is still necessary to use ground methods. The writer has found that contour maps made by the strip method, using a slope level and chain, are more dependable and more economical than maps made by the use of plane table. On a scale of 400 ft to the inch with 10-ft to 25-ft contours, such maps cost as much as one dollar per acre. When photogrammetry can develop a method for making such maps, it should be economically advantageous.

In spite of difficulties, there is still a large field for aerial photography in the logging industry. Possibilities of distinguishing the type and conditions of the forest through photographs are unlimited and the further development of color and filters will add to the value of these studies.

The author has stressed the relative value of the various types of equipment, thus clarifying the possibilities that are available to the engineer. Consideration of the subject from the viewpoint of cost is commendable, and further reports are needed to define the relationship between cost and accuracy before any economic procedure for a project can be established.

AMERICAN SOCIETY OF CIVIL ENGINEERS

Founded November 5, 1852

DISCUSSIONS

DESIGN DEVELOPMENTS—STRUCTURES OF THE TENNESSEE VALLEY AUTHORITY A SYMPOSIUM

Discussion

BY A. T. LARNED

A. T. LARNED,[12] M. AM. SOC. C. E.[12a]—Clearly and orderly, the second paper of the Symposium (by Messrs. Palo and Marks) describes the layout of a type of hydro station which has become quite standardized for large low-head, propeller type installations. The title of this paper is broad and, perhaps, should have been more explicit, as only a part of the total hydro plants is laid out with the station integral with the dam so that, for stability, advantage is taken of the mass of concrete in the dam itself. There are many other hydro developments already built and to be built in the future, with dams remote from the station and with tunnel, canal, and long penstocks utilizing water under medium or high heads, in which the design and layout of the station involve problems of a somewhat different nature than those outlined in the paper.

Functional Considerations of Design.—Quite appropriately, Messrs. Palo and Marks have emphasized the functional characteristics of power-plant layout, which enables one to visualize the over-all performance of each type of equipment and its interrelation with other types, so that each can be arranged to perform its assigned task in the most effective manner and with the minimum space requirement.

In power-plant design, the realization of directness and compactness, and the elimination of excess or waste space, assure that the lowest cost will be obtained in the construction of the plant. The designer sets the pattern and there is nothing the construction man can do later to reduce costs if the designer failed in his layout. In other words, "the money is already spent as soon as the design leaves the drafting table."

In regard to allotting space for future maintenance and repair requirements, it is of particular importance that heed should be given to the advice

NOTE.—This Symposium was published in October, 1945, *Proceedings*.

[12] Chf. Civ. Engr., Ebasco Services Inc., New York, N. Y.

[12a] Received by the Secretary October 31, 1945.

and counsel of the operating group who in the future must "live" with the plant, in order that all equipment be made easily accessible and the repair and tool rooms be arranged conveniently.

Simplification of Design.—The features of simplicity and economy of design have been stressed by Messrs. Palo and Marks, and it is evident that the outdoor and semi-outdoor types of station have been valuable contributing factors in the accomplishment of this objective. The writer is aware of no adverse experience resulting from this type of installation, and the elimination of expensive superstructure to house nothing more than a traveling crane has resulted in marked economy. Steam-plant designers have realized the advantages of the outdoor type of station and many of the newer steam installations utilize outdoor boilers, auxiliary equipment such as circulating fans, and, in some cases, outdoor turbine units.

Messrs. Palo and Marks make no mention of the rôle that the umbrella or overhung type of generator has played in the design of the outdoor type of hydro station. This arrangement of generating unit enables a substantial reduction in powerhouse costs through reduced head clearances. The advantages of the umbrella type of generator are that it reduces the guide bearings from three to two and materially shortens the span necessary for the bracket supporting the thrust bearing. This reduces the length of shaft necessary and also makes it possible to dismantle the generator for inspection and repairs without disturbing the thrust bearing, shaft, or turbine.

It is advantageous to restrict the control room to the minimum space possible, with due allowance for the addition of future electric controls. In most cases, for stations with one to three main generating units, the control room has been placed on the main operating floor between the units so that full visibility of the governors and generating equipment is possible. This avoids the need for a separate building and takes up floor space that would be wasted otherwise.

The advisability of locating the governors and actuating equipment on the generator floor to save space has been noted by Messrs. Palo and Marks. There is another reason for locating this apparatus and other auxiliaries on one floor in so far as possible, the number of men on a shift can be reduced to the minimum. This is an important consideration from the point of view of reduced operating costs and increasingly difficult labor conditions.

Model tests and tests of actual installations have shown that the entrance to the penstock or upstream side of the water passage need not be increased materially in size. A moderate increase in diameter by a properly shaped bell-mouth is all that is necessary to keep the entrance losses low. This type of construction is economical because the size of the intake gate can be kept to a minimum.

Design as Related to Concrete Construction.—The discussion of the need for, and the method of, locating construction joints (see Fig. 15) is especially helpful and should serve to impress both the engineer and the construction man with the need for care in placing concrete. Experience has proved that it is advantageous to have the construction joints located by the engineer rather than by the construction man. The need for an early decision as to the

location of these joints is well taken as the design will depend considerably upon their placement.

Although the Palo-Marks paper mentions only construction joints in the heavy substructure, it also would be well to call attention to the need for joints in the lighter concrete sections of the structure above the generator floor. Such joints are necessary for construction purposes and also to localize the cracks that would result if large areas of concrete walls were not protected by such construction.

In some of its recent designs for steam plants the writer's company has resorted to the use of special control joints in the reinforced-concrete walls and parapets of the buildings. These consisted of wood strips tacked to the forms to leave wedge-shaped joints in both the exterior and interior faces of the walls. These have been successful in eliminating the unsightly patterns of shrinkage or expansion cracks, and they control the location of the larger cracks that usually appear. The joints are filled with a concrete-colored calking compound which preseals any cracks that may occur.

A brief general statement as to the means adopted for securing watertight joints would be appreciated. The appearance of joints, after a few years, can either make or mar an otherwise perfect job.

The generation of heat in large blocks of concrete, and the damage resulting from subsequent shrinkage when the concrete is cool are well known in connection with the design and construction of dams. However, little has been published about this subject in connection with power-station structures, since most hydro developments have not been of the magnitude of those designed and built by the Tennessee Valley Authority (TVA) and other government agencies. The attention called to this factor, therefore, is timely and should help to make it easier for the engineer to sell to the construction organization the desirability of placing the concrete in the powerhouse substructure in the proper sequence and at the proper intervals of time.

Messrs. Palo and Marks have not mentioned form construction, particularly the construction of draft-tube forms. It has been found convenient to build these forms on an erection floor where wood-working machinery is convenient and working conditions neither cramped nor dangerous. The forms are built in large sections and transported to the powerhouse site by truck.

Large quantities of steel reinforcement usually are required in powerhouse substructures to carry and distribute the loads into the foundation. There is a tendency on the part of some construction men (as well as some engineers), not intimately connected with the design, to claim that the amount of reinforcement used is unnecessarily large. The Palo-Marks paper calls attention to the necessity and desirability of using considerable reinforcement both for structural strength and for resisting temperature and shrinkage stresses. In view of the large amount of reinforcing steel necessarily required, careful analysis should be made of the loads acting, or assumed to be acting, on the structure simultaneously so as not to make these loads larger than is absolutely necessary.

In the design and construction of the many hydroelectric plants with which the writer has been connected, it has not been considered necessary to provide

a gate at or near the downstream end of the draft tube except where the runner is located below tailwater. Operating experience over a period of about thirty years has confirmed the opinion that the need for draft-tube unwatering is very slight, and that provision for the installation of stop logs or a single panel bulkhead that can be used for any one of the units should suffice. In many cases, the omission of such downstream gates has made it possible to put the transformers on a platform on the downstream side of the powerhouse, thus making the electrical connections from the unit to the transformers very short and simple. In most cases, this has been a considerable advantage over the practice of placing the transformers at a distance, especially where the plant is in a place where it is necessary to go a considerable distance to find a large enough level piece of ground.

The concentration of load that may occur at the upstream nose of the piers in draft tubes, and the difficulty of caring for these loads, have been mentioned by Messrs. Palo and Marks. On several occasions the writer's firm has placed a short, built-up steel column at this point, with spread base and capital to take the load concentration. This column has been of aid also in supporting the form work for the draft tube.

Attention has been called to the presence of cracks in the side walls of the volute casings of three of the stations described in the second paper. These cracks were about 10 ft upstream from the center line of the unit. The similarity of the cracks in the three cases leads to the conclusion that a definite set of stresses has been the cause for the pattern of cracking. By referring to the cross sections of the station in question it will be noted that this is the point where the deep excavation starts for the draft tube. This reentrant angle into the concrete, if considered as a casting, could account for the failure, particularly if the line of excavation changed abruptly from vertical to horizontal. The writer has always attempted to excavate so that there is a fillet in the concrete and so that the change in direction is gradual.

The authors of the second paper (to which all the writer's comments are limited) are to be commended. It is to be hoped that the paper will stimulate further study and discussion of the many problems which it has raised.

AMERICAN SOCIETY OF CIVIL ENGINEERS

Founded November 5, 1852

DISCUSSIONS

CAVITATION IN HYDRAULIC STRUCTURES
A SYMPOSIUM

Discussion

BY C. A. MOCKMORE

C. A. MOCKMORE,[6] M. AM. SOC. C. E.[6a]—An excellent explanation of cavitation is presented by Professor Vennard. The Symposium offers some timely suggestions (which designers should bear in mind if they wish to minimize the destructive effects of cavitation)—avoidance of sharp curves and abrupt corners.

Obviously, pressures within the cavities in the flowing fluid must be low, but that does not necessitate a low pressure in the fluid a short distance from the surface of a conduit. Fig. 51(*a*) shows a cast-steel wicket gate of a water turbine operating under a head greater than 300 ft. Fig. 51(*b*) is an enlargement of one corner of this same wicket gate showing the manner in which the tough metal is worn away by cavitation. The effect of the roughness left by a milling machine during fabrication is noticeable.

Professor Vennard emphasizes the necessity that laboratory experiments should be concurrent with design to avoid the danger of cavitation. Perhaps a little extra care in fabrication would help to produce, as nearly as possible, the conditions called for in the design. Cavitation may be started by a very small irregularity in the surface of a conduit; and, once started, it may grow rapidly in destructive intensity.

Corrections for *Transactions:* In September, 1945, *Proceedings*, on page 1017, Fig. 14(*b*), direct the arrow on "El. 1365'" to the floor of the stilling basin; page 1020, line 40, change "h" to "H_m"; page 1021, Fig. 17(*a*), delete "$= 30\ h$"; page 1027, Fig. 20(*a*), in six places reading "29-In. Floor" etc., delete the hyphen and the period, thus denoting "29 In Floor" etc.; and, on page 1032, line 9, change "halves" to "half," and, in line 10, change "place" to "plate."

NOTE.—This Symposium was published in September, 1945, *Proceedings*.

[6] Prof. and Head, Dept. of Civ. Eng., Oregon State College, Corvallis, Ore.

[6a] Received by the Secretary November 13, 1945.

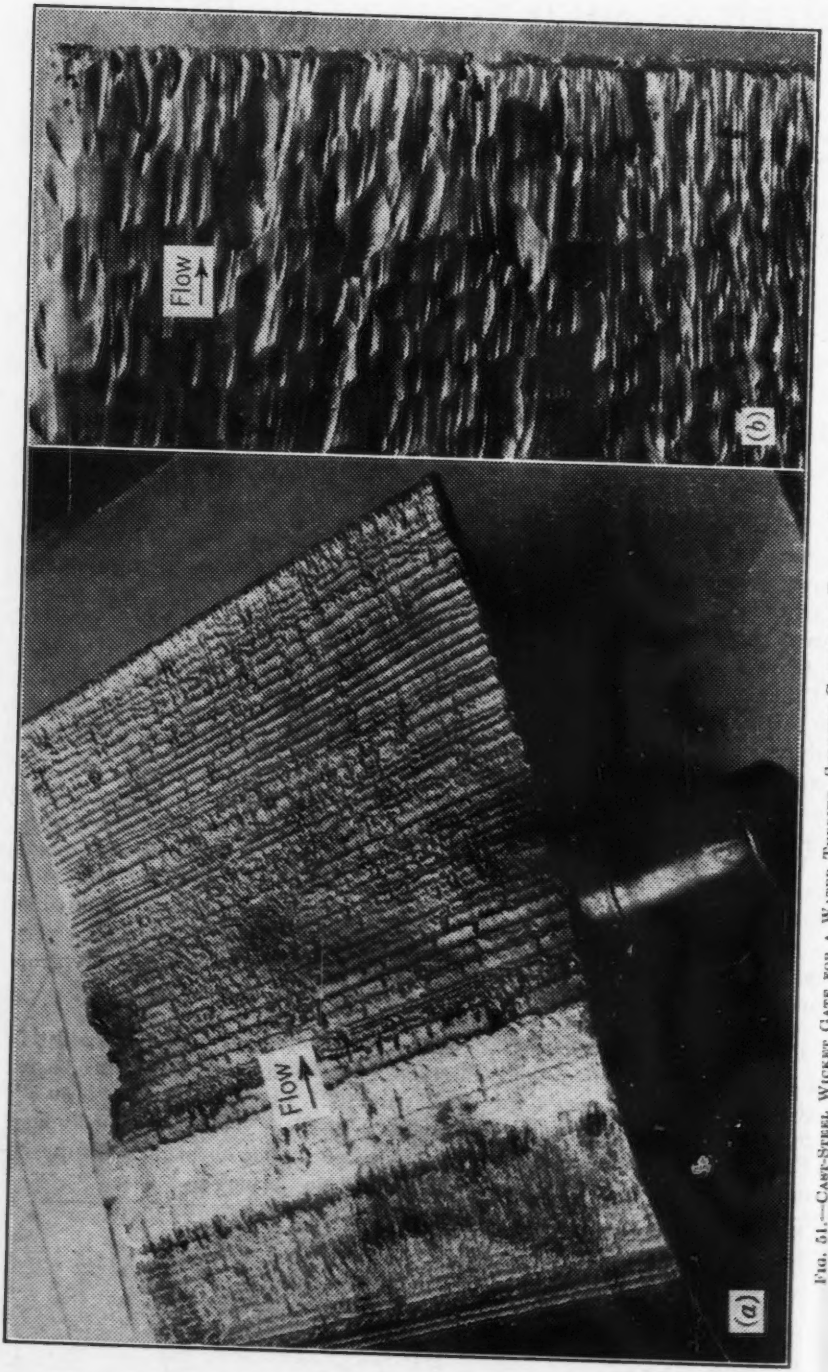

FIG. 51.—CAST-STEEL WICKET GATE FOR A WATER TURBINE, SHOWING CAVITATION EFFECTS RESULTING FROM AN IMPERFECT SURFACE FINISH

AMERICAN SOCIETY OF CIVIL ENGINEERS

Founded November 5, 1852

DISCUSSIONS

FUTURE OF LAKE MEAD AND ELEPHANT BUTTE RESERVOIR

Discussion

BY BERARD J. WITZIG

BERARD J. WITZIG,[89] ASSOC. M. AM. SOC. C. E.[89a]—Although the forecast for the future appears pessimistic, the paper presents a logical determination of the theoretical useful lives of two large reservoirs essential to the economic well-being of the Southwest. The lately emphasized concern of the engineering profession over the apparently inevitable decadence of the nation's river control resources is not new, but the mounting accumulation of records indicates that irreplaceable reservoir storage will be destroyed by sedimentation within a few generations.

Merely from a theoretical basis, the writer questions whether it is proper to assume a linear rate of loss of reservoir storage. If such factors as the method of reservoir operation, cyclic variations of rainfall and runoff, and changing erosion conditions are neglected, it seems reasonable to expect that the annual sedimentation rate would decrease with storage and with the effectiveness of the reservoir as a sediment trap. Available data for Elephant Butte Reservoir, plotted in Fig. 3, indicate that the rate of loss to 1940 was not linear. A more optimistic estimate of the life of the reservoir would be obtained if these data were extended by some exponential function, although the aforementioned omitted factors render such an extension highly academic. Linear extension undoubtedly results in the most conservative estimate of the probable useful life of the reservoir.

The average specific weight of the sediment deposited in Elephant Butte Reservoir, estimated by Mr. Stevens at 65 lb per cu ft, is probably as correct a value as can be determined from available data. However, the validity of applying this value to Lake Mead is questionable in view of other data,[90]

NOTE.—This paper by J. C. Stevens was published in May, 1945, *Proceedings*. Discussion on this paper has appeared in *Proceedings*, as follows: October, 1945, by D. C. Bondurant, John H. Bliss, Luna B. Leopold, Carl B. Brown, and G. E. P. Smith; and November, 1945, by Albert E. Coldwell, Walter B. Langbein, C. S. Howard, Charles Kirby Fox, H. V. Peterson, L. C. Crawford and P. C. Benedict, Charles P. Berkey, and Stafford C. Happ.

[89] Engr. (Civ.), U. S. Engr. Office, Buffalo, N. Y.

[89a] Received by the Secretary October 30, 1945.

[90] "The Silt Problem," by J. C. Stevens, *Transactions*, Am. Soc. C. E., Vol. 101 (1936), p. 222.

which indicate that Colorado River silts vary in specific weight from 37 lb per cu ft to more than 100 lb per cu ft.

Also, an estimate of the specific weight of sediment, based only on observations, probably errs on the low side, and the value thus computed is applicable only to the period of record and to the more or less immediate future. Additional sediment, to be deposited in the future, will impose a consolidating load on earlier deposits; and it is probable that the ultimate average specific weight of the deposits in their entirety will exceed the average for a shorter period during the earlier life of the reservoir. The older deposits will undoubtedly weigh more per unit volume than the newer deposits. Fluctuations of reservoir levels will also cause greater shrinkage in the sediments near the head and in the higher elevations of the basin than in those deposits which are continuously submerged.

Expectation of an increase in the specific weight is supported by the fact that, in 1913, the late W. W. Follett,[4] M. Am. Soc. C. E., used 53 lb per cu ft for silt in the Rio Grande; in 1935, the Soil Conservation Service[91] used 60 lb per cu ft; and Mr. Stevens adopts 65 lb per cu ft. The writer believes that within a few years the average specific weight of sediment in Elephant Butte Reservoir may exceed 70 lb per cu ft and may eventually approach 85 to 90 lb per cu ft. If data are available for the purpose, it would be of interest to learn the estimated ultimate specific weight based on the method proposed in 1943[25] by E. W. Lane, M. Am. Soc. C. E., and Victor A. Koelzer, Jun. Am. Soc. C. E.

The specific weight adopted for estimating future sedimentation rates may greatly influence the predicted useful life of a reservoir. Thus, if the average specific weight approximates 75 lb per cu ft at the end of the useful life, the reservoirs under discussion may actually have useful lives 15% longer than those estimated by the author.

However, differences of opinion on specific weights of sediments or on the estimated lives of the reservoirs do not reach the crux of the problem. The best and most economical reservoir sites have already been, or soon will be, utilized, and "a reservoir begins to die the day it is born."

Mr. Stevens suggests several measures to prolong the useful lives of Elephant Butte Reservoir and of Lake Mead. The writer agrees that land management is probably not a panacea for erosion ills, at least within economic limits, since it would probably be impracticable to reduce erosion rates below the natural norm prior to the influence of man-made conditions. Even if improvement in land management practices could decrease sedimentation rates by 50%, instead of by the 10% estimated by the author, the all-too-short estimated life of a reservoir would merely be doubled.

The possible use of density currents to void suspended silt before deposition through properly designed and located outlets in the dam has not yet been practicably demonstrated, and is generally not applicable to existing dams

[4] "Silt in the Rio Grande," by W. W. Follett, Dept. of State, International Boundary Commission, 1913.

[91] "Silting of Reservoirs," by Henry M. Eakin, revised by Carl B. Brown, *Technical Bulletin No. 524*, U. S. D. A., Washington, D. C., 1939, p. 99.

[25] See *Report No. 9* of "A Study of Methods Used in Measurement and Analysis of Sediment Loads in Streams," Iowa Inst. of Hydr. Research, Iowa City, Iowa, 1943.

and reservoirs. Outlets in future dams, where silting is expected to be serious, should be provided to explore this possibility. Further field and laboratory research on density currents in reservoirs appears to be a professional imperative.

The writer does not consider the suggested provision of upstream silt storage as more than a temporary expedient. Such a measure would merely postpone the inevitable reckoning, and would only transfer the destruction of reservoir storage to other locations. The one recommendation for this expedient would be that it might decrease erosion rates and silt loads by decreasing the effective stream gradients. The plan for developing the upstream storage suggested by the author for the Colorado River would extend the useful life of Lake Mead from an estimated 80 years to about 233 years. Probably something like this will be done, but it should be recognized that the problem is thus merely being postponed and not solved.

AMERICAN SOCIETY OF CIVIL ENGINEERS

Founded November 5, 1852

DISCUSSIONS

MOVING LOADS AND RESTRAINED BEAMS AND FRAMES

Discussion

BY J. KALB, G. ROLSMA AND F. W. GIESEKING, STANLEY S. SCHURE, AND ALEXANDER DODGE

J. KALB,[20] ESQ.[20a]—As examples of unusual structures to which the Brumfield method has been applied successfully, two interesting frames are presented herein to advance the discussion of Section 15. For example, Fig. 16 represents,

TABLE 3.—FRAME CHARACTERISTICS FOR THREE JOINTS OF FIG. 16

Member	Q	i	R	Member	C	Moment split[a]		
JOINT 2G								
G-21	2.32	0.668	0.710	G-12	0.261	(a)	0.596	0.833
2-GF	11.60	3.35	0.399	2-FG	0.454	0.212	(b)	0.167
G-23	4.03	0.902	0.556	G-32	0.373	0.788	0.404	(c)
JOINT 3G								
G-32	4.03	0.764	0.448	G-23	0.444	(a)	1	....
3-GC	1.515	0.448	0.764	3-CG	0.198	1	(b)	....
JOINT 3C								
C-32	6.58	1.20	0.343	C-23	0.534	(a)	0.275	0.536
C-34	7.40	1.39	0.330	C-43	0.595	0.247	(c)	0.464
3-CG	1.515	0.455	0.642	3-GC	0.221	0.753	0.725	(d)

[a] The lower-case letters in the moment-split column represent the possible radiating members at the joint under consideration, thus: (a), (b), (c), and (d) always refer to the members radiating downward, to the left, upward, and to the right, respectively, from the joint.

diagrammatically, one of the seven reinforced-concrete rigid-frame bents designed for a vocational high school to be constructed in New York, N. Y.

NOTE.—This paper by R. C. Brumfield was published in May, 1945, *Proceedings*. Discussion on this paper has appeared in *Proceedings*, as follows: October, 1945, by R. W. Stewart, Nathan D. Brodkin, and T. F. Hickerson; and November, 1945, by Max W. Strauss, D. A. Mackenzie, and Charles E. Schaffner.

[20] Asst. Civ. Engr. (Structural), Board of Education, New York, N. Y.

[20a] Received by the Secretary September 28, 1945.

Low Point of Roof
Finished Third Floor and Low Point of Gymnasium Roof
Finished Mezzanine Floor
Finished Gymnasium Floor
Finished Locker Room Floor
Finished Cafeteria Floor
w = 1 110 Lb per Ft (26% Live Load)
w = 1 600 Lb per Ft Live Load = 52.5%
w = 1 430 Lb per Ft Live Load = 42%
w = 3 240 Lb per Ft (17.6% Live Load)
w = 1 600 Lb per Ft Live Load = 48.7%
21×46-Tons, 6" Slab
11×18-Tons
11×20-Tons
12×22-Tons
12×18-Tons
Q = 12.3
Q = 13.0
Q = 9.8
Q = 8.33
Q = 8.65
Q = 10.95
Q = 11.6
Q = 1.515
Q = 7.4
Q = 6.58
Q = 3.79
Q = 4.03
Q = 2.32
Q = 4.65
Q = 4.94
Q = 4.88
Q = 4.41
17'3"
22'8"
15'6½"
10'6"
11'1½"
12'0½"
16'0"
15'5½"
19'9"
16'5½"
62'1"
15'4"
16'2½"
8'1"
7'8"
15'2½"
22'6½"
17'7½"
13'7½"
A
B
C
D
E
F
G
0
1
2
3
4CB
C43
3CG
C23
C34
C32
3GC
G32
0.197
0.380
0.258
0.279
0.595
0.534
0.221
0.424
0.428
0.238
0.312
0.268
0.27
0.278
0.276
0.493
0.444
0.373
0.261
0.272
0.387
0.5
0.167
0.833
0.212
0.788
0.198
0.596
0.404
0.303
0.23
0.426
0.331
0.367
0.394
0.398
0.4
34
24
36
20

FIG. 16

TABLE 4.—Analysis of Vierendeel Truss

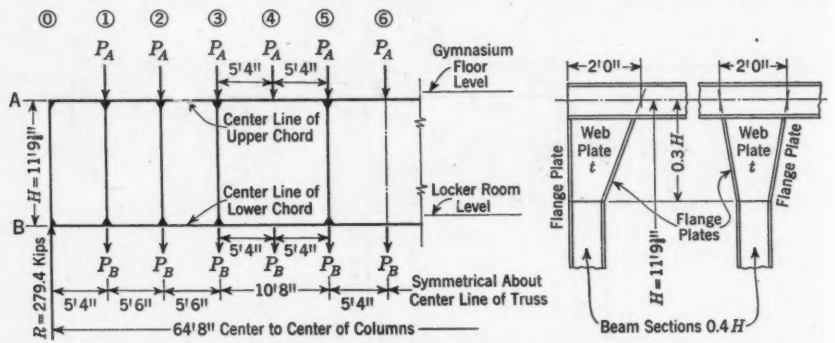

Member (see diagrams)	Physical Characteristics			Bending Moments, in Foot-Kips[a]			Direct Force, in Kips[b]	
	Beam section	Thickness (t in.) of web plates	Size of flange plates (in.)	Direct force neglected	Direct force considered	Live load[c] and direct force	Direct force neglected	Direct force considered[d]
	(1)	(2)	(3)	(4)	(5)	(6)	(7)	(8)
Joint A0:								
0-AB	12 WF 120	$\frac{1}{2}$	14 × 1	411 N	384 N	....	−279.4	
A-01	14 WF 167	....	....	411 R	384 R	....	− 69.5	− 65.0
Joint A1:								
1-AB	12 WF 120	$\frac{1}{2}$	14 × 1	653 N	609 N	....	− 2.3	
A-10	14 WF 167	....	....	356 R	325 R	....	− 69.5	
A-12	14 WF 167	....	....	297 R	284 R	....	−180.5	−168.0
Joint A2:								
2-AB	12 WF 120	$\frac{1}{2}$	14 × $\frac{3}{4}$	498 N	480 N	....	− 2.3	
A-21	14 WF 167	....	....	339 R	360 R	....	−180.5	
A-23	14 WF 211	....	....	159 R	120 R	....	−265.0	−249.5
Joint A3:								
3-AB	12 WF 120	$\frac{1}{2}$	14 × $\frac{3}{4}$	492 N	495 N	....	− 3.5	
A-32	14 WF 211	....	....	289 R	320 R	....	−265.0	
A-35	14 WF 211	....	....	203 R	175 R	225 R	−349.0	−333.5
Joint A5:								
5-AB	12 WF 79	$\frac{3}{4}$	14 × $\frac{1}{2}$	169 N	164 N	{70 R / 206 N}	− 4.6	
A-53	14 WF 211	....	....	329 R	368 R	....	−349.0	
A-55[1]	14 WF 211	....	....	160 N	204 N	344 N	−377.5	−368.1
Joint B0:								
0-BA	14 WF 120	$\frac{1}{2}$	14 × 1	411 N	384 N	....	−279.4	
B-01	....	....	....	411 R	384 R	....	+ 69.5	
Joint B1:								
B-10	....	....	....	356 R	346 R	....	+ 69.5	
1-BA	12 WF 120	....	....	653 N	607 N	....	− 2.3	(0.1483)
B-12	....	....	....	297 R	261 R	....	+180.5	
Joint B2:								
B-21	....	....	....	338 R	354 R	....	+180.5	
2-BA	12 WF 120	$\frac{1}{2}$	14 × $\frac{3}{4}$	498 N	480 N	....	− 2.3	(0.3293)
B-23	....	....	....	160 R	126 R	....	+265.0	
Joint B3:								
B-32	....	....	....	294 R	325 R	....	+265.0	
3-BA	12 WF 120	$\frac{1}{2}$	14 × $\frac{3}{4}$	492 N	495 N	....	− 3.5	(0.4953)
B-35	....	....	....	198 R	170 R	225 R	+349.0	
Joint B5:								
B-53	....	....	....	336 R	375 R	....	+349.0	
5-BA	12 WF 79	$\frac{3}{4}$	14 × $\frac{1}{2}$	169 N	164 N	{70 R / 206 N}	− 4.6	(0.7815)
B-55[1]	....	....	....	167 N	201 N	335 N	+377.5	

[a] N = normal moment and R = reverse moment. [b] Tension is positive. [c] Bending moments for maximum live load, and with direct force considered. [d] The last four items in this column (in parentheses) are the deflections at the joints indicated, in inches.

The spans, sizes, loads, Q-values, and transmission coefficients for the frame, as well as the moment split at joint 2G, are shown in Fig. 16. These were taken from computations such as those in Table 3 for joints 2G, 3G, and 3C. The values of Q are to be multiplied by 100 and the moments are in kip-feet. Members in the frame are identified by a coordinate system in which columns and supports are lettered and floors and roofs are numbered. Thus, joint C2 is in column C at floor level 2. The writer investigated the intrusion of the members in accordance with the principles developed by the author in his text,[4] because at several joints relatively limber members are framed into very stiff members.

In connection with this design three facts are particularly noteworthy:

(*a*) The original design of member 3CG called for a haunched T-beam, increasing from 46 in. at its center to 72 in. at the center line of the columns. The analysis indicated that the columns, limited in size by the architect, would be overstressed. Changing this girder to one of constant depth required recomputations of frame characteristics only for those members framing into the joints at the ends of the girder.

(*b*) The results of the transmission and collection of the moments from the various joints are indicated for joint 3C. For example, the uniform load on 4BC transmitted 19 ft-kips to member 3CG, the sense of the moment being the same. Therefore, changes in loadings resulted only in changing the value of M_R and M_L for that particular load and noting its effect on the various joints to which it is transmitted.

(*c*) The critical values of the column moments were obtained by collecting the moments to give the maximum or minimum values, using the live-load percentages of the total loads.

Table 4 demonstrates the analysis of a Vierendeel truss used in the structural steel framing of New York City school buildings, the loadings, in kips, being as follows:

Load	P_A	P_B
Dead	13.7	17.9
Live	14.0	5.2
Total	27.7	23.1

The analysis of such a truss may be summarized into the following basic steps: (1) Compute the frame characteristics; (2) prepare torque transfer strips; (3) prepare torque-distribution charts; (4) compute moments due to loads between panel points and distribute; (5) distribute and collect artificial and neutralizing torques; (6) set up and solve shear bending moment equations; (7) obtain primary moments by substituting in the collections of artificial and neutralizing torques; (8) compute the direct stress; (9) find the artificial moments due to changes in length and distribute the neutralizing torques; (10) compute the vertical forces necessary to hold the lower chords horizontal and find the moments caused by the shears by substituting as in step 7; and (11) the total moment in any member is the algebraic sum of the moments found

[4] "Restrained Beams and Rigid Frames," by R. C. Brumfield, 1941 (revision and expansion of "The Solution of Statically Indeterminate Structures"; printed in mimeograph form by Cooper Union, New York, N. Y.)

in steps 7, 9, and 10. For ordinary purposes, the practice of using two-joint distribution and neglecting the secondary stresses will limit the analysis to the first seven steps and reduce the time required approximately one half. The analysis for secondary stresses and the effect of placing the live load to give the maximum moments are included in Table 4. The deflections of this truss (see last four items in Col. 8, Table 4) are practically the same as those for the conventional type. Fig. 17 shows the distorted frame and the horizontal and vertical displacements of the panel points.

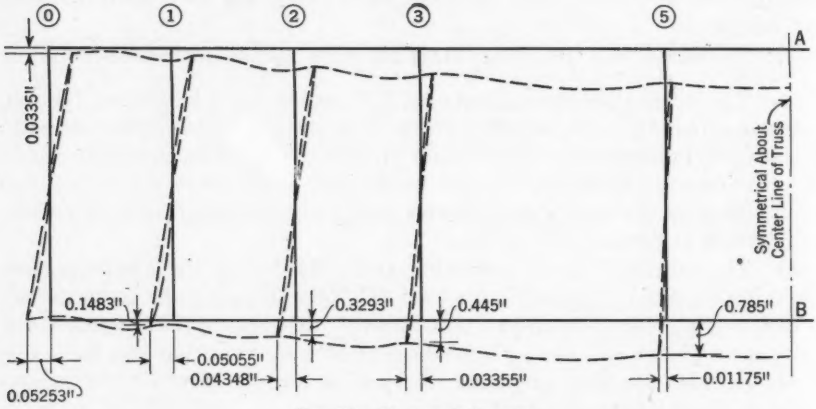

FIG. 17.—DISTORTED FRAME

As a check on the accuracy of Professor Brumfield's method, the writer analyzed a Vierendeel truss whose solution[21] has appeared elsewhere. The results were in exact agreement.

Summary.—The adaptation of frame characteristics, which is the heart and soul of Professor Brumfield's system, cloaks each frame with scientific exactness. These frame characteristics make entirely clear every detail of the flow of moment through the frame, and they readily facilitate computations and the examination of computations in case of changes in loading on any member. They simplify the computations for critical values of moment and shear for any member, regardless of type of loading, by indicating the necessary pattern of loading required to give these values, thus enabling the designer to trace their effects to that member. By the formula and the principles stated in Section 11, the writer has estimated the transmission coefficients for non-reentrant frames with gratifying results both as to time saved and accuracy of results. The concept of normal and reverse bending moment introduced by Professor Brumfield yields a clear picture of the distorted frame and eliminates the possibility of error and confusion arising in complicated frames when the plus and minus signs are used.

The writer has applied Professor Brumfield's system, successfully, not only to frames with straight beams of variable sections but also to curved beams with variable sections and to noncoplanar frames. The entire system is thorough, well integrated, and readily applied.

[21] *Transactions*, Am. Soc. C. E., Vol. 102 (1937), Table 3, p. 934.

G. ROLSMA,[22] ESQ., AND F. W. GIESEKING,[23] ESQ.[23a]—The concept of the transmission coefficient, as presented in this paper, provides a means for analyzing rigid frames regardless of shape or symmetry. Frames can be solved directly and completely for wind sidesway, moving loads, deflections, and settlement of supports. Expansion of the fundamental derivations furnishes the solution of each succeeding step. No additional theorems or assumptions are necessary. The fundamentals should be readily understood by the average engineer who is familiar with the three-moment theorem or the method of moment areas.

As a comment on Section 15 of the paper several "other applications" can be cited briefly. For example, the frame in Fig. 18(*a*) has been analyzed in the design of several stadia in New York, N. Y. A thorough study was desirable and the slight extra time required for computing coefficients was considered well spent as they were used in each succeeding step of the analysis. The frame characteristics in Fig. 18(*c*) were computed from the physical constants of the frame as outlined in Section 10 of the paper.

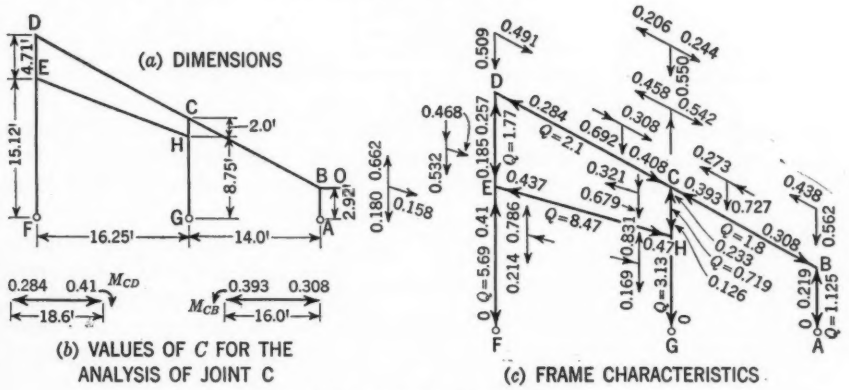

FIG. 18.—ANALYSIS OF STADIUM BENT

End moments were calculated, for all members of the frame, using Eqs. 16 and 17. For example, in the computations for joint C, $L_{CD} = 18.6$ ft and $L_{CB} = 16.0$ ft. The total design load, w, on member DB was 2.8 kips per ft, half of which was live load. Values of C_R and C_L are shown in Fig. 18(*b*). Substituting these values in Eqs. 16 and 17, $M_{CD} = \frac{28 \times 18.6^2}{4} \times \frac{0.41}{1 - 0.41 \times 0.284} \times 0.716 = 81$ ft-kips. Similarly, $M_{CB} = 56$ ft-kips. The end moments were then distributed to the frame in accordance with Section 13, except that moment-distribution charts were used, such as those for joint C in Fig. 19. Letters U, L, and R refer to the "under," "left," and "right" members, respectively, of the joint under consideration. The letters in the central column of each part of the chart indicate the joint of origin, and the lower-case letters

[22] Asst. Civ. Engr., Board of Education, City of New York, Brooklyn, N. Y.
[23] Asst. Architect, Board of Education, City of New York, Brooklyn, N. Y.
[23a] Received by the Secretary September 28, 1945.

at the sides show the particular member from which the distributed bending moment originates; thus: "a" denotes the under members, "b" denotes the left members, "c" the over members, and "d" the right members. Quantities next to the lower-case letters are live-load moments taken as a percentage of

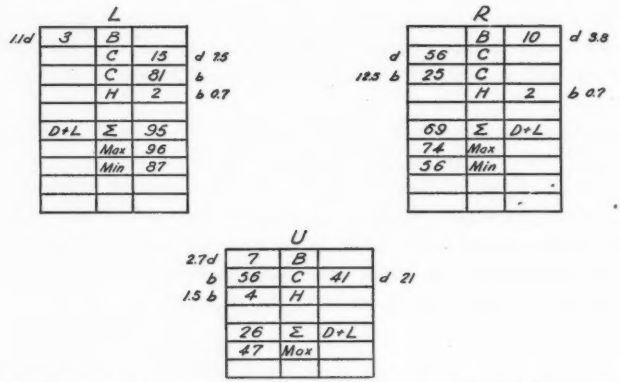

FIG. 19.—EXAMPLE OF LOAD BENDING-MOMENT COLLECTION CHART FOR MEMBERS AT JOINT C

the total moment, and are used for computing maximum and minimum moments. Moments of reverse sense are recorded in the left-hand column and normal moments in the right-hand column.

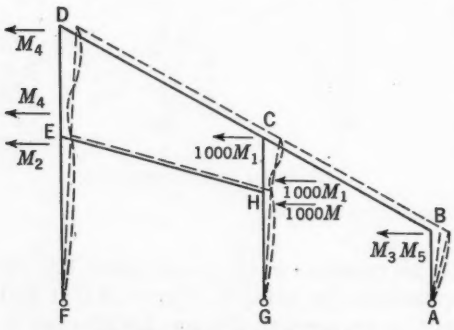

FIG. 20.—EFFECT OF SIDESWAY

For example, at the U-member of joint C the 21 ft-kips (normal in sense) constitute 50% of the total moment from the d-member of joint C indicating removal of live load from member CB to produce maximum moment of 47 ft-kips. From the moment-distribution charts, live-load plus dead-load moments, and maximum moments and minimum moments, may be obtained rapidly for each member at all joints. The frame is now statically determinate for all possible loading conditions; and the reactions, column shears, and maximum positive bending moments are readily computed.

Sidesway on an unsymmetrical frame, such as that in Fig. 18, may now be investigated easily by continuing the analysis. In general, the method is to assume that each joint has moved laterally to its final but unknown position as indicated by dashed lines in Fig. 20. At each end of all columns the designer places unknown bending moments sufficient to rotate the columns parallel to their original unstressed position. In this case 1,000 units of M were placed in top of column GH, 1,000 M_1 were placed at the top and the bottom of

column HC. By comparing column FE to column GH: $M_2 = \frac{Q\,L}{Q_2\,L_2} \times 1{,}000\,M$ $= \frac{3.13 \times 8.75}{5.69 \times 15.12} \times 1{,}000\,M = 318\,M$. Similarly, for the ends of the other columns, $M_3 = 8{,}350\,M$, $M_4 = 173\,M_1$, and $M_5 = 219\,M_1$.

Neutralizing torques, which are numerically equal but of opposite sense to the artificial bending moments placed at ends of columns, are applied at each joint and distributed to the frame. An example of a torque-distribution chart for joint C, in which 1,000 units of torque at joint C are distributed to the frame, is shown in Fig. 21. Such a chart is a valuable aid in distributing the neutral-

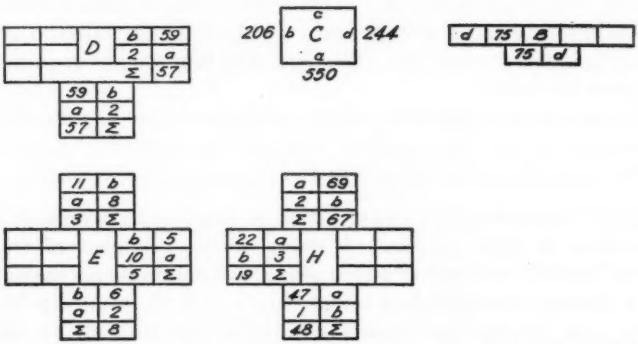

FIG. 21.—EXAMPLE OF CHART FOR THE DISTRIBUTION OF TORQUE FROM A GIVEN JOINT (JOINT C) TO ALL MEMBERS OF THE FRAME

izing moments at a joint to the frame. After distribution, these neutralizing torques and the artificial bending moments are summarized for each member at all joints. Shears in the columns may now be expressed in terms of M and M_1, and, by the laws of equilibrium, simultaneous equations may be set up and solved for numerical values of M and M_1. These values of M and M_1 are then substituted back into the joint summary for each member, thus obtaining values of bending moments due to lateral deflection. A summary chart for joint C, similar in arrangement to Figs. 19 and 21, can then be prepared to show the artificial bending moments and neutralizing torques, and final moments due to sidesway.

Most engineers do not have time to study, thoroughly, all methods proposed; also, personal preferences often dictate the method to be used in solving rigid frames. Actually, one method may be more suitable for a particular problem than another, depending on the desired degree of accuracy and extent of analysis. The concept of transmission coefficients as presented, therefore, offers the following advantages:

(1) It is a perfectly general method of analysis and not a special means of solving a limited number of cases due to form or symmetry. In the frame presented by the writers the members are of uniform section. If some or all were of variable section, the procedure would be the same except that then the restraint triangles require modification.

(2) No approximations of the degree of end restraints of the members are necessary anywhere in the structure except at the base or foundation levels.

(3) The manner of bookkeeping suggested offers opportunity for detecting errors speedily and for observing the paths of moments through the frame. The resulting moments are obtained directly and accurately.

(4) The formulas, readily understood, lead to short cuts expressing, in a brief mathematical expression, ideas which would require many lines of written explanation. This is particularly true of the formula for moving loads which, together with the prepared graph, provides a direct and rapid method for placing moving loads of any composition upon restrained beams in position for the required maximum condition. Therefore, influence lines are not required. The case of frames loaded with uniform live load is illustrated in Fig. 19, the use of loading patterns and the attendant separate studies required for each pattern being obviated.

(5) The use of the concept of normal and reserve bending moment in place of the plus and minus signs removes much of the confusion in the old use of signs. The distortion of the frame is also more readily visualized.

The paper is a noteworthy contribution to engineering literature pertaining to the analysis of rigid frames. A study of the "concept of transmission coefficients" and the manner of approaching various problems cannot help but result in a greater understanding of the action of rigid frames under all types of loading and the method should not prove too difficult to master and remember.

STANLEY S. SCHURE,[24] ESQ.[24a]—The Brumfield method of analysis has several advantages over other comparable methods. For example, it is more direct and, in a number of cases, more simple than the Cross method. After he has computed the frame characteristics, the designer will be familiar with the structure. The effect of different loadings, or of changes in the original loading, can easily be traced.

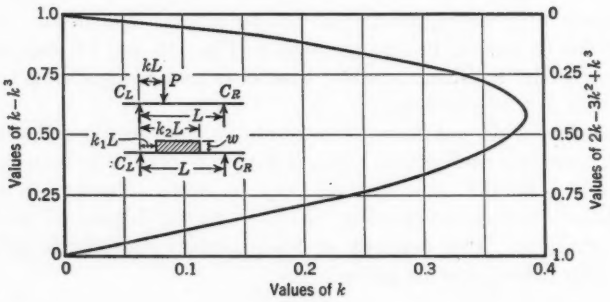

FIG. 22

To demonstrate this point, consider an ordinary continuous beam resting simply on five supports, with the four spans unequal in length. Assume the

[24] Structural Designer, Standard Oil Development Co., Elizabeth, N. J.

[24a] Received by the Secretary October 2, 1945.

end supports to be partly fixed so that finite values of C will occur at the extremities by the beam. Formulas for the fixed moments in each span (see inset, Fig. 22) are computed as follows:
For concentrated loads—

$$M_R = -P\,L\,A_R\,[(k - k^3) - C_L\,(2\,K - 3\,K^2 + K^3)] \ldots\ldots (61a)$$

and

$$M_L = -P\,L\,A_L\,[(2\,k - 3\,k^2 + K^3) - C_R\,(k - k^3)] \ldots\ldots (61b)$$

For uniform loads—

$$M_R = -w\,L^2\,A_R \left[\frac{k^2{}_2 - k^2{}_1}{2}\,(1 - 2\,C_L) + (k^3{}_2 - k^3{}_1)\,C_L - \frac{k^4{}_2 - k^4{}_1}{4}\,(1 + C_L)\right] \ldots\ldots (62a)$$

and

$$M_L = -w\,L^2\,A_L \left[\frac{k^2{}_2 - k^2{}_1}{2}\,(2 - C_R) - (k^3{}_2 - k^3{}_1) + \frac{k^4{}_2 - k^4{}_1}{4}\,(1 + C_R)\right] \ldots\ldots (62b)$$

When $k_1 = 0$ and $k_2 = 1$, Eqs. 62 become

$$M_R = -\frac{w\,L^2}{4}\,A_R\,(1 - C_L) \ldots\ldots (63a)$$

and

$$M_L = -\frac{w\,L^2}{4}\,A_L\,(1 - C_R) \ldots\ldots (63b)$$

which may also be derived by substituting A_R-values and A_L-values in Eqs. 16 and 17, respectively. Values of $k - k^3$ and $2\,k - 3\,k^2 + k^3$ can be selected from curves such as Fig. 22. The succeeding step is to compute the frame characteristics similar to Table 1. For the example presented herein these characteristics are shown in Table 5. Finally, the restrained moments for

TABLE 5.—COMPUTATION OF FRAME CHARACTERISTICS, CONTINUOUS BEAM ON FIVE SUPPORTS

Member	Stiffness Index $Q\,(2 - C) = i$		Restraint index R	Transmission Coefficient C (Eq. 5)	
				Value	Member
(1)	(2)	(3)	(4)	(5)	(6)
Joint B					
BA	0.667 (2 − 0.174)	1.22	0.660	0.335	AB
BC	0.357 (2 − 0.155)	0.660	1.22	0.185	CB
Joint C					
CB	0.357 (2 − 0.184)	0.648	1.593	0.155	BC
CD	1.0 (2 − 0.407)	1.593	0.648	0.378	DC
Joint D					
DC	1.0 (2 − 0.378)	1.622	0.456	0.407	CD
DE	0.270 (2 − 0.303)	0.456	1.622	0.125	ED

each load, and the unbalanced moments from each span, are tabulated and the total moment is determined as shown in Table 6. As stated, the method

TABLE 6.—Analysis of a Continuous Four-Span Beam Resting on Five Supports (End Supports Partly Fixed)

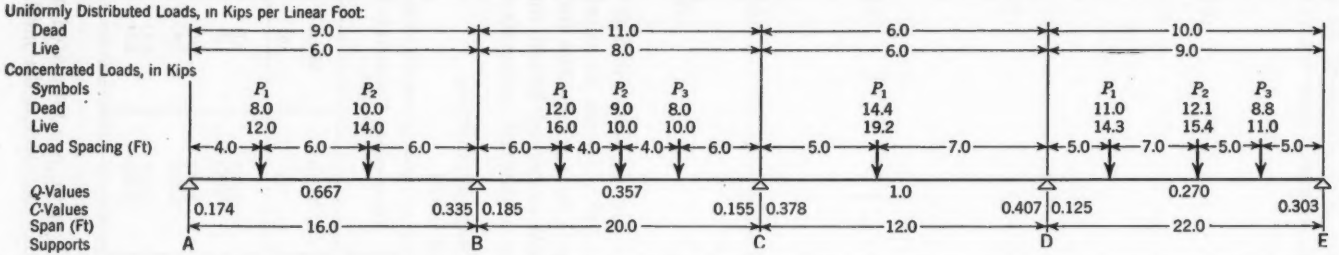

A (Eq. 19)	0.185			0.356		0.195			0.160		0.447			0.481		0.130			0.315	
λ-values			λ					λ					λ					λ		
Load	Dead	Live		Dead	Live	Dead	Live		Dead	Live	Dead	Live		Dead	Live	Dead	Live		Dead	Live
Uniform	7.1	4.7		16.8	11.2	18.1	13.2		14.3	10.4	5.7	5.7		6.5	6.5	11.0	9.9		33.4	30.1
P_1	6.0	9.0	0.25	7.9	11.9	14.8	19.7	0.3	8.0	10.7	18.6	24.8	0.417	17.2	23.0	8.1	10.5	0.227	13.2	17.1
P_2	5.9	8.3	0.667	18.0	25.2	11.1	12.4	0.5	9.1	10.0	....	....		....	....	7.4	8.8	0.545	28.6	36.4
P_3	....	....		....	....	6.8	8.5	0.7	7.8	9.8	....	....		....	....	2.9	4.0	0.775	17.2	21.5
	←	←		→	→	←	←		→	→	←	←		→	→	←	←		→	→
Fixed-end moment	19.0	22.0		42.7	48.3	30.8	53.8		39.2	40.9	24.3	30.5		23.7	29.5	29.4	33.2		92.4	105.1
Distribution:						←	←		←	←	→	→		→	→	←	←		←	←
From AB	....	....		....	....	42.7	48.3		6.6	7.5	6.6	7.5		2.7	3.1	2.7	3.1		0.8	0.9
	→	→		→	→						←	←		←	←	→	→		→	→
From BC	8.9	9.4		50.8	53.8	....	....		....	....	39.2	40.9		16.0	16.7	16.0	16.7		4.9	5.1
	←	←		←	←	→	→		→	→						←	←		←	←
From CD	0.8	1.0		4.5	5.6	4.5	5.6		24.3	30.5	....	....		....	....	23.7	29.5		7.2	9.0
	→	→		→	→	←	←		←	←	→	→		→	→					
From DE	0.3	0.4		2.1	2.3	2.1	2.3		11.1	12.6	11.1	12.6		29.4	33.2	....	....		....	....
Final Moments:																				
	←			→		←			→		←			→		←			→	
Dead load	10.6			91.1		91.1			45.8		45.8			39.8		39.8			89.3	
Live load—																				
		←			→		←			→		←			→		←			→
Maximum		23.0			104.4		104.4			71.4		71.4			65.8		65.8			110.2
		→			←		→			←		→			←		→			←
Minimum		9.8			5.6		5.6			20.1		20.1			16.7		16.7			9.9

is direct and simple. In a large percentage of cases the loads are concentrated or uniformly distributed, as in this example. For special loadings, such as locomotives, trucks, and variable distributions, the method described in Section 5 is applicable.

In computing frame characteristics the writer suggests a modification which produces the same results as the author's method. This procedure avoids the use of a slide rule and thus eliminates errors. It involves the use of tables of reciprocals such as those found in most handbooks. For instance, the writer would add the following data in a column to be inserted between Cols. 3 and 4, Table 1:

Member	$\frac{1}{i}$
Joint B_1	
B10	2.1930
1BA	2.5253
1BC	3.4843
Joint C_1	
C10	2.1930
1CB	3.4384
1CD	3.4130
Joint D_1	
D10	1.6448
1DC	3.4722
1DE	2.5253

The proper values of $1/i$ are then added and the co-reciprocal of their sum is as the necessary R-value. For example, in member 1BC, joint B_1, $2.1930 + 2.5253 = 4.7183$. The co-reciprocal of this value (0.212) is the value of $R_{1BC}\left(= \frac{1}{\frac{1}{i_1} + \frac{1}{i_2}}\right)$. Similarly for member 1DC, joint D_1, $1.6448 + 2.5253 = 4.1701$, whose co-reciprocal (0.240) is the required value of R_{1DC}.

ALEXANDER DODGE,[25] ASSOC. M. AM. SOC. C. E.[25a]—The analysis of the frame shown in Table 1 was predicated on the assumption that no sidesway existed, which would hold true only if the ends A_1 and E_1 were hinged. However, this assumption is in conflict both with the sketch, in which the ends A_1 and E_1 are shown to be freely supported, and with the statement (see Section 10) "A free support, such as point A_1." It is inconceivable that the term "a free support" could ever be applied to the hinged end of a member. Furthermore, in modern rigid frames of the type shown, the bearing ends A_1 and E_1 are usually made free to move in a horizontal direction (to minimize shrinkage and temperature stresses) by the introduction of rockers or metal sliding plates; and the problem of determining the degree of lateral support, as a rule, is given due consideration in design. Therefore, with the information

[25] Engr., U. S. Engrs., Portland, Ore.

[25a] Received by the Secretary October 24, 1945.

at hand, the degree of lateral support for this frame is an unknown quantity, depending on the position of a load and the amount of the downward reactions, as well as the coefficients of friction at points A_1 and E_1. This point should be clarified, so that no doubt is left in the reader's mind as to the type of a structure that is being analyzed. With loads placed as shown in Fig. 12, both ends A_1 and E_1 will be raised from their supports, provided this movement is not prevented by dead-load reactions, which, however, were not taken into consideration in the analysis. Therefore, the transmission coefficients will be changed and unbalanced shears in the columns will cause lateral deflections. Consequently, the characteristics of the frame will be altered to such an extent that an entirely new solution will result, although the changes will be slight because of the almost perfect symmetry of the frame and the loading.

The stated purpose of the paper (see "Synopsis") is to develop methods "for distributing the moments to the frame in a single operation," but the author has failed to show how this could be done because sidesway, present in the analysis of this frame, is disregarded. Moreover, the analysis of any rigid frame without sidesway can be reduced to an analysis of a continuous beam, and Eqs. 10 to 38 represent very special cases of structural concepts, belonging to the "beam class" rather than to the "frame class" of problems. The designer is interested not only in the bending moment under concentrated loads, but also (even for the very simple case treated in the paper) in negative moments at intermediate points; and these latter moments must be determined by some method not treated in the paper. A pure couple requires an entirely different set of computations using a very different concept, which makes the Brumfield analysis lengthy, nonuniform, and cumbersome.

The derivation of exact partly restrained end moments due to loads on a member has been demonstrated by A. Strassner.[26] He showed the practical applications of the concept of transmission coefficients and presented a method of distributing the moment to the frame of a general type in two operations—(1) by distributing the moment in a single operation on the assumption that no sidesway exists and (2) finding the sidesway corrections (also a single operation). Mr. Strassner's original work is mostly graphical—probably the reason why his method has never attained popularity in the United States. Subsequently, an entirely algebraic method, called the "coefficients of unit moment" method,[27] was developed which took variable moment of inertia, as well as sidesway adjustments, into consideration.

On the assumption that there is no sidesway, the general equation of the exact partly restrained end moment at end A of a member AB, due to applied load on the member, is given by:

$$M'_A = M_A (1 + t_{ab}) + M_B t_{ba} Z'_{ab} \quad \ldots\ldots\ldots\ldots\ldots\ldots (64)$$

in which t_{ab} and t_{ba} (the writer's "coefficients of unit moment" and Professor Brumfield's "torque split") represent the exact moment induced in a member

[26] "Neuere Methoden zur Statik der Rahmentragwerke," by A. Strassner, Vol. 1, Ernst, Berlin, 1925–1927.

[27] "Solution of Rigid Frames by Coefficients of Unit Moment," by Alexander Dodge, thesis presented to the University of Washington at Seattle, Wash., in 1939, in partial fulfilment of the requirements for the professional degree of Civil Engineer.

at a joint due to a unit moment applied at the same joint; and Z'_{ab} is the coefficient of unit moment, or the moment at the partly restrained end A of the beam AB due to a unit moment at the hinged end B. Furthermore,

$$M_A = \frac{\frac{\phi_\beta 6I}{L^2}(M_{sa}) - \frac{\phi_\alpha 12I}{L^2}(M_{sb})}{4\phi_\alpha\phi_{ab} - \phi^2_\beta} \quad \ldots\ldots\ldots\ldots (65a)$$

and

$$M_B = \frac{\frac{\phi_{ab} 12I}{L^2}(M_{sa}) - \frac{\phi_\beta 6I}{L^2}(M_{sb})}{4\phi_\alpha\phi_{ab} - \phi^2_\beta} \quad \ldots\ldots\ldots\ldots (65b)$$

In Eqs. 65: ϕ_β, ϕ_α, and ϕ_{ab} are form factors, or constants of integration depending upon the variation in moment of inertia of a beam; and M_{sa} and M_{sb} are numerical values of the moment of the simple-beam, M/I-area, due to external loading on beam AB taken about points A and B, respectively. For a constant moment of inertia, Z'_{ab} in Eq. 64 is equal to:

$$Z'_{ab} = \tfrac{1}{2} f = C_{BA} \quad \ldots\ldots\ldots\ldots (66a)$$

After a slight rearrangement, Eq. 4 may be written:

$$C_{BA} = \tfrac{1}{2}\left[\frac{1}{1 + \frac{1}{2\left(\frac{Q}{i_1} + \frac{Q}{i_2}\right)}}\right] \quad \ldots\ldots\ldots\ldots (66b)$$

combining Eqs. 66:

$$\frac{1}{1 + \frac{1}{2\left(\frac{Q}{i_1} + \frac{Q}{i_2}\right)}} = f \quad \ldots\ldots\ldots\ldots (67)$$

The left side of Eq. 67 is the mathematical expression of the symbolic definitions, but the "end fixity," f, has been shown to represent the clear physical concept, simply derived from the knowledge of the stiffnesses of the joining beams only;[28] that is,

$$f = \frac{\Sigma S_p}{\Sigma S_p + S} \quad \ldots\ldots\ldots\ldots (68)$$

A very simple relation also exists between the "end fixity" and the "transmission coefficient." When f is equal to unity (100% end fixity for the fixed end), the value of C equals 0.5; and, when f is equal to zero (0% end fixity for the hinged end), the value of C becomes zero also. For any variation of the moment of inertia and for a partial fixity, the simple linear relation still exists between f and C. Eq. 64 was developed with the expectation that it might be used on a broad scale in engineering practice, but this expectation has never

[28] *Proceedings*, Am. Soc. C. E., September, 1945, p. 1121.

been realized because in rigid frame analyses sidesway adjustments may modify, considerably, the results found by Eq. 64. Eqs. 18 through 38 belong to the same category and from the practical standpoint can scarcely prove satisfactory to designers.

The exact partly restrained end moment in a member due to end translation is expressed by Eq. 64, except that, in this particular case (compare Eq. 65*a*):

$$M_A = \frac{M_B\,(\phi_\beta + 2\,\phi_a)}{\phi_\beta + 2\,\phi_{ab}} \qquad (69)$$

Computation of "symbolic" quantities is a tedious process that has no physical meaning in a designer's mind. It will always be the source of numerous errors, especially if the computations are not performed as a matter of daily routine work. The introduction of unusual terms and definitions, such as S, e, ϵ, i, and R, which have no clear physical concepts, complicates the analysis unnecessarily, serves no particular purpose, and could be avoided. For example, if the frame in Fig. 12 were analyzed on the assumption that ends A_1 and E_1 were hinged, the necessary paper work would be limited to

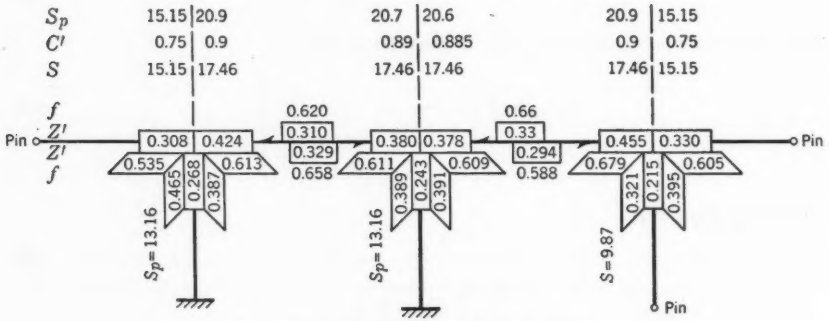

FIG. 23.—COEFFICIENTS OF UNIT MOMENT

computations shown in Fig. 23, in which the author's basic Q-values have been replaced by the exact stiffnesses of the members as shown in Table 7.

TABLE 7.—EQUIVALENT S-VALUES, FRAME IN FIG. 12

Stiffness	A_1B_1	B_1B_0	B_1C_1	C_1C_0	C_1D_1	D_1D_0	D_1E_1
Q	0.198	0.304	0.172	0.304	0.172	0.304	0.198
S	15.15	....	17.46	....	17.46	9.87	15.15
S_p	....	13.16	....	13.16	....	....	....

Since the Cross method of analysis has been developed, it has been known that for members with fixed ends $S_p = 4\,I/L$ and for members with hinged ends $S = 3\,I/L$. Although Fig. 23 contains all characteristics that are recorded in Fig. 12, computation of the values shown in Table 1 is not necessary, and the procedure begins directly with step 6 of Section 10. The "moment split" m (the writer's "moment joint coefficient," J) for the members B_1A_1 and B_1B_0,

respectively, will be

$$m_{ba} = \frac{S_p}{\Sigma S_p} = \frac{15.15}{15.15 + 13.16} = 0.535$$

$$m_{bb} = \frac{13.16}{28.31} = 0.465$$

$$\Sigma m_b = 1.000$$

The computations in step 7 would then be, by Eq. 68, $f = \frac{28.31}{28.31 + 17.46}$ $= 0.620$; and $C_{1CB} = Z' = \frac{1}{2}f = 0.310$. In step 8 with $f = 0.620$ and the corresponding value[28] of $C' = 0.89$, the exact stiffness of the member B_1C_1 at joint C_1 is readily determined by the relation—

$$S_p = \frac{C' S}{C_d} \qquad (70)$$

—that is, $S_p = \frac{0.89 \times 17.46}{0.75} = 20.7$. In Eq. 70 the symbol C_d is a constant that can be read from design charts prepared by Thor Germundsson,[29] Assoc. M. Am. Soc. C. E. For a member of uniform section this constant is equal to 0.75. The value of S_p having been determined, the moment splits are computed thus: $m_{cb} = \frac{20.7}{20.7 + 13.16} = 0.611$; and $m_{cc} = \frac{13.16}{33.86} = 0.389$. The operations are repeated in this very simple and direct way until all characteristics are obtained.

The torque splits, or "coefficients of unit moment," are also evaluated very simply and directly. For example, for joint B_1,

$$t_{ba} = \frac{S_p}{\Sigma S_p} = \frac{15.15}{15.15 + 13.16 + 20.9} = 0.308$$

$$t_{bb} = \frac{13.16}{49.21} = 0.268$$

$$t_{bc} = \frac{20.9}{49.21} = 0.424$$

$$\Sigma t_b = 1.000$$

Other "coefficients of unit moment" or "torque splits" are found in a similar manner.

The writer objects strongly to the term "torque split" for the reason that, in a structural analysis, the word "torque" is associated with twisting action, causing primarily shear stresses in a member. Moreover, the design of structures often incorporates the analysis of noncoplanar members, in which a moment acting at the joint may be resisted partly by the bending of some members and partly by the twisting of the other members. The term "torque

[29] "Design of Continuous Frames Having Variable Moment of Inertia," by Thor Germundsson *Civil Engineering*, October, 1932, p. 647.

split" would apply more consistently to the analysis of a spandrel girder receiving a twisting moment when this moment is split in unequal amounts to two segments of the girder; but, for the sake of clearness as well as uniformity in engineering literature, it would be advisable to stay within the customary definitions of bending and twists.

To distribute a moment to a frame of the general type (that is, a frame with a sidesway and variable moment of inertia) in a single operation, it is necessary to determine "true frame characteristics" or "true moment coefficients." At the designer's discretion, there are several optional methods of computing the "true moment coefficients." The following discussion does not infer that it presents the only procedure available but, rather, that it offers the simplest and the most systematic treatment of the problem. The true moment coefficients due to a unit moment m_{BC} may be derived as follows:

1. Compute the torque split ("coefficients of unit moment") shown in Fig. 24;

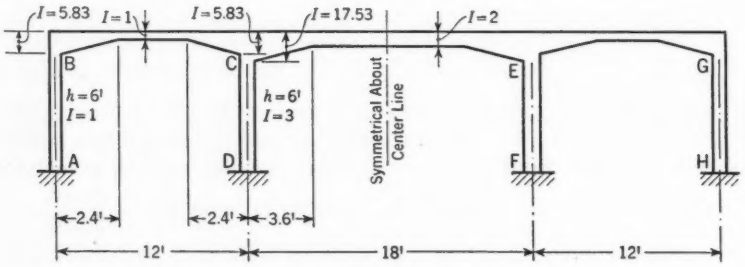

(*a*) GENERAL DATA

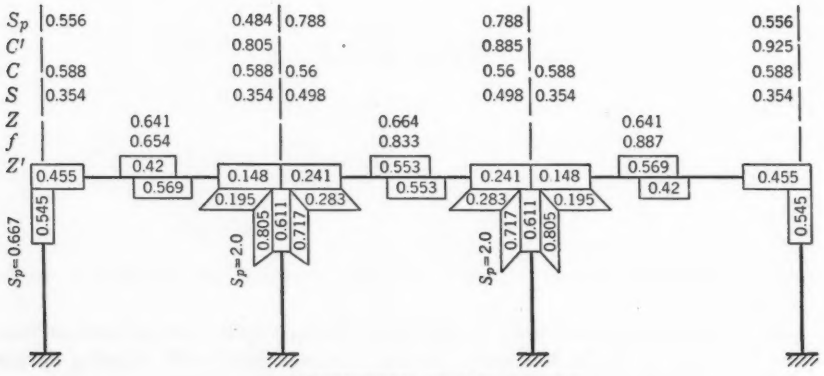

(*b*) COEFFICIENTS OF UNIT MOMENT

FIG. 24.—SOLUTION OF A RIGID FRAME

2. Compute "beam coefficients" due to $m_{BC} = +1$ on the assumption that no sidesway exists and record them in Col. 2, Table 8 (this step is the equivalent of the author's procedure outlined in Section 13);

3. Find the horizontal reaction R_{mB} due to m_{BC}, which prevents the translation of the joints ($R_{mB} = \frac{1}{6}$ (0.273 + 0.545 − 0.186 − 0.093 + 0.032 + 0.016 − 0.003 − 0.001) = + 0.097 kips);

TABLE 8.—COMPUTATION OF INFLUENCE ORDINATES

Moments	Coefficients of Unit Moment, for Positive Unit Values of:						Influence Ordinates for Moment[a]		
	m_{BC}	m_{CB}	m_{BC}	m_{CB}	m_{BC}	m_{CB}	$M_{Bf} = -2.18$	$M_{Cf} = 0.44$	Total (kip-ft)
	Beam		Sidesway		True Moment				
(1)	(2)	(3)	(4)	(5)	(6)	(7)	(8)	(9)	(10)
M_{AB}	− 0.273	0.031	+ 0.043	0.051	− 0.230	0.082	0.50	0.04	0.54
M_{BC}	+ 0.545	− 0.062	− 0.033	− 0.039	+ 0.512	− 0.101	− 1.12	− 0.04	− 1.16
M_{CB}	− 0.259	0.852	− 0.034	− 0.040	− 0.293	0.812	0.64	0.36	1.00
M_{CD}	+ 0.186	− 0.611	+ 0.089	0.104	+ 0.275	− 0.507	− 0.60	− 0.22	− 0.82
M_{DC}	+ 0.093	− 0.305	+ 0.126	0.146	+ 0.219	− 0.159	− 0.48	− 0.07	− 0.55
M_{CE}	+ 0.073	− 0.241	− 0.054	− 0.064	+ 0.019	− 0.305	− 0.04	− 0.13	− 0.17
M_{EC}	+ 0.040	− 0.133	− 0.054	− 0.064	− 0.014	− 0.197	0.03	− 0.09	− 0.06
M_{EF}	− 0.032	0.107	+ 0.089	0.104	+ 0.057	0.211	− 0.12	0.09	− 0.03
M_{FE}	− 0.016	0.054	+ 0.126	0.146	+ 0.110	0.200	− 0.24	0.09	− 0.15
M_{EG}	− 0.008	0.026	− 0.034	− 0.040	− 0.042	− 0.014	0.09	− 0.01	0.08
M_{GE}	− 0.003	0.011	− 0.033	− 0.039	− 0.036	− 0.028	0.08	− 0.01	0.07
M_{HG}	+ 0.001	− 0.005	+ 0.043	0.051	+ 0.044	0.046	− 0.10	0.02	− 0.08

[a] Ordinates of the influence line for moment (in kip-ft) caused by a unit load at the quarter points of beam BC.

4. Compute sidesway moments in the frame due to $H = 1$, as shown in Table 9;

TABLE 9.—SIDESWAY MOMENTS CAUSED BY VARIOUS FIXED-END MOMENTS

Sidesway moments	$M_{AB} = 1$ and $M_{BA} = 1$	$M_{DC} = 3$ and $M_{CD} = 3$	$M_{FE} = 3$ and $M_{EF} = 3$	$M_{HG} = 1$ and $M_{GH} = 1$	$H = -1.793\ k$	$H = +1\ k$
M_{AB}	0.727	0.093	− 0.616	0.001	0.805	− 0.448
M_{BA}	0.455	0.186	− 0.033	0.003	0.611	− 0.341
M_{CB}	− 0.259	− 0.444	0.078	− 0.008	− 0.633	+ 0.353
M_{CD}	0.186	1.167	0.323	− 0.032	1.644	− 0.916
M_{DC}	0.093	2.083	0.161	− 0.016	2.321	− 1.295
M_{CE}	0.073	− 0.723	− 0.401	0.040	− 1.011	+ 0.563
M_{EC}	0.040	− 0.401	− 0.723	0.073	− 1.011	+ 0.563
M_{EF}	− 0.032	0.323	1.167	0.186	1.644	− 0.916
M_{FE}	− 0.016	0.161	2.083	0.093	2.321	− 1.295
M_{EG}	− 0.005	0 078	− 0.444	− 0.259	− 0 633	+ 0.353
M_{GH}	0.003	− 0.033	0.186	0.455	0 611	− 0.341
M_{HG}	0.001	− 0.016	0.093	0.727	0.805	− 0.448

5. Find "sidesway coefficients" due to $-R_{mB}$, and record them in Col. 4, Table 8; and

6. Find the "true moment coefficients" due to m_{BC} by adding the values of Cols. 2 and 4, and record them in Col. 6, Table 8.

The Germundsson charts were used for the computation of beam constants, or the elastic properties of members which are independent of the framed structure. These computations are shown in Table 10. Steps 1 and 2 are

computed by slide rule.[30] Computations for step 4 are similar to those for step 2. The sidesway moments from any horizontal force applied at the top of columns are found first. These values are reduced to moments generated by the force $H = 1$, as shown in Table 9.

TABLE 10.—COMPUTATION OF BEAM MOMENTS

Members	a	b	$Z = r$	C	$S = C_s I/L$ [a]
BC and EG	2.4/12 = 0.2	1/5.83 = 0.171	0.641	0.588	4.25/12 = 0.354
CE	3.6/18 = 0.2	2/17.55 = 0.114	0.664	0.56	4.48 × 2/18 = 0.498
AB and HG	....	....	0.5	0.75	4/6 = 0.667
DC and EF	....	....	0.5	0.75	4 × 3/6 = 2.0

[a] In this formula the symbol C_s is a constant that can be read from the design charts.[29]

Thus far the discussion has been limited strictly to the computation of the "true moment coefficients" due to $m_{BC} = +1$. True moment coefficients will be changed, of course, with the point of application of a unit moment, but for any new position, such as will be defined by the subscript of the unit moment m_{CB}, the additional work recorded in Cols. 3, 5, and 7, Table 8, is negligible. After the sixth step, it is possible to distribute a moment to the frame in a single operation. Nevertheless, because the derivation of these coefficients may be divided into two distinct operations—an analysis of a frame without sidesway and evaluation of sidesway corrections—it would be more correct to describe the analysis as moment distribution in two operations. Thus, for a two-story frame, there will be two sidesway corrections, and the analysis will require three distinct operations. A rigid frame with N sidesway forces will have N corrections and $N + 1$ distinct operations.

For practical purposes, contrary to the author's opinion, the writer still believes that the design of structures for moving loads is rendered much easier by influence lines than by any other method. This will be even more true of a structure that must be designed for various conditions of loading; but any important structure may be expected to have a set of design conditions. Even in a preliminary design of a continuous beam, the author's formulas could scarcely compete with the old fixed-end moment formulas, because, in the former, as a result of a series of abstract computations, the chances for mistakes are innumerable, and there is no way to "feel" the errors. However, in the latter the maximum limit of moments is given at once, and the values of the exact moments, depending on the end fixity, may be correctly estimated without the complete analysis. It will now be shown how simple moments due to a unit load placed, say, at the quarter point of beam BC may be determined. The fixed-end moments from this load will be: $M_{Bf} = -0.182 \times 12 = -2.18$ kip-ft; and $M_{Cf} = 0.037 \times 12 = 0.44$ kip-ft.

These moments multiplied by the values of Cols. 6 and 7, Table 8, will yield the products recorded in Cols. 8 and 9, respectively. Summation of Cols. 8 and 9 in Col. 10 gives the final distributed moments and, at the same time, the values of influence ordinates. If the computations of Cols. 8, 9, and 10 were

[30] *Proceedings*, Am: Soc. C. E., September, 1945, p. 1124.

repeated for a unit load placed at the center line and three-quarter point of the span, the complete values of the influence ordinates, for a load on beam BC, would be obtained. From a practical standpoint, these load positions were found to be entirely satisfactory for the accurate construction of influence lines. The writer, at least, has never had occasion to use more points than those suggested herein.

The definitions of "normal" and "reverse," as applied to bending moments, are definitely inferior to the brief and simple definition: "Clockwise moments are positive." The value of this simpler definition may be realized and appreciated to the greatest extent by one familiar with an analysis of frames in three dimensions, such as the twist analysis of a dam or the analysis of a structure on an elastic foundation. How difficult it would be to perform these analyses with the definitions proposed by the writer may be realized by consideration of the equation of joint equilibrium, which would be stated as follows: The summation of normal bending and clockwise twisting moments, minus reverse bending and counterclockwise twisting moments, plus or minus an externally applied couple at the joint, is equal to zero. In contrast to this phraseology is the simplicity of the commonly adopted statement of joint equilibrium, namely: "The summation of moments is equal to zero; clockwise moments are positive." Contrary to the author's opinion, the old definition of "clockwise moments are positive" fits the analysis of beams radiating in all directions exceptionally well—especially when many loading conditions must be investigated. The old definition fixes the sense of the bending moment in such a manner as to avoid confusion.

The author's statement (Section 13) that "One distribution also is sufficient for all purposes, including live-load and dead-load moment distribution, wind moments, and sidesway * * *" is not clear. Because the allowable unit stresses, as a rule, vary with the particular combination of loadings, a separate distribution should be made for each of the aforementioned loads.

Of incidental interest, but nonetheless important, is the question of nomenclature. Every new paper on this subject yields its own set of nomenclature and abbreviations. If writers would take full advantage of the commonly accepted symbols and restrict the introduction of new symbols to the absolute minimum, they would render the engineering profession a priceless service as well as facilitate the task of education. For example, there are only three really important structural concepts that need to be known for analysis of structures. They have been established previously and again are presented in this paper but, being differently derived, are given new definitions and symbols. Excluding foreign sources, the equivalent symbols for these concepts are known as follows: Transmission coefficient C equals carry-over factor f equals coefficient of unit moment Z'; torque split t equals distribution factor d equals coefficient of unit moment K; and moment split m equals joint moment coefficient J.

It is not clear why the span of a simple structure should be designated by three symbols such as 1BC, and why the same subscript should be needed to define the bending moment. In most structural analyses in two dimensions, two letters (or two subscripts in the case of a moment) are sufficient. If the

first subscript were always selected to designate the location, the term M_{AB} would define the moment at point A in span (or member) AB. The same system would hold true for shear, angle, deflection, and twisting moment. In the case of an angle, two subscripts will be needed only when the efficiency of a joint is less than 100%. For isolated members, or for single spans, the second subscript, of course, would be omitted because the first subscript completely defines the location of the point. A similar system of lower-case letter subscripts could be adopted for the description of other properties of members. The selection of lower-case letters, although not absolutely necessary, would facilitate recognition of apparently equal terms, such as S_{AB} and S_{ab}, at a glance. The first term would refer to the shear and the second to the stiffness at point A of member AB. The transmission coefficient, or the exact carry-over factor with the subscript *ab* in the same system, would signify the exact moment at point A due to a unit moment at point B, which, evidently, would be contrary to the author's notation.

Sometimes a distinction may need to be made between hinged, fully fixed, or partly fixed, end conditions. In such cases the writer suggests the use of lower-case letters *o*, *f*, and *p*, respectively, for the third subscript. This appears to be a contradiction of the foregoing statement, but in reality it is not, because in the latter case three independent structures are being analyzed. Instead of verbal descriptions, a simple subscript is utilized for this distinction. For example, M_{ABf} would define the fixed-end moment at point A of member AB. Were one or both of the capital subscripts missing, M_f would still be recognized as a fixed-end moment. Not all the three subscripts *o*, *f*, or *p* would have to be retained in the same analysis; the predominating subscript might be omitted at the discretion of the designer.

For analyzing multistoried frames, with many members and joints, a grid pattern of numbering may be used to advantage. In this pattern, a joint is defined by the intersection of two lines and, therefore, one letter and one number will be needed for identification. The grid pattern of numbering will not be in conflict with the foregoing described system of abbreviations, if it is remembered that the first two subscripts define the point and the third subscript, the direction. For instance, M_{1BC} will define the moment at point 1B in the member BC.

ENGINEERING
LIBRARY

JAN 1 1946

PROCEEDINGS

American Society
of
Civil Engineers

DECEMBER
1945

VOLUME 71 NO. 10

AMERICAN SOCIETY OF CIVIL ENGINEERS

OFFICERS FOR 1945

PRESIDENT

J. C. STEVENS

VICE-PRESIDENTS

Term expires January, 1946:

RICHARD E. DOUGHERTY
FRANKLIN THOMAS

Term expires January, 1947:

E. E. HOWARD
A. C. POLK

DIRECTORS

Term expires January, 1946:

R. E. BAKENHUS
DEAN G. EDWARDS
C. B. BREED
C. F. GOODRICH
N. W. DOUGHERTY
FRED C. SCOBEY

Term expires January, 1947:

S. C. HOLLISTER
GAIL A. HATHAWAY
RALEIGH W. GAMBLE
WILBUR M. WILSON
FRANK C. TOLLES
WILLIAM D. SHANNON
ROYCE J. TIPTON

Term expires January, 1948:

CHARLES W. BRYAN, JR.
THORNDIKE SAVILLE
HOWARD T. CRITCHLOW
JOHN H. GARDINER
H. F. THOMSON
O. H. KOCH

PAST-PRESIDENTS

Members of the Board

EZRA B. WHITMAN
MALCOLM PIRNIE

TREASURER

CHARLES E. TROUT

SECRETARY

WILLIAM N. CAREY

ASSISTANT TREASURER

GEORGE W. BURPEE

ASSISTANT SECRETARY

JAMES E. JAGGER

PROCEEDINGS OF THE SOCIETY

SYDNEY WILMOT
Manager of Publications

HAROLD T. LARSEN
Editor of Proceedings

COMMITTEE ON PUBLICATIONS

N. W. DOUGHERTY, *Chairman*

S. C. HOLLISTER
FRED C. SCOBEY
H. F. THOMSON
WILBUR M. WILSON
J. C. STEVENS, *ex officio*

Issue	Page Numbers
January	1– 126
February	127– 268
March	269– 410
April	411– 600
May	601– 790
June	791– 996
September	997–1154
October	1155–1312
November	1313–1470
December	1471–1612

AMERICAN SOCIETY OF CIVIL ENGINEERS

COMING MEETINGS

BOARD OF DIRECTION MEETINGS

January 14–15, 1946:

A Quarterly Meeting will be held in New York, N. Y.

ANNUAL MEETING

NEW YORK, N. Y.

January 16–18, 1946

The Reading Room of the Society is open from 9:00 A.M. to 5:00 P.M. every day, except Saturdays when it is closed at 12:00 noon. It is closed all day on Sundays and holidays.

Members, particularly those from out of town, are cordially invited to use this room on their visits to New York, to have their mail addressed there, and to utilize it as a place for meeting others. There is an ample file of current periodicals, the latest technical books, and the room is well supplied with writing tables.